Université de Montréal

Polyamides and polyesters made of bile acids in the main chain

par
Olga Ivanysenko

Département de chimie
Faculté des arts et des sciences

Mémoire présenté à la Faculté des etudes supérieures
en vue de l'obtention du grade de maîtrise (M.Sc.) en chimie

Septembre 2012

Université de Montréal
Faculté des études supérieures et postdoctorales

Ce mémoire intitulé :

Polyamides and polyesters made of bile acids in the main chain

Présenté par :
Olga Ivanysenko

a été évalué par un jury composé des personnes suivantes :

Prof. William Skene, président-rapporteur
Prof. Julian Zhu, directeur de recherche
Prof. Suzanne Giasson, membre du jury

Abstract

Bile acids have drawn attention in the synthesis of polymers for biomedical and pharmaceutical applications due to their natural origin. The objective of this work is to synthesize main-chain bile acid-based polymers. The step-growth polymerization was used to prepare two important classes of polymers used in textile fibers, polyamides and polyesters.

Heterofunctional bile acid-based monomers were synthesized and used in order to overcome stoichiometric imbalances during step-growth polymerization. The lithocholic acid derivative bearing amine and protected carboxylic functional groups was polymerized in bulk at high temperatures, yielding polyamides that were poorly soluble in common organic solvents. Soluble triazole-linked polyamides and polyesters were obtained when the cholic acid derivative bearing azide and alkyne functional groups was polymerized under mild conditions via copper(I)-catalyzed azide-alkyne cycloaddition. Two different catalytic systems, copper(I) bromide and copper(II) sulfate, were tested. Only copper(I) bromide proved to be an effective catalyst for the system, allowing the synthesis of the polymers with a degree of polymerization of ca. 50 and an unimodal molecular weight distribution (PDI < 1.7). The main-chain cholic acid-based polymers are thermally stable (307 °C ≤ T_d ≤ 372 °C) with high glass transition temperatures (137 °C ≤ T_g ≤ 167 °C) and Young's moduli in excess of 280 MPa, depending on the chemical structure of the linker.

Keywords: bile acids, polycondensation, azide-alkyne cycloaddition, polyamides, polyesters

Résumé

La préparation de polymères à base d'acides biliaires, molécules biologiques, a attiré l'attention des chercheurs en raison des applications potentielles dans les domaines biomédicaux et pharmaceutiques. L'objectif de ce travail est de synthétiser de nouveaux biopolymères dont la chaîne principale est constituée d'unités d'acides biliaires. La polymérisation par étapes a été adoptée dans ce projet afin de préparer les deux principales classes de polymères utilisés en fibres textiles: les polyamides et les polyesters.

Des monomères hétéro-fonctionnels à base d'acides biliaires ont été synthétisés et utilisés afin de surmonter le déséquilibre stœchiométrique lors de la polymérisation par étapes. Le dérivé de l'acide lithocholique modifié par une fonction amine et un groupement carboxylique protégé a été polymérisé en masse à températures élevées. Les polyamides obtenus sont très peu solubles dans les solvants organiques. Des polyamides et des polyesters solubles en milieu organique ont pu être obtenus dans des conditions modérées en utilisant l'acide cholique modifié par des groupements azide et alcyne. La polymérisation a été réalisée par cycloaddition azoture-alcyne catalysée par l'intermédiaire du cuivre(I) avec deux systèmes catalytiques différents, le bromure de cuivre(I) et le sulfate de cuivre(II). Seul le bromure de cuivre(I) s'est avéré être un catalyseur efficace pour le système, permettant la préparation des polymères avec un degré de polymérisation égale à 50 et une distribution monomodale de masse moléculaire (PDI < 1.7). Les polymères synthétisés à base d'acide cholique sont thermiquement stables (307 °C ≤ T_d ≤ 372 °C) avec des températures de transition vitreuse élevées (137 °C ≤ T_g ≤ 167 °C) et modules de Young au-dessus de 280 MPa, dépendamment de la nature chimique du lien.

Mots-clés: acide biliaire, polycondensation, cycloaddition azoture-alcyne, polyamides, polyesters

Table of contents

List of tables

List of figures

List of symbols and abbreviations

ATRP	atom transfer radical polymerization
ATR	attenuated total reflectance
BisGMA	2,2-bis(4-(2-hydroxy-3-methacryloxypropoxy) phenyl)propane
Bpy	2,2'-bipyridine
BSA	bovine serum albumin
CA	cholic acid
CAC	critical aggregate concentration
CDA	chenodeoxycholic acid
$CHCl_3$	chloroform
CuAAC	copper(I)-catalyzed azide-alkyne cycloaddition
DCA	deoxycholic acid
DCC	N,N'-dicyclohexylcarbodiimide
DCM	dichloromethane
DIPC	diisopropylcarbodiimide
DIPEA	N,N-diisopropylethylamine
DMA	dynamic mechanical analysis
DMAP	4-(dimethylamino)pyridine
DMSO	dimethyl sulfoxide
DMF	N,N-dimethylformamide
DSC	differential scanning calorimetry
E	storage modulus
E'	Young’s modulus
EDC·HCl	1-ethyl-3-(3-dimethylaminopropyl)carbodiimide hydrochloride
ED-ROP	entropy-driven ring-opening polymerization
ED-ROMP	entropy-driven ring-opening-metathesis polymerization
EG	ethylene glycol
Et_3N	thriethylamine

FTIR	Fourier transform infrared spectroscopy
g	gram
GCA	glycocholate
GPC	gel permeation chromatography
h	hour(s)
HCA	hydroxycinnamic acid
HOBt	1-hydroxybenzotriazole monohydrate
HRMS	high-resolution mass spectrometry
Hz	Hertz
LCA	lithocholic acid
LCST	lower critical solution temperature
M	molar per litre
mg	miligram
mL	millilitre
mmol	millimole
M_n	number-average molecular weight
MPEG	methoxy poly(ethylene glycol)
MsCl	methanesulfonyl chloride
M_w	weight-average molecular weight
NIPAM	N-isopropylacrylamide
nm	nanometer
NMR	nuclear magnetic resonance spectroscopy
OEG	oligo(ethylene glycol)
PAGE	poly(allyl glycidyl ether)
PDI	polydispersity index
PEG	poly(ethylene glycol)
Ph_3P	triphenylphosphine
PMDETA	N,N,N',N',N''-pentamethylethylenetetramine
PNIPAM	poly(N-isopropylacrylamide)

ppm	part per million
PTSA	p-toluenesulfonic acid
Py	pyridine
SA	sodium ascorbate
T_g	glass transition temperature
T_d	decomposition temperature
TCA	taurocholate
TGA	thermogravimetric analysis
THF	tetrahydrofuran
TLC	thin layer chromatography
TMDP	trimethylene dipiperidine
TsCl	4-toluenesulfonyl chloride
UDMA	1,6-bis(methacryloyloxy-2-ethoxycarbonylamino)-2,4,4-trimethylhexane

"In the middle of difficulty lies opportunity"
Albert Einstein

Acknowledgements

First of all, I would like to thank Prof. Zhu for giving me a great opportunity to join his team, for his help and support during my educational journey at the Université de Montréal. I also thank him for letting me work independently, which helped me to progress as a student and a scientist.

I thank Sylvain Essiembre, Pierre Ménard-Tremblay, Cédric Malveau, Antoine Hamel and Geneviève Beaudry-Dubois for training me on the instruments used for polymer characterizations.

I would like to thank all my colleagues and friends. I thank Kim for sharing with me her professional experience and baking chocolate cookies. I thank Gwen for taking care of the chemical orders and other things in the lab, which made work in the lab efficient and pleasant. I thank Anna for her help with the fiber cutter.

Finally, I wish to give my deepest thanks to Rodolphe and my family in Ukraine. I thank Rodolphe for his constant and endless love, care, and support. It is hard to find enough words to express how much I appreciate your presence in my life and giving it even more sense and motivation than before. I thank my dearest mother for her countless sacrifices and for always believing in me.

1 Introduction

Biomaterials play an important role in medicine and biotechnology.[1] Due to the growing demands for tissue and organ transplants, tissue engineering has attracted much attention over the last few decades. Materials are required to have appropriate mechanical properties, not to cause excessive immune responses, to be non-toxic, biocompatible, and sometimes biodegradable with degradation products that can be readily absorbed or excreted.[2] However, the choice of biomaterials is still limited.

Both natural and synthetic biopolymers have been used as biomaterials.[3] Biopolymers are often limited by their poor stability, inappropriate mechanical properties; and possibility of triggering immune responses.[2,4-9] It is necessary to modify the chemical structures of natural polymers to improve their mechanical properties, degradation and biocompatibility.[7, 10]

We have used natural compounds such as bile acids in the preparation of various polymers intended for biomedical and pharmaceutical applications. These include polymers with bile acids as end groups,[11] pendant groups[12, 13] or in the main chain,[14, 15] and as the core of star-shaped polymers.[16, 17] Materials derived from bile acids can maintain some of their properties, including biocompatibility, high stability of the steroid skeleton, amphiphilicity and chirality, and self-assembly capacity that are valuable for biomedical, pharmacological and supramolecular applications.[18, 19]

1.1 Bile acids

Bile acids are important steroidal compounds that are stored in the gallbladder and they aid in the digestion of food in the gastro-intestinal tract of animals. They form micelles with lipids/fats/cholesterol in the intestine to enable fat digestion and they are present in large quantities also in the human body (~ 250 g). Only two primary bile acids, cholic acid (CA) and chenodeoxycholic acid (CDCA), are biosynthesized from cholesterol in the human liver (Figure 1.1).[20 21]

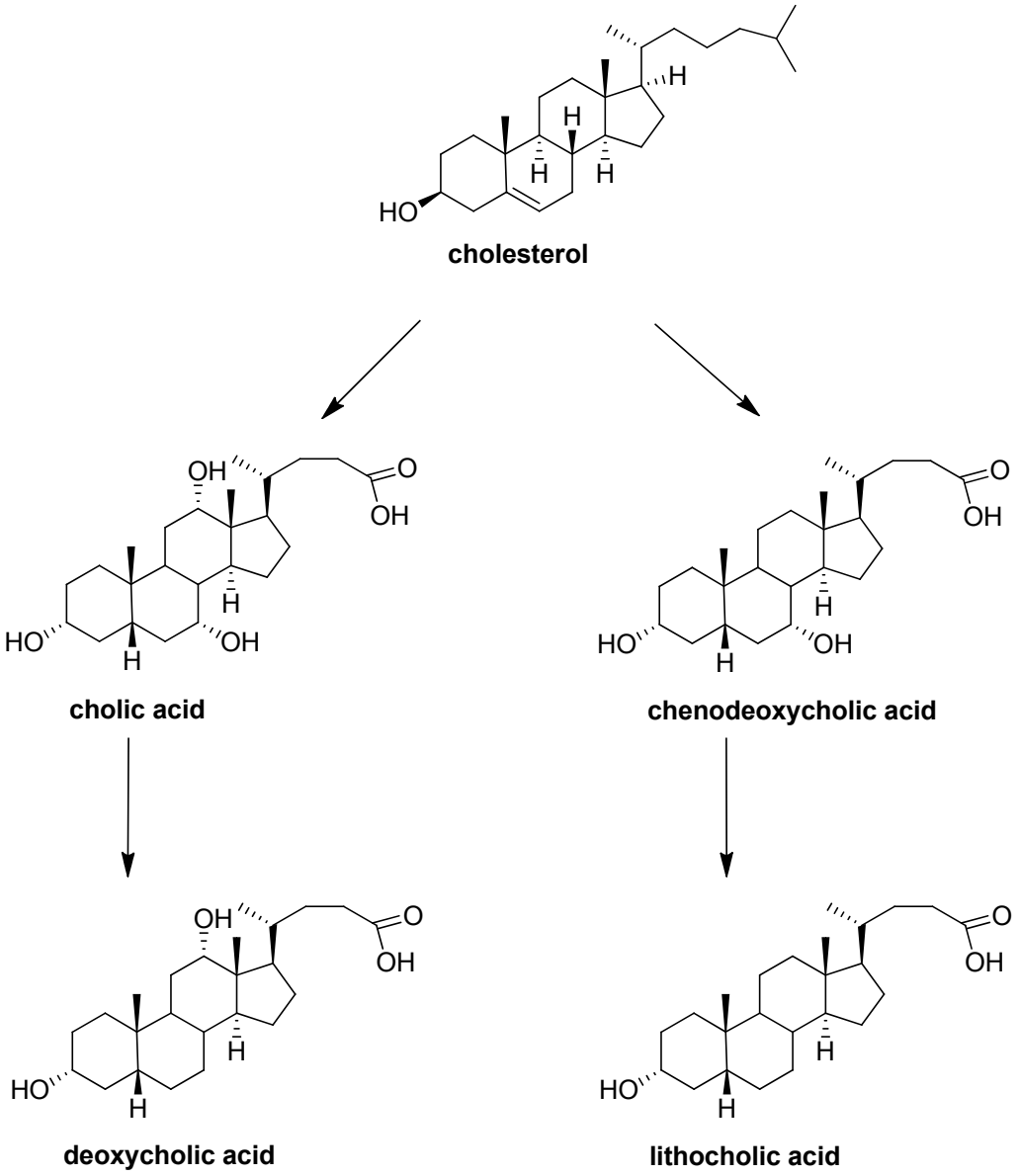

Figure 1.1: Conversion of cholesterol into the primary and secondary bile acids.

The primary bile acids are converted into secondary bile acids, deoxycholic acid (DCA) and lithocholic acid (LCA), by intestinal bacteria (Figure 1.1).[22, 23] The bile acids are almost completely absorbed from the intestine, after which they recirculate to the liver

via the portal vein. This process is called enterohepatic circulation, which happens 6-15 times per day, and is an important factor in serum cholesterol homeostasis.[18] Reduced biosynthesis of bile acids can cause the precipitation of cholesterol in the gallbladder and the formation of gallstones. Bile acids are conjugated with an amino acid, either glycine (75 %) or taurine (25 %), and they often exist as bile salts.[20] The most abundant bile salt in humans is cholate. The average bile acid pool of healthy human adults contains 38-40 wt% cholate conjugates, 35 wt% chenodeoxycholate conjugates, 25 wt% deoxycolate conjugates and 1-2 wt% lithocholate conjugates, as shown in Table 1.1.[24]

All bile acids possess a rigid steroid skeleton and an aliphatic side chain. The steroid nucleus of bile acids has a saturated tetracyclic hydrocarbon perhydropentanophenanthrene, containing three six-member rings and a five-member ring, where the cis connection between rings A and B imparts a curvature to the steroid skeleton, making possible the formation of a cavity. The hydroxyl groups are directed to one side to form a hydrophilic face with the carboxyl group at the C24-position. The other face is hydrophobic where three methyl groups are present.[25] Therefore, bile acids can form micelles induced by back-to-back hydrophobic interactions.[26, 27]

Bile acids also possess several chiral centers. The modification of hydroxyl and carboxylic groups of bile acids can give rise to a diverse range of bile acid-based compounds. The carboxylic acid group may be esterified, reduced, amidated or subjected to salt formation with metal ions, alkaloids or organic bases.[20, 28] Cholic acid has three OH groups which exhibit very different reactivities depending on their locations at the steroid skeleton. The reactivity of hydroxyl groups towards oxidation is 7-OH > 12-OH > 3-OH. The order of acelylation, hydrolysis, reduction, or hydrogenation is 3-OH > 7-OH > 12-OH.[29] Moreover, the hydroxyl group at C3-position is more reactive than the more sterically hindered OH groups at axial C7- and C12-positions.

Due to their natural abundance and unique chemical structure, bile acids are the candidate of choice for designing and modulating the properties of synthetic biomaterials with bile acids as end groups,[11] pendent groups[12, 13] or in the main chain,[30, 31] and star-shaped polymers with bile acids as the core.[16, 17]

Table 1.1: The most important bile acids and their amino acid conjugates.

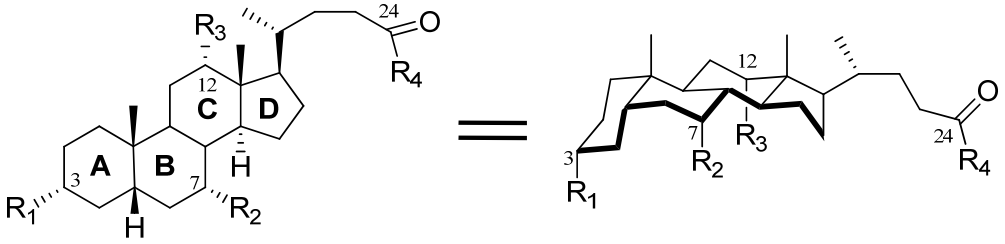

Bile acid	abbrev.*	R_1	R_2	R_3	R_4	% in bile
Chenodeoxycholic acid	CDA	OH	OH	H	OH	Trace
Glycochenodeoxycholate	GCDA	OH	OH	H	$NHCH_2CO_2^-$	30
Taurochenodeoxycholate	TCDA	OH	OH	H	$NHCH_2CH_2SO_3^-$	5
Cholic acid	CA	OH	OH	OH	OH	Trace
Glycocholate	GCA	OH	OH	OH	$NHCH_2CO_2^-$	30
Taurocholate	TCA	OH	OH	OH	$NHCH_2CH_2SO_3^-$	10
Deoxycholic acid	DCA	OH	H	OH	OH	Trace
Glycodeoxycholate	GDCA	OH	H	OH	$NHCH_2CO_2^-$	15
Taurodeoxycholate	TDCA	OH	H	OH	$NHCH_2CH_2SO_3^-$	10
Lithocholic acid	LCA	OH	H	H	OH	Trace
Glycolithocholate	GLCA	OH	H	H	$NHCH_2CO_2^-$	1-2
Taurolithocholate	TLCA	OH	H	H	$NHCH_2CH_2SO_3^-$	

* Abbreviation

1.2 Polymeric materials containing bile acids

1.2.1 Bile acid as an end-group on the polymer chain

Bile acids were attached to polymers, often poly(ethylene glycol) (PEG), bearing reactive end groups, such as OH and NH_2. Deoxycholic acid end-capped PEG polymers were synthesized. They formed spherical micelles in aqueous media.[11] Similar core-shell

type nanoparticles were observed for cholic acid-based PEG conjugates (Figure 1.2).[32] When three hydrophobic deoxycholic acid molecules were attached to one end of methoxy poly(ethylene glycol) (MPEG) smaller spherical micelles were formed in water and a lower critical aggregation concentration (CAC) value was obtained than those of monosubstituted ones due to the increased hydrophobicity.[33] It was shown that these micellar systems might be suitable as delivery system of bioactive agents.[32, 33]

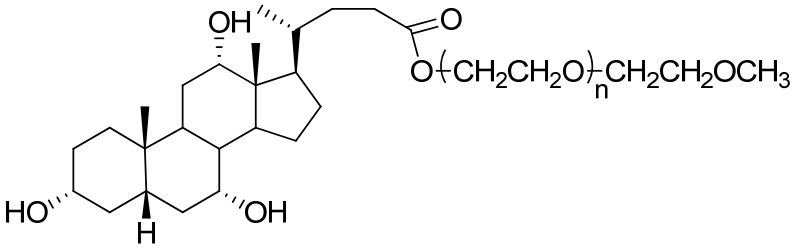

Figure 1.2: MPEG end-capped with cholic acid.

Cho et al.[34] reported the preparation and characterization of novel nanocarriers for liver specific drug targeting. Diamine-terminated PEG with a galactose moiety from lactobionic acid was conjugated with cholic acid. Spherical nanoparticles were observed by transmission electron microscopy.

Li et al.[35] demonstrated a novel method to prepare narrowly-dispersed silver nanoparticles using a hydrogel of PEG 400 end-modified with cholic acid. Other examples of well-known thermoresponsive polymers, such as poly(*N*-isopropylacrylamide) (PNIPAM), were modified with cholic acid at one terminus. The drug release from CA-PNIPAM thermoresponsive micelles may be applied to a site-specific drug delivery system by modulating the temperature of the target site.[36]

1.2.2 Bile acid as the core of star-shaped polymers

The cholic acid was used as a hydrophobic core for star-shaped polymers. Zhuo et al. have prepared such polymers using cholic acid as an initiator for ring-opening polymerization of DL-lactide[16, 37-39] and ε-caprolactone.[40-42] Cholic acid-functionalized star

oligo/poly(DL-lactide)s or star oligo/poly(ε-caprolactone)s (Table 1.2, **1a** and **1b**) showed faster hydrolytic degradation rates[16, 41] compared to linear homopolymer poly(DL-lactide) or poly(ε-caprolactone). The degradation mechanism changed from bulk erosion to surface erosion with decreasing molecular weight.[16] They had both improved cell adherence and proliferation,[39, 41] which are useful as drug carriers[37, 40] and gene delivery.[38]

Table 1.2: Star-shaped polymers with cholic acid as a core.

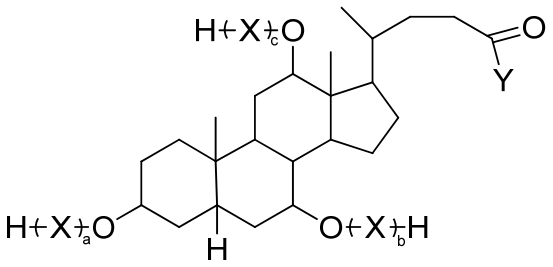

	X	Y
1a	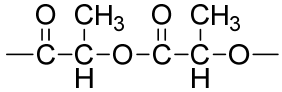	OH a+b+c=m=15, 30, 60 or 120
1b	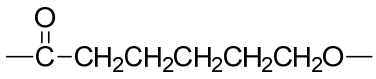	OH a+b+c=m=20, 40, 80 or 160
1c	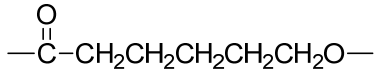	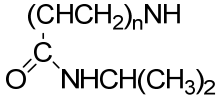 a+b+c=m=20 or 40
1d	—CH_2CH_2O—	$NH(CH_2CH_2O)_{d+1}H$ a=b=c=d=5, 10, 15, 30, 50 or 75
1e	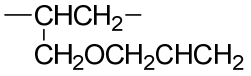	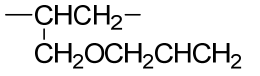 a=b=c=d=5, 10 or 15

Also, Zhou et al.[42] prepared "intelligent" drug delivery system of star-shaped copolymers, comprised of a thermoresponsive PNIPAM segment and three hydrophobic poly(ε-caprolactone) arms using the same synthetic approach. The amphiphilic star-shaped copolymers were capable of self-assembling into spherical micelles in water at room temperature (Table 1.2, **1c**).

In order to better control the length of branches and polydispersity (PDI) of star-shaped polymers, atom transfer radical polymerization (ATRP)[43] and anionic polymerization[17, 44-46] were used by our group. The grafting of PEG chains of different lengths onto the cholic acid core was successfully achieved by anionic polymerization of ethylene oxide (EO), providing star polymers with very low PDI. The PEGylated cholic acid derivatives (Table 1.2, **1d**) formed spherical micellar aggregates in water, providing an interesting reservoir for hydrophobic compounds that may be useful as drug delivery vehicles.

The hydroxyl group of PEG end-chains may be further modified to introduce other functional groups for different applications.[44] Star-polymers derived from cholic acid with poly(allyl glycidyl ether) (PAGE) arms were also prepared via anionic polymerization, yielding polymers with well-defined molecular weight and low PDI (Table 1.2, **1e**). Because of the strong hydrophobicity of PAGE chains, the $CA(AGE_n)_4$ star polymers were not soluble in water. The double bonds of the allyl groups on the polymer chain were used to introduce either amine or carboxylic acid groups for obtaining amphiphilic polymers with cationic and anionic groups, respectively. These had interesting thermoresponsive properties in water over a wide range of temperatures (5-75 °C).[17]

The length of the polymer chains was shown to have a strong effect on the polymer aggregation. The amphiphilic properties of these materials and their aggregation may be useful for potential pharmaceutical applications.[17, 43, 44] Recently, our group reported the synthesis of new star-shaped polymers having cholic acid as a core and four branches of PAGE and PEG block copolymers via anionic polymerization.[46] The introduction of PAGE segments into $CA(PEG)_4$ significantly reduced their crystallinity, while displaying two step transition, depending on the length of the PEG blocks.

1.2.3 Bile acid as a cross-linker

Multifunctional monomers may serve as crosslinking reagents in polymeric gels and solid materials. A modern trend in the design of new dental materials is to use natural compounds in order to improve biocompatibility.[47] Cholic acid derivatives with multiple methacrylate groups were prepared in a controlled way by using methacrylic acid, methacryloyl chloride, and methacryloyl anhydride as acylating agents (Figure 1.3).[48]

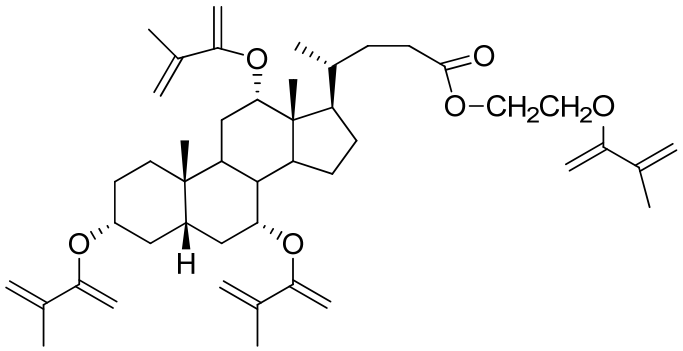

Figure 1.3: Structure of cholic acid-based compound bearing four methacrylate groups.

Di-, tri-, and tetra-methacrylate derivatives of bile acids (Figure 1.3) showed lower polymerization shrinkage, improved mechanical properties at high temperatures, and significantly less cytotoxic than common dental monomers (with no effect on cell viability over their entire range of solubility). Potential final biodegradation products also displayed lower cytotoxicity than 2,2-bis(4-(2-hydroxy-3-methacryloxypropoxy) phenyl)propane (BisGMA) or 1,6-bis(methacryloyloxy-2-ethoxycarbonylamino)-2,4,4-trimethylhexane (UDMA).[49, 50]

1.2.4 Bile acid as a pendant group from the polymer chain

The hydroxyl groups of bile acids can be modified for directly introducing vinyl groups or via a spacer, leading to polymers having bile acids as pendant groups. These polymers can be prepared using radical polymerization techniques. However, the bile acid

can be also grafted to the main-chain polymers that have reactive groups, such as OH or NH_2, through coupling reactions with the carboxyl group of bile acids.

Methacryloyl groups can be attached to cholic acid derivatives via the OH group at the C3-position without protection at C7- and C12- hydroxyl groups because of the higher reactivity of the OH at the C3-position (Figure 1.4). The carboxylic group at the C24-position must be protected with a methyl ester to avoid side attacks and to increase the solubility of the monomer.

Cholic acid-based polymers were prepared by free-radical polymerization in solution from 3α- and 3β-methacrylate and methacrylamide derivatives of cholic acid (Figure 1.4, **2a** and **2b**).[51] After the selective hydrolysis of methyl ester protecting groups, without affecting the methacrylic ester or amide bond, the hydrophilicity of the cholic acid-based polymers increased. Amphiphilic polymers made from the methacrylic derivatives of cholic acid **2a** can assemble into fibrils of 1 nm in diameter and they can further bundle into lamella plates in aqueous media.

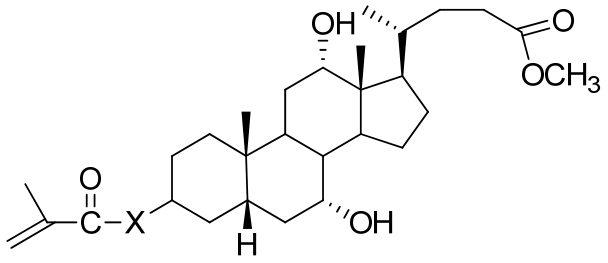

2a	X = O
2b	X = NH
2c	X = $(OCH_2CH_2)_nO$; n=0, 1, 2, 4, 6

Figure 1.4: The chemical structures of 3-methacryloyl cholic acid derivatives.

After immersing the fibrils into simulated body fluid with ion concentrations equivalent to those of human plasma, plate-like single crystals of hydroxyapatite formed on the surface of the polymer fibril assembly. These may be useful in the matrix design of biomimetic mineralization and in the development of scaffold materials for hard tissue engineering.[12]

In addition, a cholic acid-containing polymer was prepared by a hybrid imprinting method involving the use of a template-containing monomer **2a**.[52] The high selectivity for cholic acid binding originates from imprinting with templates of a certain shape and certain spatial arrangement of functional groups via hydrogen bonding.

Furthermore, random copolymers of methacrylic monomers **2a** with styrene,[53] and **2a** and **2b** with monomers of higher hydrophilicity, such as methacrylic acid and 2-hydroxyethyl methacrylate, were successfully synthesized.[54, 55] In order to improve the hydrophilicity of bile acid-containing polymers, EG and OEG spacers between cholic acid and methacrylate residues of different lengths were incorporated into the structure of bile acid-based polymers (Figure 1.4, **2c**).[56] Water absorption tests showed the hydrophilicity of the polymers was improved with increasing length of the OEG spacers. The copolymerization of monomer **2c** with N-isopropylacrylamide (NIPAM) leads to temperature- and pH-responsive polymers. The lower critical solution temperature (LCST) value of bile acid-based copolymers was lower than LCST value of NIPAM homopolymer, but it increased with longer OEG spacers and higher pH values and it decreased with higher content of bile acid-based monomers.[57]

Roh et al.[58] introduced cholic acid and deoxycholic acid as pendant groups into norbornene and maleic anhydride copolymers in order to obtain photoresist materials (Figure 1.5, **3**). The polymer had an excellent transmittance at 193 nm and it possessed good thermal stability up to 255 °C.[58] Recently, our group reported copolymers of cholic acid-based nonbornene and triethylene glycol monomethyl ether nonbornene derivatives that were prepared by ring-opening metathesis polymerization (ROMP), having multishape memory properties (Figure 1.5, **4**). The polymers displayed good shape fixing and recovery in different thermal processing stages over the broad glass transition range.[13]

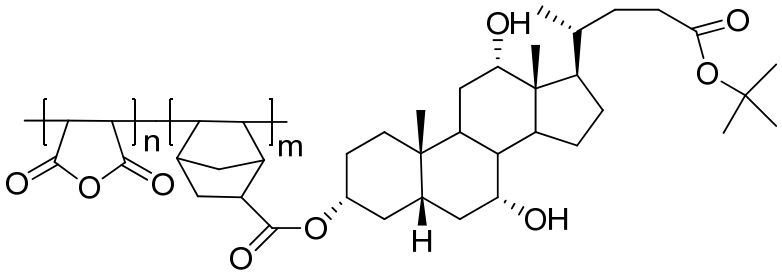

3

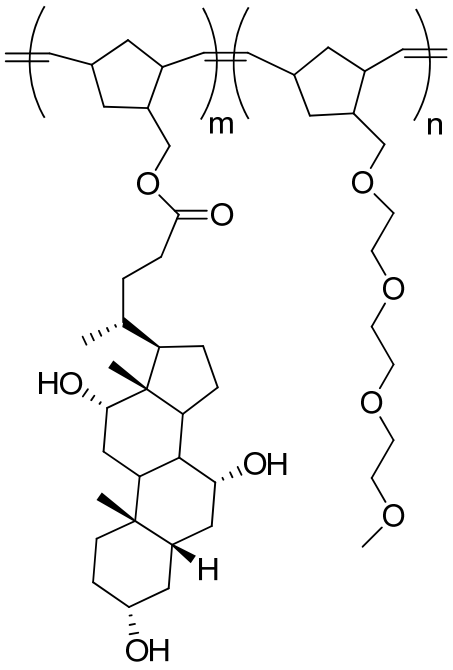

4

Figure 1.5: Chemical structures of copolymers based on norbornyl cholic acid derivatives.

Moreover, a cholic acid was modified with a methacryloyl group via spacer at the C24-position.[59-61] The synthesized monomers (Figure 1.6, **5a-c**) were then copolymerized with N-alkyl acrylamides. The cholic acid-based monomer **5a** was used to obtain a series of

crosslinked imprinted polymers.[59] The copolymerization of **5b** with NIPAM leads to water-soluble and temperature-responsive materials.[60]

The synthesis of a comb-shaped cholic acid-containing polymer **5c** by ATRP was reported by Zhu et al.[61] for the first time. The formation of the comb-shaped polymer was evidenced by the semicrystalline nature and high glass transition temperature (T_g) of the polymer.

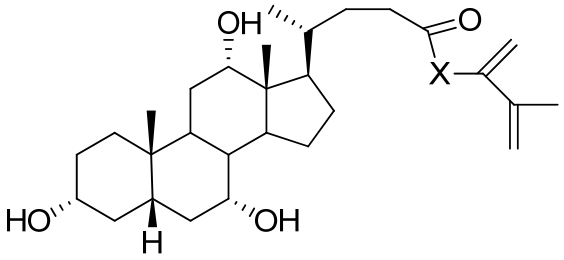

5a X = $NH(CH_2)_6O$

5b X = $NHCH_2CH_2NH$

5c X = $(OCH_2CH_2)_3O$

Figure 1.6: The chemical structures of 3-methacryloyl cholic acid derivatives.

Bile acids can also be attached through the COOH groups at the C24-position of polymers bearing reactive groups, such as OH or NH_2. Low degrees of substitution (5-15 %) were attempted in order to study the self-aggregation of these new water-soluble amphiphilic polymers.[28] Many different natural biopolymers were modified with bile acids, such as polysaccharides (dextran,[62-65] chitosan,[66-68] glycol chitosan,[69-72] heparin[73] or cellulose[74]) and proteins (bovine serum albumin, BSA).[75]

Cholic acid and deoxycholic acid, or their conjugates with amino acids, were covalently bound to dextran through the ester linkage, using N,N'-dicyclohexylcarbodiimide (DCC) as the coupling reagent and 4-(dimethylamino)pyridine (DMAP) as a catalyst.[62, 63] Modified dextran polymers with good surface-active properties and foaming capacities self-assembled to form aggregates in water.[62] In order to avoid the

use of carbodiimide coupling reagents, dextran was oxidized to dextran dialdehyde by sodium periodate, which was then conjugated with cholic acid hydrazide through an acyl hydrazide linkage (Figure 1.7).[64, 65]

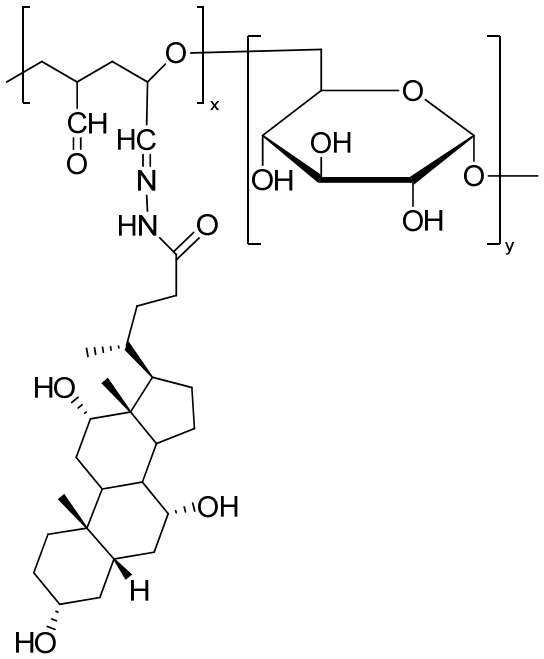

Figure 1.7: Polymers formed by conjugation of cholic acid hydrazide and dextran dialdehyde.

These hydrophobically modified dextrans showed low CAC, depending on both the degrees of oxidization and substitution and they aggregated into nanometer-sized spheres having a hydrophobic core and a hydrophilic shell in aqueous media. The size of the nanoparticles depended on the pH of the medium due to the aldo–enol transition of the dextran dialdehyde. The nanoparticles were stabilized by crosslinking the surface aldehyde groups with adipic dihydrazide. The drug-loading and release behavior of indomethacin was not affected by the crosslinking. However, it decreased the drug release rate from nanoparticles.[65]

Bile acids were also grafted to chitosan[66-68] and glycol chitosan[69-72] in order to improve the hydrophibicity of the polymers. Chitosan was made hydrophobic by modifying

the deoxycholic acid (Figure 1.8), formed colloidally stable self-aggregates in water above the CAC, depending on the degree of substitution with bile acid.[67] These polymers may be useful for anticancer drug release and DNA delivery.[68]

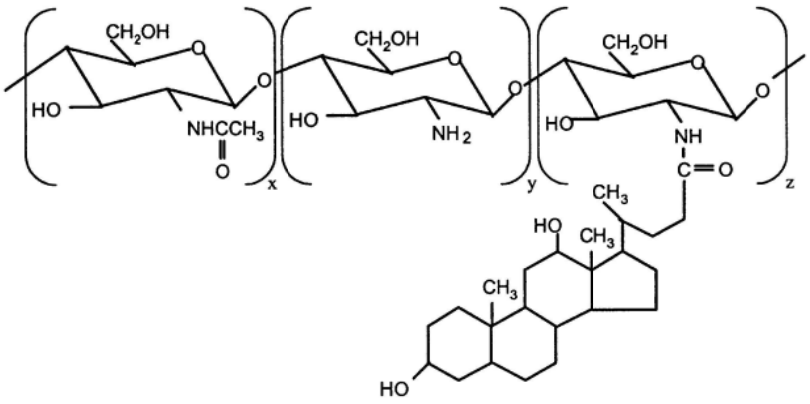

Figure 1.8: Chemical structure of deoxycholic acid-modified chitosan.[68]

In order to improve the stability of aggregates, more hydrophilic compounds were used when 5β-cholanic acid was attached to the glycol chitosan.[69] The size of the self-aggregates depended on the degree of substitution. These nanoparticles can be used as drug carriers and gene-delivery.[70, 72]

1.2.5 Bile acids in the polymer main chain

Although a variety of polymers based on bile acids have been synthesized, the synthesis of main-chain bile acid-based polymers is still challenging. Polycondesation is often used to prepare these polymers.[14, 76-83] High-molecular weight main-chain bile acid-based polyesters were synthesized using *p*-toluenesulfonic acid (PTSA) as the catalyst at high reaction temperatures. Thus, branched low molecular weight polymers were obtained with deoxycholic and cholic acids and they had a poor solubility in common organic solvents.[76]

In order to overcome these issues, milder polymerization conditions were applied. Wagener et al.[14] used diisopropylcarbodiimide (DIPC) and catalytic amounts of a 1:1

mixture of DMAP and PTSA at room temperature to polymerize lithocholic, deoxycholic and cholic acids selectively only at the C3-position of the steroid skeleton (Figure 1.9).

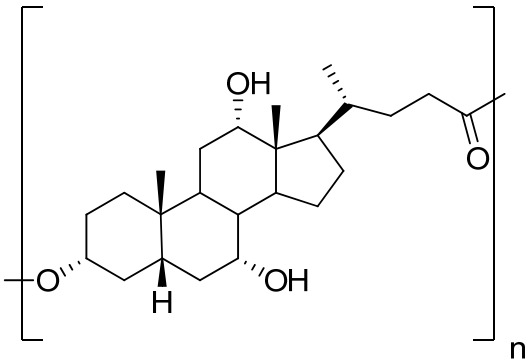

Figure 1.9: Main-chain cholic acid-based polyesters.

This methodology allowed the synthesis of linear, uncrosslinked lithocholic acid- and deoxycholic acid-based polyesters of moderate molecular weight (59 000 and 64 000 $g \cdot mol^{-1}$, respectively). However, a low molecular weight of ~ 2 800 $g \cdot mol^{-1}$ was obtained for cholic acid-based polymers. These polymers showed partial crystallinity and high thermal stability up to 380 °C.

Using a different synthetic strategy with a lipase enzyme, Noll and Ritter[77] synthesized unbranching cholic acid-based oligomers. Under similar conditions, the oligocondensation in the presence of 1,1-methacryloylaminoundecanoic acid was performed that yielded a polymerizable methacrylic monomer (Figure 1.10).

Another recent attempt to synthesize cholic acid- and deoxycholic acid-based polyesters via polycondensation reactions with 3-succinoylloxy-derivatives was reported by Simionescu and co-workers.[78] As reported previously,[14] they obtained polyesters with high-temperature stability and low degrees of crystallinity (25-30 %).

Lithocholic acid-based polyanhydrides were firstly reported by our group (Figure 1.11).[79] Biodegradable polyanhydrides were prepared from 3α-lithocholic acid dimers. These polymers were synthesized by linking two lithocholate methyl ester molecules with

sebacoyl chloride,[79, 81] subsequent selective hydrolysis of the methyl ester, activation by refluxing with acetic anhydride, and finally polymerization with sebacic acid.

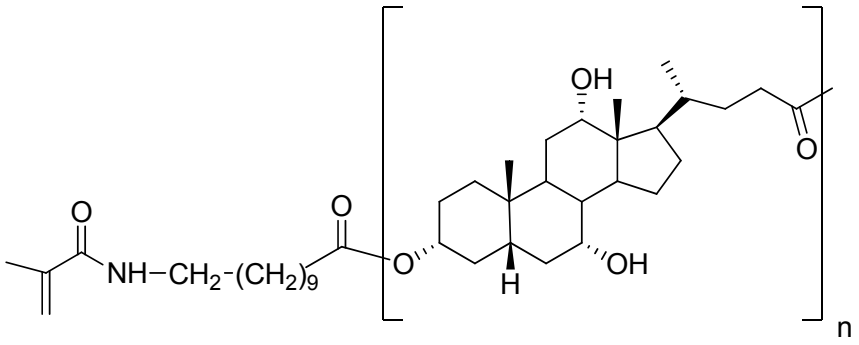

Figure 1.10: 11-Methacryloylaminoundecanoic acid oligo(cholic acid ester).

The polymer properties were controlled by adjusting the comonomer content during the polymerization. When the proportion of sebacic acid increased from 0 to 90 %, the glass transition temperature (T_g) dropped from 85 to 13 °C, meanwhile the melting temperature increased from 63 to 77 °C as the content of sebacic acid increased from 50 to 90 % and ~ 250 °C for lithocholic acid-based homopolymer. In addition, the degradation study showed an increase of nearly 20 times in degradation rate when the sebacic acid content reached 90 %.[79]

Alternatively, Domb et al.[82] obtained lithocholic acid-based polyanhydrides by using lithocholic acid and oligo(sebacic anhydride) prepolymer as a starting material to form a diacid. Polycondensation of the diacid activated with acetic anhydride and different amounts of oligo(sebacic anhydride) prepolymer yielded polymers with high molecular weights (up to 70 000 $g \cdot mol^{-1}$). It was found that the polymer melting temperatures increased from 54 to 112 °C with increasing the lithocholic content from 10 to 70 %.

In 2005, Akashi's research group[83] reported the copolymerization of lithocholic acid and hydroxycinnamic acid (HCA) in bulk at high temperature (~ 200 °C), using acetic anhydride and sodium acetate as the coupling agent and catalyst, respectively, affording lithocholic acid-based oligomers.

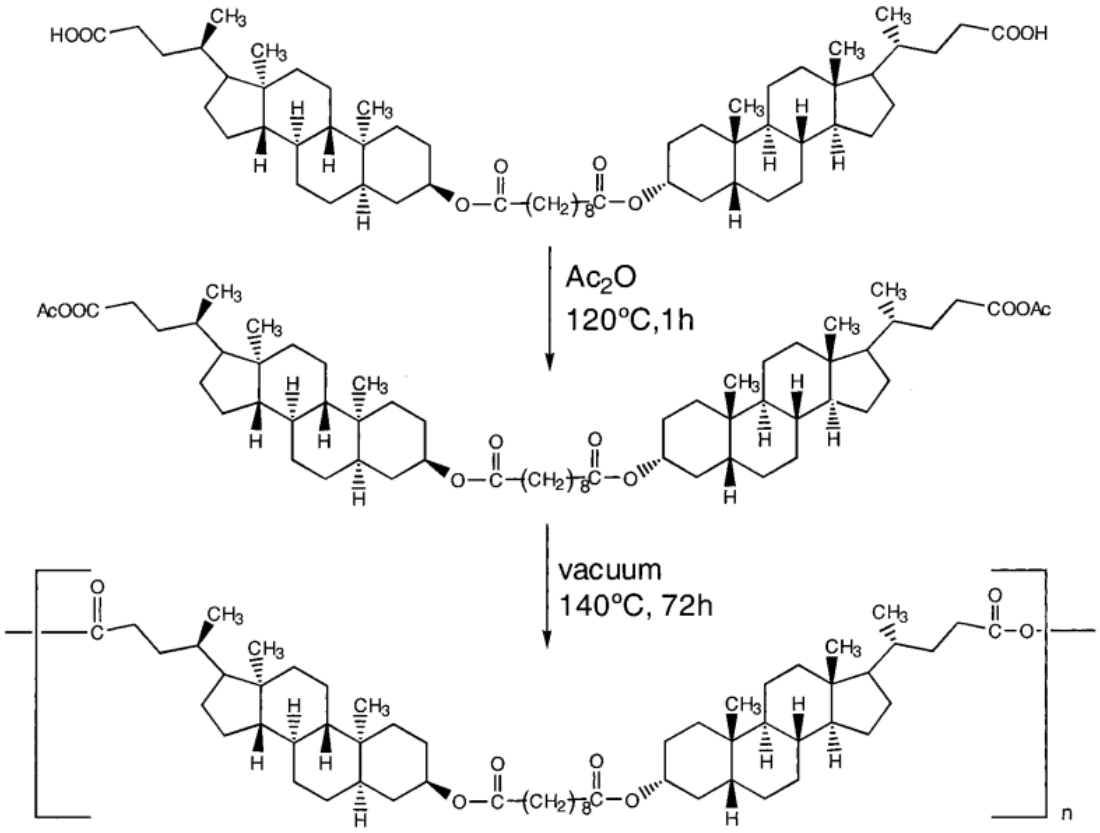

Figure 1.11: Synthetic scheme of lithocholic acid-based polyanhydride from dimers.[79]

When the lithocholic acid molar fraction of poly(HCA-co-LCA)s was 45 mol % and lower, copolymers had a nematic liquid crystalline phase. Moreover, spin-coated films of these copolymers showed high cell adhesion properties caused by high molecular hexagonal orientation.

In order to prepare bile acid-based polymers with a high molecular weight and low PDI, our group tried the entropy-driven ring-opening-metathesis polymerization (ED-ROMP) technique with the second generation Grubbs catalyst.[15, 30, 84] ED-ROMP appears to be a method of choice for the synthesis of high-molecular-weight polyesters based on bile

acids.[85] Furthermore, with this synthetic method, the utilization of large amounts of coupling agents and catalyst are not required. This lowers the toxicity of the material.

Lithocholic acid-based polyesters (Figure 1.12) were obtained with high molecular weights (> 160 000 g·mol^{-1}) and glass transition temperatures below room temperature (12 ≤ T_g ≤ 20 °C). They also displayed typical rubberlike elasticity (1.2 ≤ E ≤ 2.1 MPa) with maximum elongations higher than 400 % at 37 °C.[30]

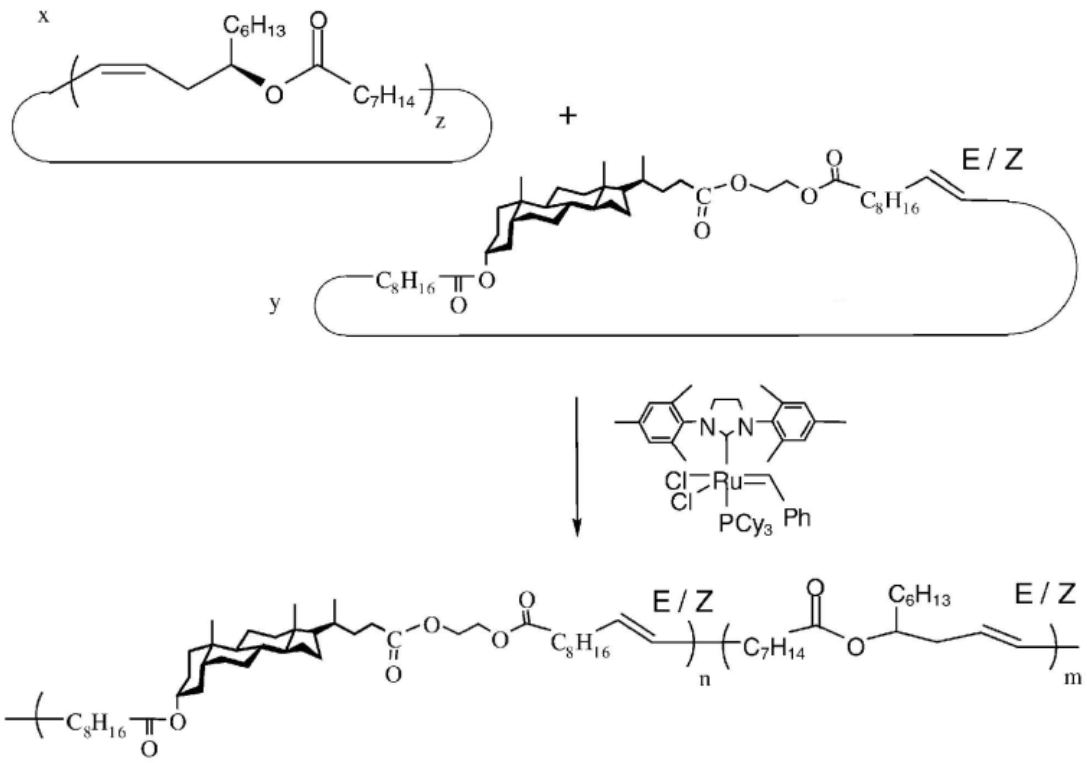

Figure 1.12: Synthesis of copolymers of lithocholic and ricinoleic acid using ED-ROMP.[84]

In order to tune the mechanical properties of lithocholic acid-based polyester, a series of mixed copolyesters of lithocholic and ricinoleic acid were synthesized with varying co-monomer ratios (Figure 1.12). When the ricinoleide composition was varied from 7.4 to 46

%, the T_g of the bile acid-based polyesters decreased from 11.2 to -23.7 °C, whereas the Young's modulus at 37 °C decreased.[84]

Using the same methodology, Gautrot and Zhu[15] also reported the synthesis of a series of lithocholic acid-based polyamides; cholic acid-based polyesters and polyamides; and their copolymers with recinoleic acid. These bile acid-based polymers displayed T_g ranging from 13 to 63 °C. The presence of hydroxyl groups in cholic acid-based polymers increased the T_g by about 35 °C. Similarly, the introduction of an amide bond into the polymer structure increased the T_g. The polymers behaved as typical elastomers with maximum elongations greater than 350-400 % and high-performance shape memory polymers in both warm and cold drawing modes. The copolymers of cholic acid and recinoleic acid displayed T_g near body temperature and retained their shape memory properties.[15] No crystallinity was observed, which is unusual for uncrosslinked polymers with shape memory properties. The shape memory properties of bile acid-based polymers may result from a combination of chain entanglements and the size of ordered domains.[86] Furthermore, it was shown that these degradable polymers are useful for the design of biomedical devices, such as all-polymeric stent grafts and smart suture materials.[15]

Although ED-ROMP is a powerful methodology for the synthesis of main-chain bile acid-based polymers of high molecular weight, the use of expensive Grubbs catalysts, the multistep synthesis of macrocyclic precursor from bile acids and high dilutions are required for successful synthesis in good yield. Therefore, Hodge et al.[87] recently applied lipase-catalyzed polymerization that was previously utilized for cholic acid by Noll and Ritter.[77] But, no polymer was obtained with unsubstituted lithocholic acid or its cyclic dimers and trimers. Nevertheless, the lipase-catalyzed entropy-driven ring-opening polymerization (ED-ROP) of larger lithocholic acid-based macrocycles gave polymers and copolymers in high yields.

Recently, Kulkarni and Gangwal[88] reported the synthesis of new low molecular weight biodegradable poly(β-amino esters) with deoxycholic acid in the polymer main chain. This was done by 1,4-addition of trimethylene dipiperidine (TMDP) to diacrylates of deoxycholyl glycol ester by Michael addition (Figure 1.13).

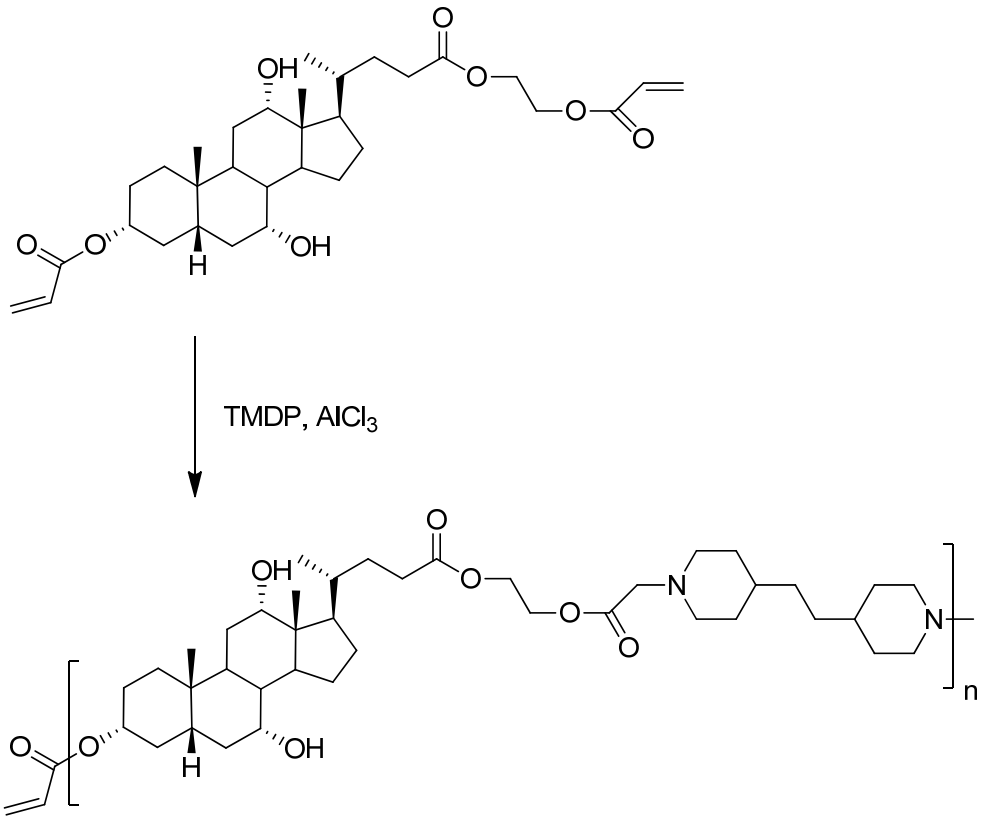

Figure 1.13: Synthesis of poly(deoxycholyl glycol TMDP β amino ester).

1.3 Synthesis of linear polymers by copper(I)-catalyzed azide-alkyne cycloaddition

The copper(I)-catalyzed azide-alkyne cycloaddition (CuAAC) often known as the 'click' reaction, was first reported in 2001 by Sharpless and coworkers (Figure 1.14).[89] This reaction is highly selective, tolerates a number of other functional groups, and in general, proceeds under mild conditions in high yields.

Polymers with different topologic structures, including linear, block, star polymers and dendrimers were synthesized with the 'click' reaction.[90] In step-growth polymerization, it allows the design of a new class of macromolecules with 1,4-disubstituted 1,2,3-triazole

within the repeating unit, among them photonically active, thermally stable and biologically compatible compounds.[91]

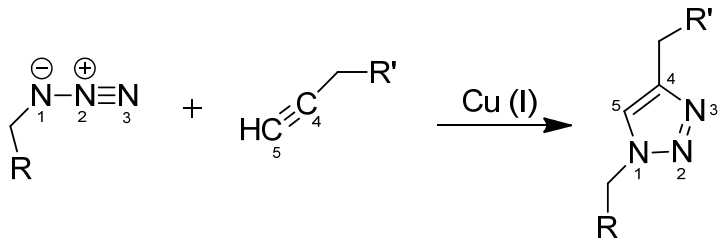

Figure 1.14: The copper(I)-catalyzed azide-alkyne cycloaddition reaction.

The step-growth polymerization of diazide and dialkyne monomers by CuAAC has been investigated.[92, 93] The catalyst often used is Cu(I), added as a salt or generated in situ by the reduction of $CuSO_4$ with sodium ascorbate (SA). The latter is preferred because of its lower cost, high purity of the active catalyst and stability towards oxygen.

For use in purely organic solvents, several different ligated copper species were prepared, making the system widely applicable. The addition of weak reducing agents to the reaction mixture renders the reaction much less susceptible to oxygen. The ligands used include triethylamine, 2,6-lutidine, and N,N-diisopropylethylamine (DIPEA), as well as N,N,N',N',N''-pentamethylethylenetetramine (PMDETA) or 2,2'-bipyridine (bpy) (Figure 1.15).

The main disadvantage of the step-growth polymerization of dialkyne and diazide monomers is the difficulty to achieve stoichiometry between antagonist 'click' functionalities. As a result, broad distributions of linear and cyclic chains of low molecular weights are often obtained. Therefore, heterofuctional monomers were also used for the synthesis of triazole-linked main-chain polymers.[94, 95]

Relatively high monomer concentrations (1 M) were employed in order to limit the formation of cyclic species.[95] More recently, Bernard et al.[96] synthesized linear starch-based polytriazoles with high glass transition ($T_g \geq 125$ °C) and decomposition ($T_d \geq 325$ °C) temperatures. The polymerization of two monofunctional monomers led to head-to-

head polymers. In contrast, the polymerization of heterofunctional monomers yielded head-to-tail polymers.[90]

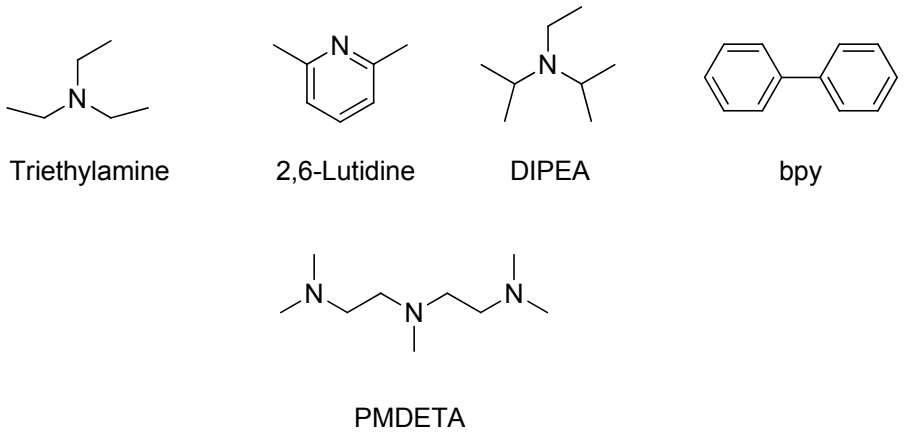

Figure 1.15: Effective ligands used to promote the Cu(I)-catalyzed triazole formation for polymer synthesis.

Looking for an alternative approach to obtain main-chain bile acid-based polymers with high molecular weight and low polydispersity, Pandey and coworkers[31] applied CuAAC. Both azide and alkyne functionalities were introduced into bile acids (Figure 1.16).

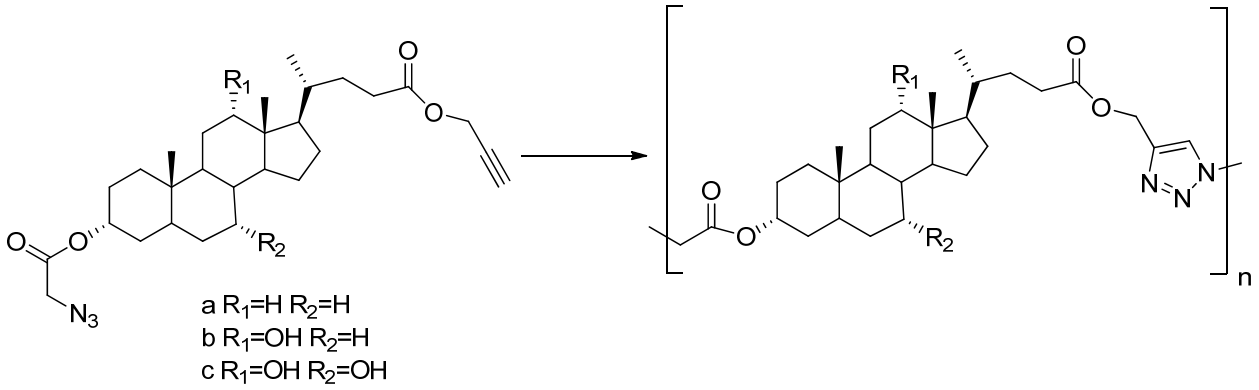

Figure 1.16: Main-chain bile acid-based polyesters synthesized via CuAAC.

The polymerization reaction of bile acid-based monomers with copper(II) sulfate and SA as the catalytic system gave regioselective 1,4-disubstituted 1,2,3-triazole containing polyesters with a low polydispersity (PDI ~ 1.3) and a molecular weight (M_n) of 75 000 $g \cdot mol^{-1}$ for lithocholic acid, 55 000 $g \cdot mol^{-1}$ for deoxycholic acid, and 27 000 $g \cdot mol^{-1}$ for cholic acid. These bile acid-based polyesters showed the capacity to stabilize silver nanoparticles. When the hydroxyl groups at the C7- and C12- positions were replaced with formyloxy groups, an oligomeric mixture was obtained with the similar reaction conditions.[97] Li et al.[98] reported that the bile-acid-based monomers (Figure 1.16) could form a well-defined rod single crystal. When the crystals were heated, the Huisgen cycloaddition between the azide and alkyne took place in the absence of copper(I)-catalyst, leading to higher molecular weight polymers (M_n ~ 70 000 - 113 000 $g \cdot mol^{-1}$). The nonregioselective polyaddition was shown by NMR in about 3:2 signal ratios for the 1,4- and 1,5-disubstituted 1,2,3-triazoles.

1.4 Objectives

The main objective of this work was to design and prepare new biopolymers with bile acids using step-growth polymerization. Different strategies and approaches were adopted to synthesize main-chain bile acid-based polymers with a variety of linkers, such as amides, esters, triazoles, urethanes, and imines (Figure 1.17), to explore the polymer properties and its uses. Because no such studies have been reported, the structure-property relationships, such as T_g, T_d, crystallinity, and solubility, were investigated as a function of the molecular weight, type of linker, and bile acid types.

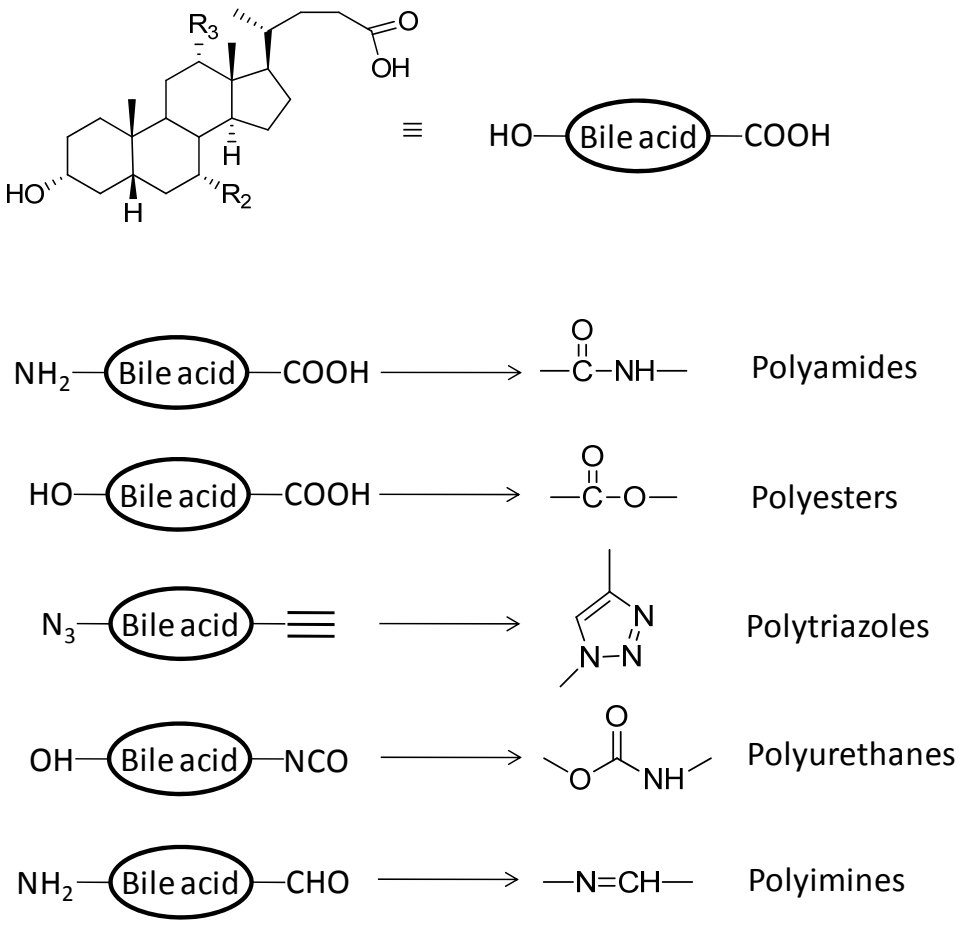

Figure 1.17: Strategies of step-growth polymerization

The syntheses involved the preparation of heterofunctional bile acid-based monomers. Until now, polycondensation has been the preferred synthetic method for preparing polyamides and polyesters. As an alternate, we prepared bile acid-based polymers via CuAAC using mild conditions.

2 Experimental part

2.1 Materials

Cholic acid (CA, 98%), lithocholic acid (LCA, 99 %), propargyl amine (98 %), hydrochloric acid (HCl, 37 %), thriethylamine (Et_3N, 98.5 %), methanesulfonyl chloride (MsCl, 99 %), propargyl alcohol (99 %), 1-ethyl-3-(3-dimethylaminopropyl)carbodiimide hydrochloride (EDC·HCl, crystalline), 1-hydroxybenzotriazole monohydrate (HOBt, 98 %), sodium azide (NaN_3, 99.5 %), triphenylphosphine (Ph_3P, 99.5 %), copper(I) bromide (CuBr, 99.999%), copper(II) sulfate pentahydrate ($CuSO_4 \cdot 5H_2O$, 98%), 2-methyl-2-propanol (*t*-BuOH, 99.7 %); N,N,N',N",N" pentamethyldiethylene triamine (PMDETA) (99 %), lithium bromide (LiBr, 99 %), and sodium ascorbate (SA, 98 %) were purchased from Aldrich and they were used as received. 4-Toluenesulfonyl chloride (TsCl, 98 %, Aldrich) was purified by recrystallization from chloroform and petroleum ether twice. Pyridine (Py, 99.8 %, Aldrich) and N,N-dimethylformamide (DMF, 99.8 %, Aldrich) and dichloromethane (DCM) were dried over CaH_2 under a dry nitrogen atmosphere for 24 h and distilled under reduced pressure or under atmospheric pressure prior to use. Tetrahydrofuran (THF), methanol, chloroform ($CHCl_3$), hexane, petroleum ether, diethyl ether and ethyl acetate were purchased from VWR. Silica gel 230-400 mesh for chromatography was purchased from Qingdao Meicao Co., China. The thin-layer chromatography (TLC) was performed on aluminum supported silica gel (60 mesh, Sigma-Aldrich Chemicals Co.) and visualized with cerium molybdate stain (Hanessian's stain). Water was deionized with a Millipore MilliQ system.

2.2 Monomer syntheses

2.2.1 Synthesis of the lithocholic acid derivative

A heterofunctional monomer **5** was synthesized in four steps from lithocholic acid **1**[80, 99, 100] (Figure 2.1).

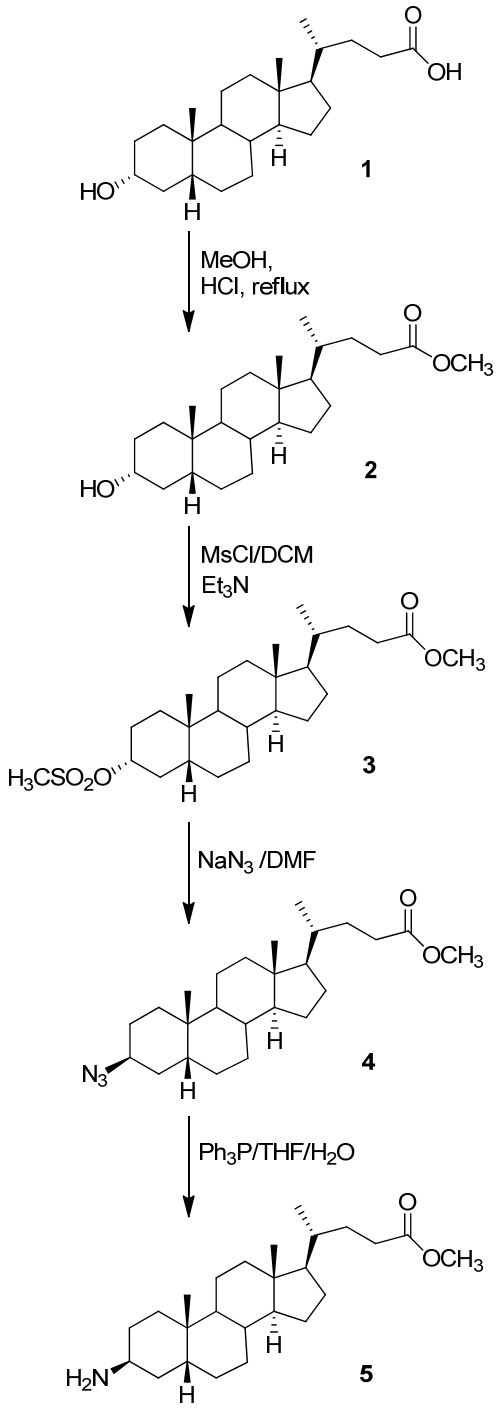

Figure 2.1: Reaction scheme for the synthesis of the heterofunctional monomer **5** from lithocholic acid **1**.

Esterification of lithocholic acid (1). A solution of lithocholic acid (**1**, 12.5 g, 33.5 mmol) in methanol (65 mL) was catalyzed by concentrated hydrochloric acid (0.5 mL). The mixture was stirred and heated to reflux for 1 h. The solution was cooled with an ice bath and the product was filtered, followed by vacuum drying to afford **2** in 95 % yield.

3α-Hydroxy-5β-cholan-24-oic acid methyl ester (2). ^{1}H NMR (400 MHz, $CDCl_3$, δ, ppm): 3.65 (3H, s, OC**H**$_3$-**26**), 3.60 (1H, m, C**H**-**3**), 0.91 (3H, s, C**H**$_3$-**21**), 0.89 (3H, s, C**H**$_3$-**19**), 0.63 (3H, s, C**H**$_3$-**18**). ATR-FTIR υ_{max} (cm^{-1}): 3516, 2931, 2859, 1710.

Mesylation of lithocholic acid methyl ester (2). To a cooled solution (~0 °C) of **2** (2.7 g, 6.91 mmol) in dry DCM (25 mL) was added Et_3N (1.45 mL, 10.37 mmol) under N_2. Methanesulfonyl chloride (MsCl, 0.60 mL, 7.60 mmol) was added dropwise to the mixture over 10 min at 0 °C under N_2. The reaction mixture was kept stirring at 0 °C for 15 min, then crushed ice was added to the reaction. The reaction mixture was extracted with DCM (2×75 mL). The resulting solution was washed with water (3×50 mL), brine (2×50 mL), and then dried over anhydrous sodium sulfate. The solvent was evaporated under reduced pressure to give the crude **3** as a white solid in 89 % yield. It was used as is without further purification.

3α-Mesyloxy-5β-cholan-24-oic acid methyl ester (3). ^{1}H NMR (400 MHz, $CDCl_3$, δ, ppm): 4.65 (1H, m, C**H**-**3**), 3.66 (3H, s, OC**H**$_3$-**26**), 3.00 (3H, s, C**H**$_3$, mesylate) 0.93 (3H, s, C**H**$_3$-**21**), 0.91 (3H, d, *J*=6.42 Hz, C**H**$_3$-**19**), 0.64 (3H, s, C**H**$_3$-**18**).

Azidation of lithocholic acid derivative (3). A suspension of **3** (2.7 g, 5.76 mmol) and sodium azide (1.12 g, 17.28 mmol) in dry DMF (30 mL) was heated at 90 °C overnight. After filtering, the solution was concentrated under reduced pressure and it was quenched by adding crushed ice (100 mL). The product was extracted with ethyl acetate (3×100 mL). The combined extracts were washed with water (3×75 mL), brine (3×75 mL), and they were dried over anhydrous sodium sulfate. The filtered solution was concentrated under reduced pressure. Column chromatography with ethyl acetate:hexane (4:1), followed by vacuum-drying, afforded pure **4** as a white solid in 78 % yield.

3β-Azido-5β-cholan-24-oic acid methyl ester (4). ^{1}H NMR (400 MHz, $CDCl_3$, δ, ppm): 3.95 (1H, m, C**H-3**), 3.66 (3H, s, OC$\underline{\mathbf{H}}_3$**-26**), 0.95 (3H, s, C$\underline{\mathbf{H}}_3$**-21**), 0.91 (3H, d, *J*=6.43 Hz, C$\underline{\mathbf{H}}_3$**-19**), 0.64 (3H, s, C$\underline{\mathbf{H}}_3$**-18**). ATR-FTIR υ_{max} (cm^{-1}): 2932, 2855, 2086, 1732.

Reduction of lithocholic acid derivative (4). To a solution of azide ester **4 (**1.86 g, 4.31 mmol) in THF (70 mL) were added Ph_3P (1.71 g, 6.47 mmol) and water (3 mL). The reaction mixture was stirred at reflux overnight. After the solvent was evaporated under reduced pressure, the residue was purified by column chromatography with ethyl acetate:hexane (4:1) and then methanol:triethylamine (45:1) to afford **5** as a white solid in 68 % yield.

3β-Amine-5β-cholan-24-oic acid methyl ester (5). ^{1}H NMR (400 MHz, $CDCl_3$, δ, ppm): 3.66 (3H, s, OC$\underline{\mathbf{H}}_3$**-26**), 3.26 (1H, m, C**H-3**), 0.96 (3H, s, C$\underline{\mathbf{H}}_3$**-21**), 0.91 (3H, d, *J*=6.42 Hz, C$\underline{\mathbf{H}}_3$**-19**), 0.64 (3H, s, C$\underline{\mathbf{H}}_3$**-18**). ATR-FTIR υ_{max} (cm^{-1}): 3358, 2920, 2857, 1728. T_m (DSC) 127 °C.

2.2.2 Syntheses of the cholic acid derivatives

Heterofunctional monomers **9a** and **9b** were synthesized in three steps starting from cholic acid [80, 99, 101, 102] (Figure 2.2).

Propargylation of cholic acid (6). Compounds **7a** (amide) and **7b** (ester) were synthesized by the following this procedure. Cholic acid (**6**, 2.45 g, 6.00 mmol) was placed in a flame-dried round-bottom flask equipped with a stir bar. Propargyl amine (0.78 mL, 12.0 mmol) or propargyl alcohol (0.70 mL, 12.0 mmol) in dry DMF (10 mL) was added to the flask under nitrogen atmosphere. The solution was cooled to 0 °C and then it was degassed with nitrogen for 10-15 min, after which, EDC·HCl (1.73 g, 9.0 mmol) and HOBt (0.41 g, 3.00 mmol) were added. After 30 minutes, the mixture was allowed to warm to room temperature and it was stirred for 24 h. The reaction was quenched by pouring the mixture into a beaker filled with crushed ice. The crude product was extracted with ethyl acetate (3×100 mL). The combined extracts were washed with water (100 mL), 5 % LiBr (aq, 50 mL), and brine (50 mL). They were then dried over anhydrous sodium sulfate and concentrated under reduced pressure.

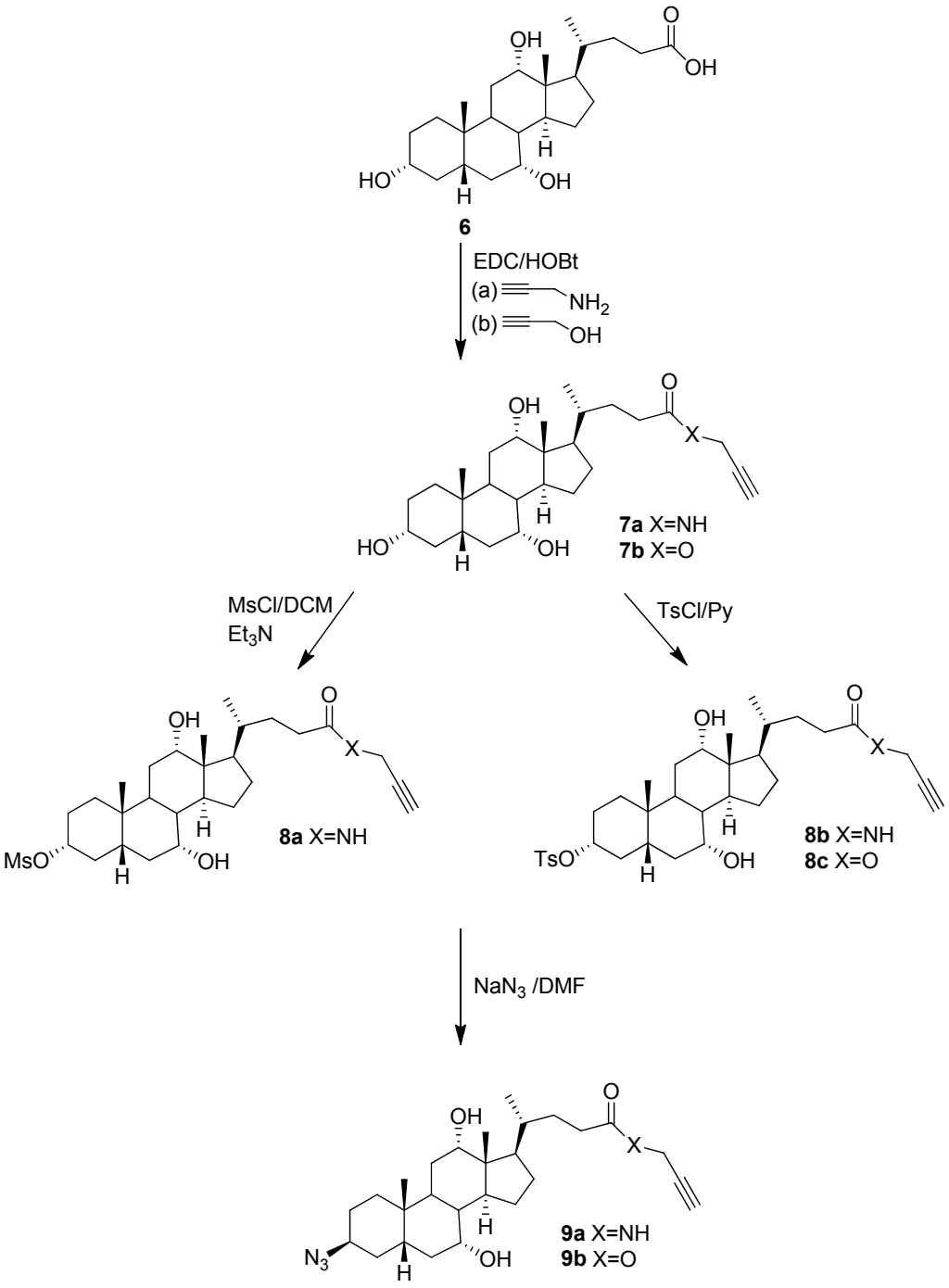

Figure 2.2: Reaction scheme for the synthesis of ω-alkyne-α-azide cholic acid derivatives **9a** and **9b** from cholic acid **6**.

Column chromatography with ethyl acetate:hexane (9:1 or 4:1), followed by vacuum-drying, afforded pure alkynes **7a** and **7b** as white solids in 84 % and 81 % yields, respectively.

N-Propargyl-3α, 7α, 12α-trihydroxy-5β-cholan-24-amide (7a). ^{1}H NMR (400 MHz, DMSO-d_6, δ, ppm): 8.19 (1H, t, *J*=5.43 Hz, CON**H**), 3.82 (2H, m, NH-C**H**$_2$), 3.78 (1H, s, C**H-12**), 3.61 (1H, s, C**H-7**), 3.18 (1H, m, C**H-3**), 3.06 (1H, t, J=2.51 Hz, alkyne C**H**), 0.92 (3H, d, *J*=6.45 Hz, C**H**$_3$**-21**), 0.81 (3H, s, C**H**$_3$**-19**), 0.58 (3H, s, C**H**$_3$**-18**). ^{1}H NMR (400 MHz, $CDCl_3$, δ, ppm): 6.11 (1H, s, CON**H**), 4.05 (2H, m, NH-C**H**$_2$), 3.98 (1H, s, C**H-12**), 3.85 (1H, s, C**H-7**), 3.45 (1H, m, C**H-3**), 2.23 (1H, t, *J*=2.46 Hz, alkyne C**H**), 0.98 (3H, d, *J*=6.14 Hz, C**H**$_3$**-21**), 0.88 (3H, s, C**H**$_3$**-19**), 0.68 (3H, s, C**H**$_3$**-18**). ^{13}C NMR (125 MHz, DMSO-d_6, δ, ppm): 172.26 (**C**=O), 81.31 (**-C**≡CH), 72.60 (-C≡**C**H), 70.89 (**C**H**-12**), 70.31 (**C**H**-3**), 66.13 (**C**H**-7**), 31.46 (NH-**C**H$_2$), 22.53 (**C**H$_3$**-19**), 17.00 (**C**H$_3$**-21**), 12.25 (**C**H$_3$**-18**). ATR-FTIR υ_{max} (cm^{-1}): 3392, 3301, 2926, 2864, 2113, 1649. HRMS (ESI) *m/z*: calculated for $C_{27}H_{44}NO_4$ 446.3265, found 446.3275 (M + H$^+$).

Propargyl-3α, 7α, 12α-trihydroxy-5β-cholan-24-oate (7b). ^{1}H NMR (400 MHz, DMSO-d_6, δ, ppm): 4.67 (2H, d, *J*=2.37 Hz, O-C**H**$_2$), 4.31 (1H, d, *J*=4.38 Hz, OH), 4.11 (1H, d, *J*=3.50 Hz, OH), 4.0 (1H, d, *J*=3.36 Hz, OH), 3.78 (1H, s, C**H-12**), 3.62 (1H, s, C**H-7**), 3.52 (1H, t, *J*=2.43 Hz, alkyne C**H**), 3.18 (1H, m, C**H-3**), 0.93 (3H, d, *J*=6.29 Hz, C**H**$_3$**-21**), 0.81 (3H, s, C**H**$_3$**-19**), 0.59 (3H, s, C**H**$_3$**-18**). ^{13}C NMR (125 MHz, DMSO-d_6, δ, ppm): 172.49 (**C**=O), 78.47 (**-C**≡CH), 77.33 (-C≡**C**H), 70.87 (**C**H**-12**), 70.32 (**C**H**-3**), 66.13 (**C**H**-7**), 51.33 (**C**H$_2$-O), 22.51 (**C**H$_3$**-19**), 16.77 (**C**H$_3$**-21**), 12.22 (**C**H$_3$**-18**). ATR-FTIR υ_{max} (cm^{-1}): 3396, 3290, 2929, 2872, 2097, 1737. HRMS (ESI) *m/z*: calculated for $C_{27}H_{46}NO_5$ 464.3371, found 464.3384 (M + NH_4^+).

Mesylation of 7a. To a cooled solution (~0 °C) of **7a** (2 g, 4.50 mmol) in dry pyridine (20 mL) was added methanesulfonyl chloride (MsCl, 0.35 mL, 4.50 mmol) dropwise to the mixture over 10 min under N_2. The reaction mixture was kept stirring at 0 °C for 1 h. The solvent was then removed under reduced pressure and the residue was dissolved in ethyl acetate (150 mL). The resulting solution was washed with water (3×50 mL) and brine (2×50 mL), then it was dried over anhydrous sodium sulfate. Column

chromatography with ethyl acetate:hexane (4:1), followed vacuum-drying, afforded **8a** as a white solid in 58 % yield.

N-Propargyl-3α-mesyloxy-7α,12α-dihydroxy-5β-cholan-24-amide (8a). ^{1}H NMR (400 MHz, $CDCl_3$, δ, ppm): 5.94 (1H, s, CON**H**), 4.50 (1H, m, C**H-3**), 4.04 (2H, m, NH-C**H$_2$**), 3.99 (1H, s, C**H-12**), 3.86 (1H, s, C**H-7**), 2.98 (3H, s, mesyl C**H**$_3$), 2.23 (1H, t, *J*=2.55 Hz, alkyne C**H**), 0.99 (3H, d, *J*=6.23 Hz, C**H**$_3$**-21**), 0.90 (3H, s, C**H**$_3$**-19**), 0.67 (3H, s, C**H**$_3$**-18**).

Tosylation of 7a and 7b. **7a** (2.00 g, 4.50 mmol) or **7b** (1.90 g, 4.26 mmol) was dissolved in anhydrous pyridine (10 mL) in a flame-dried round bottom flask with a stir bar. The solution was then cooled to 0 °C using an ice-water bath and it was degassed for 10-15 min under nitrogen atmosphere. A cold pyridine solution (10 mL) of 4-toluenesulfonyl chloride (0.88 g, 4.50 mmol) or (0.83 g, 4.26 mmol) was added dropwise to the mixture over 15 min. The reaction mixture was stirred at 0 °C for 1 h and then it was warmed to room temperature and stirred overnight. The solvent was removed under reduced pressure and the residue was dissolved in ethyl acetate (150 mL). The resulting solution was washed with water (3×50 mL) and brine (2×50 mL), and then it was dried over anhydrous sodium sulfate. The solvent was removed to give crude **8b** and **8c** as white solids in 86 % and 88 % yields, respectively, which were used without further purification.

N-Propargyl-3α-(4-methylphenyl)sulfonyloxy-7α,12α-dihydroxy-5β-cholan-24-amide (8b). ^{1}H NMR (400 MHz, DMSO-d_6, δ, ppm): 8.19 (1H, t, *J*=5.38 Hz, CON**H**), 7.78 (d, *J*=8.25 Hz, 2H aromatic), 7.46 (d, *J*=7.95 Hz, 2H aromatic), 4.25 (1H, m, C**H-3**), 3.81 (2H, m, NH-C**H$_2$**), 3.75 (1H, s, C**H-12**), 3.58 (1H, s, C**H-7**), 3.42 (3H, s, tosyl C**H**$_3$), 3.06 (1H, t, *J*=2.46 Hz, alkyne C**H**), 0.92 (3H, d, *J*=6.32 Hz, C**H**$_3$**-21**), 0.78 (3H, s, C**H**$_3$**-19**), 0.56 (3H, s, C**H**$_3$**-18**).

Propargyl-3α-(4-methylphenyl)sulfonyloxy-7α,12α-dihydroxy-5β-cholan-24-oate (8c). ^{1}H NMR (400 MHz, DMSO-d_6, δ, ppm): 7.78 (d, *J*=8.29 Hz, 2H), 7.47 (d, *J*=8.07 Hz, 2H), 4.67 (2H, m, O-C**H**$_2$), 4.25 (1H, m, C**H-3**), 3.76 (1H, s, C**H-12**), 3.58 (1H, s, C**H-7**), 3.51 (1H, s, *J*=2.43 Hz, alkyne C**H**), 2.42 (3H, s, tosyl C**H**$_3$), 0.91 (3H, d, *J*=6.31 Hz, C**H**$_3$**-21**), 0.78 (3H, s, C**H**$_3$**-19**), 0.57 (3H, s, C**H**$_3$**-18**).

Azidation of 8a. A suspension of **8a** (1.00 g, 1.91 mmol) and sodium azide (0.37 g, 5.74 mmol) in dry DMF (7 mL) was heated at 45 °C for 5 days. After filtering, the solution was quenched by adding crushed ice (30 mL). The crude product was extracted with ethyl acetate (3×35 mL). The combined extracts were washed with water (3×50 mL) and brine (2×50 mL), and then they were dried over anhydrous sodium sulfate. The filtered solution was concentrated under reduced pressure. Column chromatography with ethyl acetate:hexane (4:1), followed by vacuum-drying, afforded pure **9a** as a white solid in 78 % yield.

Azidation of 8b and 8c. A similar procedure as for the azidation of **8a** was used. A suspension of **8b** (2.00 g, 3.43 mmol) or **8c** (2.00 g, 3.42 mmol) and sodium azide (0.67 g, 10.3 mmol) in dry DMF (10 mL) was heated at 45 °C for 4 days. After filtering, the solution was quenched by adding crushed ice (50 mL), and the product was extracted with ethyl acetate (3×50 mL). The combined extracts were washed with water (3×50 mL) and brine (2×50 mL), and then they were dried over anhydrous sodium sulfate. The filtered solution was concentrated under reduced pressure. Column chromatography with ethyl acetate:hexane (4:1), followed by three recrystallizations from a mixture of ethyl acetate and hexane at 0 °C, then vacuum-drying, afforded pure **9a** and **9b** as white solids in 74 % and 71 % yields, respectively.

N-Propargyl-3β-azido-7α,12α-dihydroxy-5β-cholan-24-amide (9a). ^{1}H NMR (400 MHz, DMSO-d_6, δ, ppm): 8.19 (1H, t, *J*=5.21 Hz, CON**H**), 4.15 (1H, d, *J*=3.27 Hz, 1OH), 4.10 (1H, d, *J*=3.47 Hz, 1OH), 3.99 (1H, s, C**H-3**), 3.81 (2H, m, NH-C**H$_2$**), 3.78 (1H, s, C**H-12**), 3.62 (1H, s, C**H-7**), 3.06 (1H, t, *J*=2.42 Hz, alkyne C**H**), 0.92 (3H, d, *J*=6.34 Hz, C**H$_3$-21**), 0.85 (3H, s, C**H$_3$-19**), 0.58 (3H, s, C**H$_3$-18**). ^{1}H NMR (400 MHz, $CDCl_3$, δ, ppm): 5.85 (1H, s, CON**H**), 4.04 (2H, m, NH-C**H$_2$**), 3.98 (1H, s, C**H-12**), 3.90 (1H, s, C**H-3**), 3.86 (1H, s, C**H-7**), 2.23 (1H, t, *J*=2.48 Hz, alkyne C**H**), 0.98 (3H, d, *J*=6.17 Hz, C**H$_3$-21**), 0.93 (3H, s, C**H$_3$-19**), 0.70 (3H, s, C**H$_3$-18**). ^{13}C NMR (125 MHz, DMSO-d_6, δ, ppm): 172.24 (**C**=O), 81.30 (-**C**≡CH), 72.59 (-C≡**C**H), 70.88 (**C**H-**12**), 66.05 (**C**H-**7**), 58.26 (**C**H-**3**), 31.45 (NH-**C**H$_2$), 22.63 (**C**H$_3$-**19**), 17.00 (**C**H$_3$-**21**), 12.23 (**C**H$_3$-**18**). ATR-FTIR υ_{max} (cm^{-1}): 3417,

3306, 2924, 2867, 2095, 1651. HRMS (ESI) *m/z*: calculated for $C_{27}H_{43}N_4O_3$ 471.3330, found 471.3345 ($M + H^+$).

Propargyl-3β-azido-7α,12α-dihydroxy-5β-cholan-24-oate (9b). ^{1}H NMR (400 MHz, DMSO-d_6, δ, ppm): 4.67 (2H, d, *J*=2.37 Hz, O-C**H**$_2$), 4.12-4.15 (2H, m, 2OH), 3.99 (1H, s, C**H-3**), 3.78 (1H, s, C**H-12**), 3.62 (1H, s, C**H-7**), 3.51 (1H, t, *J*=2.42 Hz, alkyne C**H**), 0.92 (3H, d, *J*=6.32 Hz, C**H**$_3$**-21**), 0.85 (3H, s, C**H**$_3$**-19**), 0.59 (3H, s, C**H**$_3$**-18**). ^{13}C NMR (125 MHz, DMSO-d_6, δ, ppm): 172.58 (**C**=O), 78.57 (**-C**≡CH), 77.43 (-C≡**C**H), 70.96 (**C**H**-12**), 66.15 (**C**H**-7**), 58.36 (**C**H**-3**), 51.44 (**C**H$_2$-O), 22.73 (**C**H$_3$**-19**), 16.88 (**C**H$_3$**-21**), 12.30 (**C**H$_3$**-18**). ATR-FTIR υ_{max} (cm^{-1}): 3435, 3290, 2926, 2870, 2094, 1731. HRMS (ESI) *m/z*: calculated for $C_{27}H_{45}N_4O_4$ 489.3435, found 489.3437 ($M + NH_4^+$).

Alternatively, **9a** was synthesized from cholic acid **6** starting by activating the OH group at C3-position and subsequent reaction with sodium azide, followed by coupling with propargyl amide (Figure 2.3).

Tosylation of cholic acid (6). To a cooled solution of cholic acid **6** (2.00 g, 4.90 mmol) in anhydrous pyridine (10 mL), a cold pyridine solution (10 mL) of 4-toluenesulfonyl chloride (0.93 g, 4.90 mmol) was added dropwise under nitrogen atmosphere. The reaction mixture was kept at 0 °C for 1 h, then it was warmed to room temperature and it was stirred overnight. The solvent was removed under reduced pressure and the residue was dissolved in ethyl acetate (350 mL). The resulting solution was washed with water (3×100 mL) and brine (2×100 mL), and the extracts were dried over anhydrous sodium sulfate. The solvent was removed to give crude **7c** as a white solid in 68 % yield, which was used for the next step without further purification.

3α-(4-Methylphenyl)sulfonyloxy-7α,12α-dihydroxy-5β-cholan-24-oic acid (7c). ^{1}H NMR (400 MHz, DMSO-d_6, δ, ppm): 11.93 (1H, s, COO**H**), 7.77 (d, *J*=8.21 Hz, 2H aromatic), 7.45 (d, *J*=8.07 Hz, 2H aromatic), 4.25 (1H, m, C**H-3**), 3.75 (1H, s, C**H-12**), 3.59 (1H, s, C**H-7**), 2.42 (3H, s, tosyl C**H**$_3$), 0.90 (3H, d, *J*=5.32 Hz, C**H**$_3$**-21**), 0.78 (3H, s, C**H**$_3$**-19**), 0.56 (3H, s, C**H**$_3$**-18**).

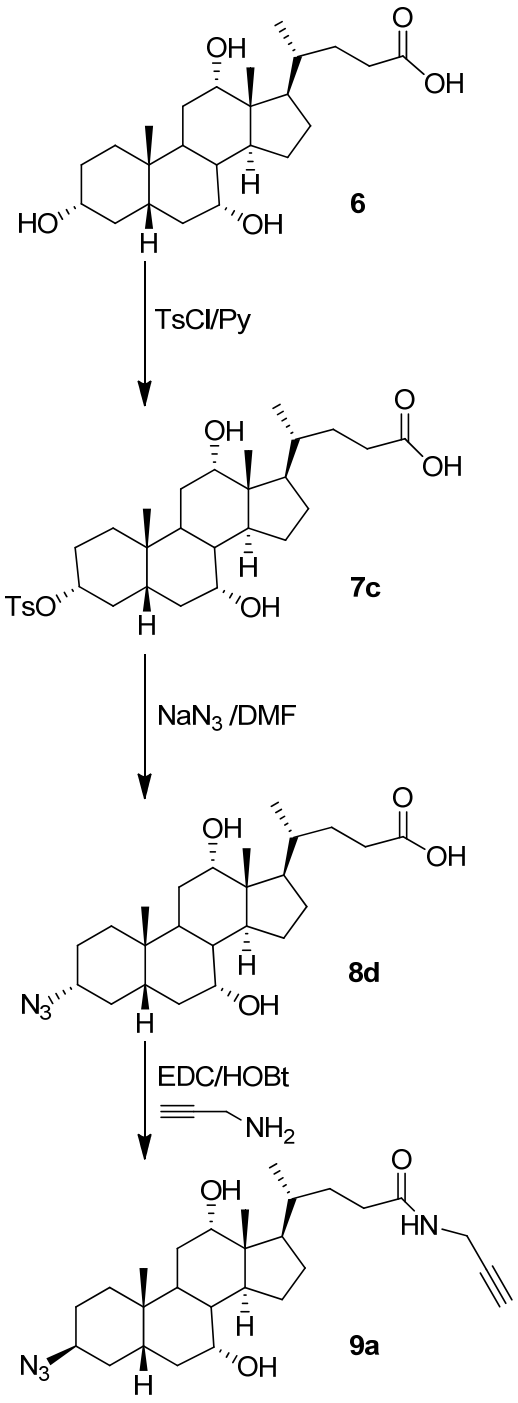

Figure 2.3: Alternative reaction scheme for the synthesis of ω-alkyne-α-azide cholic acid derivative **9a** from cholic acid **6**.

Azidation of 7c. A suspension of **7c** (1.0 g, 1.78 mmol) and sodium azide (0.35 g, 5.33 mmol) in DMF (5 mL) was heated at 90 °C overnight. After filtering, the solution was quenched by adding crushed ice (50 mL). The crude product was extracted with ethyl acetate (3×75 mL). The combined extracts were washed with water (3×50 mL) and brine (2×50 mL), and then they were dried over anhydrous sodium sulfate. The filtered solution was concentrated under reduced pressure. Column chromatography with ethyl acetate:hexane (4:1), followed by recrystallization from a mixture of ethyl acetate and hexane at 0 °C, and vacuum-drying, afforded pure **8d** as a white solid in 60 % yield.

3β-Azido-7α,12α-dihydroxy-5β-cholan-24-oic acid (8d). ^{1}H NMR (400 MHz, DMSO-d_6, δ, ppm): 4.15-4.12 (2H, m, 2OH), 3.99 (1H, s, C**H-3**), 3.76 (1H, s, C**H-12**), 3.61 (1H, s, C**H-7**), 0.91 (3H, d, J=6.33 Hz, C$\mathbf{H_3}$**-21**), 0.85 (3H, s, C$\mathbf{H_3}$**-19**), 0.58 (3H, s, C$\mathbf{H_3}$**-18**).

Propargylation of 8d. **9a** was synthesized by following the propargylation procedure of cholic acid **6**. **8d** (0.4 g, 0.92 mmol) was placed in a flame-dried round-bottom flask equipped with a stir bar. Propargyl amine (0.12 mL, 1.85 mmol) in dry DMF (5 mL) was added to the flask under nitrogen atmosphere. The solution was cooled to 0 °C and it was degassed with nitrogen for 10-15 min, after which, EDC·HCl (0.26 g, 1.38 mmol) and HOBt (62.2 mg, 0.46 mmol) were added. After 30 minutes, the mixture was allowed to warm to room temperature and it was stirred for 24 h. The reaction was quenched by pouring the mixture into a beaker filled with crushed ice. The crude product was extracted with ethyl acetate (3×20 mL). The combined extracts were washed with water (25 mL), 5 % LiBr (aq, 15 mL), and brine (15 mL), then they were dried over anhydrous sodium sulfate. The solvent was concentrated under reduced pressure. Column chromatography with ethyl acetate:hexane (4:1), followed by vacuum-drying, afforded pure **9a** as a white solid in 69 % yield.

N-Propargyl-3β-azido-7α,12α-dihydroxy-5β-cholan-24-amide (9a). ^{1}H NMR (400 MHz, DMSO-d_6, δ, ppm): 8.19 (1H, t, *J*=5.21 Hz, CON**H**), 4.15 (1H, d, *J*=3.27 Hz, 1OH), 4.10 (1H, d, *J*=3.47 Hz, 1OH), 3.99 (1H, s, C**H-3**), 3.81 (2H, m, NH-**C**$\mathbf{H_2}$), 3.78 (1H, s, C**H-12**), 3.62 (1H, s, C**H-7**), 3.06 (1H, t, *J*=2.48 Hz, alkyne C**H**), 0.92 (3H, d, *J*=6.34 Hz, C$\mathbf{H_3}$**-21**), 0.85 (3H, s, C$\mathbf{H_3}$**-19**), 0.58 (3H, s, C$\mathbf{H_3}$**-18**).

2.3 Polymer syntheses

2.3.1 Synthesis of lithocholic acid-based polyamide via polycondensation

Synthesis of polyamide 10 (Figure 2.4)[79]. The polymerization was achieved by melt polycondensation of lithocholic acid derivative **5**. To a flask equipped with a nitrogen capillary inlet tube for nitrogen and a sidearm to the vacuum was added **5** (0.25 g, 0.064 mmol). The flask was heated to 180 °C in a sand bath under a flow of nitrogen. After **5** was molten, the polymerization was allowed to proceed under vacuum for 5, 8 and 12 h. After the reaction, the flask was cooled to room temperature. The product was purified by precipitating it from chloroform (2 mL) into cold diethyl ether.

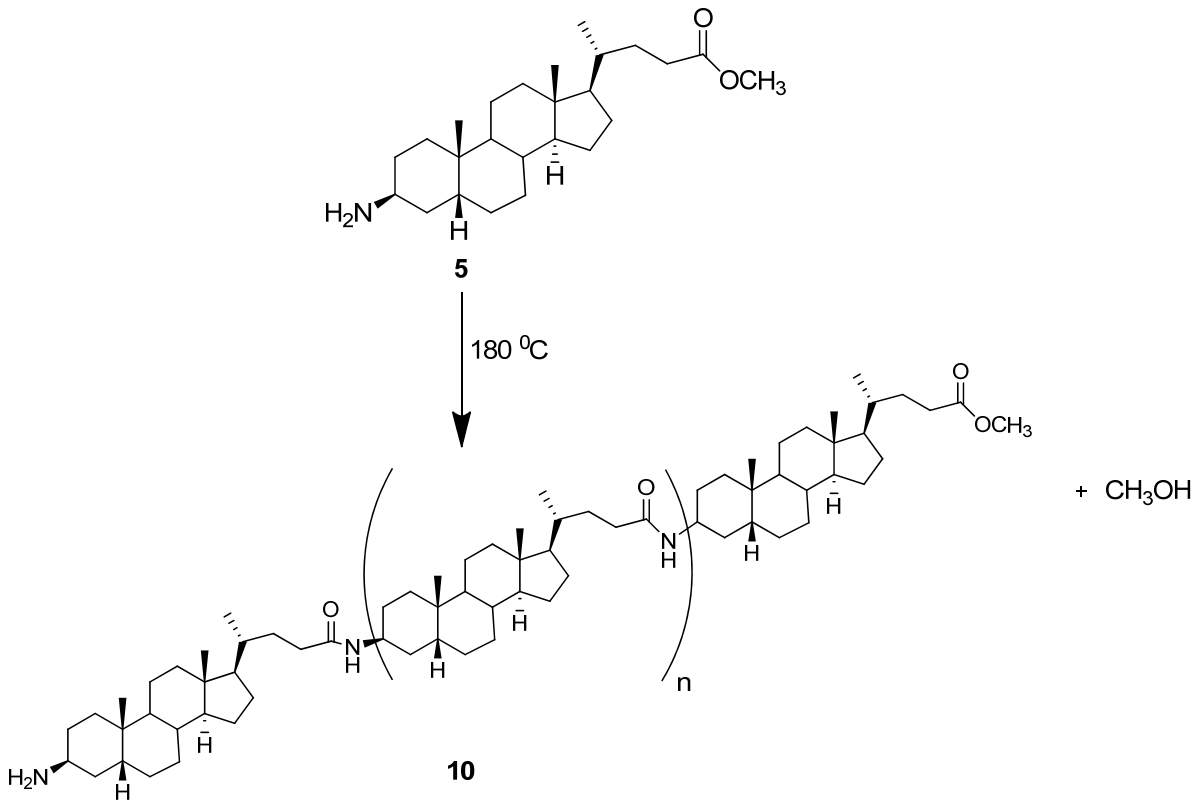

Figure 2.4: Reaction scheme for the synthesis of main-chain lithocholic acid-based polyamides via polycondensation.

Polyamide 10. ^{1}H NMR (400 MHz, $CDCl_3$, δ, ppm): 5.66 (1H, s, N**H**), 4.17 (1H, m, C**H-3**), 3.66 (3H, s, OC**H**$_3$**-26,** end group), 0.96 (3H, s, C**H**$_3$**-21**), 0.92 (3H, d, *J*=6.51 Hz, C**H**$_3$**-19**), 0.64 (3H, s, C**H**$_3$**-18**). ATR-FTIR υ_{max} (cm^{-1}): 3323, 2927, 2862, 1729, 1643, 1532. GPC ($CHCl_3$): M_n 2 500 $g \cdot mol^{-1}$, M_w 3 900 $g \cdot mol^{-1}$, PDI 1.56.

2.3.2 Synthesis of cholic acid-based polyamides and polyesters via copper(I)-catalyzed azide-alkyne cycloaddition

Synthesis of polyamide 11 and polyester 12 (Figure 2.5).

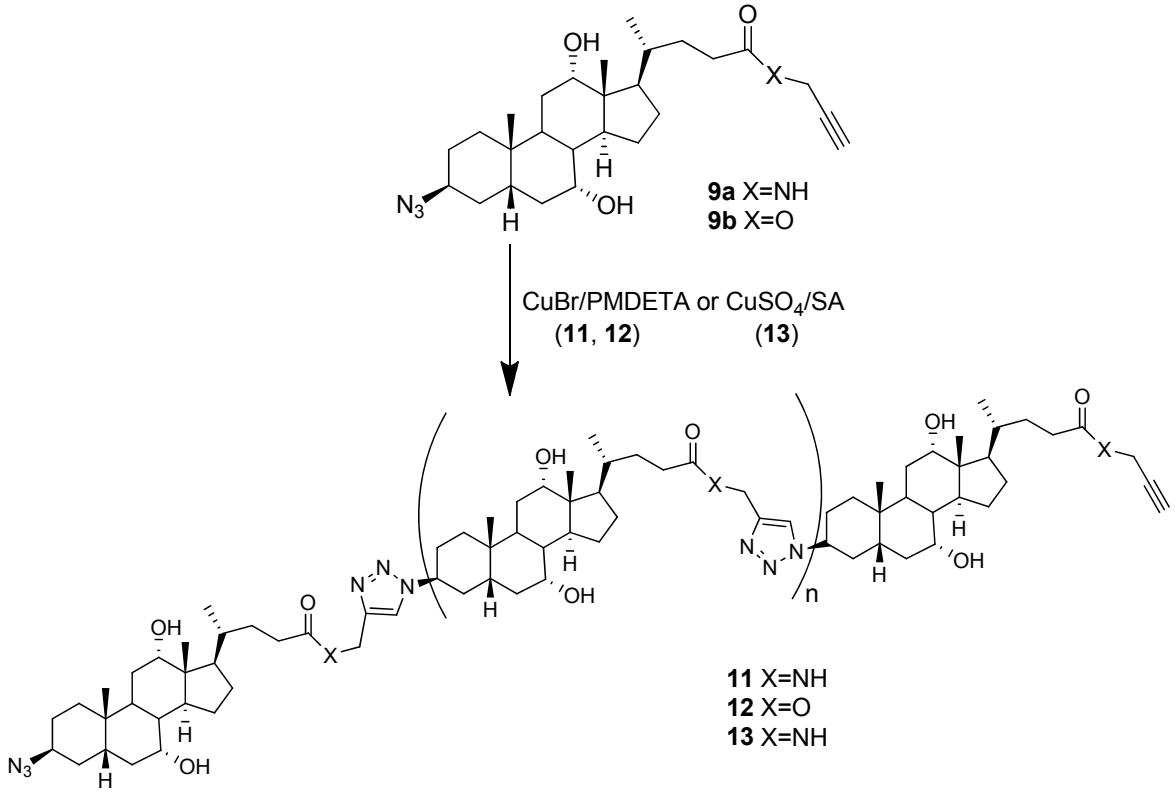

Figure 2.5: Reaction scheme for the synthesis of main-chain cholic acid-based polyamides and polyesters via copper(I)-catalyzed azide-alkyne cycloaddition.

Anhydrous DMF (5.0 mL) was added via a N_2-purged syringe to a flame-dried round-bottom flask containing **9a** (320 mg, 0.68 mmol) or **9b** (335 mg, 0.71 mmol) and it was degassed with nitrogen for 15-20 min. PMDETA (0.72 mL, 3.40 mmol) was then introduced via a N_2-purged syringe to the monomer solution. The resulting mixture was transferred to another flame-dried flask containing copper(I) bromide (2.0 mg, 0.014 mmol) under nitrogen. The mixture was then stirred under nitrogen at 80 °C for 120 h in the dark. After cooling to room temperature, the polymer was purified by precipitating it from a DMSO:DMF mixture (3 mL, 1:1*v/v*) into acetone. Vacuum-drying afforded a slightly yellow solid (ca. 280 mg) in 88 % and 84 % yields for **11** and **12**, respectively.

Polyamide 11. ^{1}H NMR (400 MHz, DMSO-d_6, δ, ppm): 8.22 (1H, t, *J*=5.56 Hz, CON**H**), 7.91 (1H, s, C**H** triazole), 4.59 (1H, s, C**H-3**), 4.27 (2H, m, NH-C**H**$_2$), 4.24 (1H, m, 1OH), 4.15 (1H, m, 1OH), 3.79 (1H, s, C**H-12**), 3.64 (1H, s, C**H-7**), 0.92 (3H, d, *J*=5.66 Hz, C**H**$_3$**-21**), 0.79 (3H, s, C**H**$_3$**-19**), 0.58 (3H, s, C**H**$_3$**-18**). ^{13}C NMR (125 MHz, DMSO-d_6, δ, ppm): 172.41 (**C**=O), 144.35 (**C**H triazole), 121.72 (**C**-CH triazole), 70.91 (**C**H-**12**), 66.08 (**C**H-**7**), 55.69 (**C**H-**3**), 31.54 (NH-**C**H$_2$), 22.66 (**C**H$_3$-**19**), 17.04 (**C**H$_3$-**21**), 12.24 (**C**H$_3$-**18**). ATR-FTIR υ_{max} (cm^{-1}): 3377, 2933, 2867, 1650. GPC (DMF): M_n 23 900 g·mol^{-1}, M_w 40 400 g·mol^{-1}, PDI 1.69.

Polyester 12. ^{1}H NMR (400 MHz, DMSO-d_6, δ, ppm): 8.17 (1H, s, C**H** triazole), 5.10 (2H, m, O-C**H**$_2$), 4.63 (1H, s, C**H-3**), 4.23 (1H, d, *J*= 2.94, 1OH), 4.16 (1H, d, *J*= 3.03, 1OH), 3.78 (1H, s, C**H-12**), 3.64 (1H, s, C**H-7**), 0.90 (3H, d, *J*=5.80 Hz, C**H**$_3$**-21**), 0.78 (3H, s, C**H**$_3$**-19**), 0.56 (3H, s, C**H**$_3$**-18**). ^{13}C NMR (125 MHz, DMSO-d_6, δ, ppm): 172.95 (**C**=O), 144.36 (**C**H triazole), 123.77 (**C**-CH triazole), 70.87 (**C**H-**12**), 66.07 (**C**H-**7**), 56.94 (O-**C**H$_2$), 55.90 (**C**H-**3**), 22.64 (**C**H$_3$-**19**), 16.80 (**C**H$_3$-**21**), 12.19 (**C**H$_3$-**18**). ATR-FTIR υ_{max} (cm^{-1}): 3424, 2942, 2867, 173, 1660. GPC (DMF): M_n 25 500 g·mol^{-1}, M_w 41 600 g·mol^{-1}, PDI 1.63.

Synthesis of polyamide (13).[31] The solvent (*t*-BuOH, 35 mL) was placed in a round-bottom flask equipped with a stir bar and condenser, and it was degassed by bubbling nitrogen gas for 30 min. **9a** (250 mg, 0.53 mmol) was added while stirring the solution vigorously under nitrogen. Sodium ascorbate (63.1 mg, 0.11 mmol) in a 1.0 mL of

deionized water was introduced into the mixture, followed by the dropwise addition of copper sulfate pentahydrate (39.8 mg, 0.053 mmol) in 2.0 mL of deionized water. The reaction was carried out at 60 °C under nitrogen for 120 h in the dark. After cooling to room temperature, the solvent was removed under vacuum and a minimum amount of DMSO was added to dissolve the product, followed by precipitating (twice) in water. The resulting product was dried by freeze-drying. The polymer was redissolved in DMSO (1 mL), precipitated in ethyl acetate, and dried under vacuum, affording a slightly yellow solid in 48 % yield.

Polyamide 13. ^{1}H NMR (400 MHz, DMSO-d_6, δ, ppm): 8.20 (1H, t, *J*=5.49 Hz, CON**H**), 7.90 (s, 1H, C**H** triazole), 4.59 (1H, s, C**H**-3), 4.27 (2H, m, NH-C**H**$_2$), 4.22 (1H, m, 1OH), 4.14 (1H, m, 1OH), 3.99 (1H, s, C**H**-3 end group) , 3.80 (1H, s, C**H**-12), 3.64 (1H, s, C**H**-7), 3.06 (1H, t, *J*=2.45 Hz, alkyne C**H** end group), 0.92 (3H, d, J=4.91 Hz, C**H**$_3$-21), 0.85 (3H, s, C**H**$_3$-19), 0.58 (3H, s, C**H**$_3$-18). ^{13}C NMR (125 MHz, DMSO-d_6, δ, ppm): 172.40 (**C**=O), 144.38 (**C**H triazole), 121.73 (**C**-CH triazole), 81.31 (-**C**≡CH end group), 72.60 (-C≡**C**H end group), 70.91 (**C**H-12), 66.08 (**C**H-7), 58.26 (**C**H-3 end group), 55.69 (**C**H-3), 31.54 (NH-**C**H$_2$), 22.65 (**C**H$_3$-19), 17.04 (**C**H$_3$-21), 12.24 (**C**H$_3$-18). ATR-FTIR υ_{max} (cm^{-1}): 3435, 3307, 2935, 2869, 2097, 1654. GPC (DMF): M_n 5 200 g·mol^{-1}, M_w 7 700 g·mol^{-1}, PDI 1.48.

2.4 Preparation of polymer films

Polymer films were prepared by evaporating a concentrated polymer solution from DMF (100 mg/mL) in a PTFE mold (1.5 × 2 cm) at 145 °C under atmospheric pressure for 24 h. They were then cured for 1 h at 160 °C and for 1 h at 180 °C.

Small rectangular samples (4 mm × 10 mm) were cut from these films and they were used for dynamic mechanical tests. The film dimensions were measured with a digital caliper with a precision of 0.01 mm.

2.5 Characterization

2.5.1 Nuclear magnetic resonance spectroscopy (NMR)

^{1}H NMR and ^{13}C NMR spectra were recorded on a Bruker AV-400 spectrometer operating at 400 MHz and on a Bruker AV-500 spectrometer operating at 125 MHz, respectively. Samples were dissolved in deuterated chloroform ($CDCl_3$) and dimethyl sulfoxide (DMSO-d_6) as indicated in the text. The solvents also served as the internal reference (7.26 or 2.50 ppm for ^{1}H, and 39.43 ppm for ^{13}C, respectively). The chemical shifts are given in ppm and coupling constants (*J*) in Hz.

2.5.2 Attenuated total reflectance Fourier transform infrared spectroscopy (ATR-FTIR)

FT-IR spectra were recorded on a TA Instruments Nicolet 6700 spectrometer equipped with an attenuated total reflectance (ATR) accessory. A total of 64 scans were signal-averaged in the range from 4000 to 400 cm^{-1} at a resolution of 4 cm^{-1}. Background measurements were taken before the sample was loaded onto the ATR unit for measurements.

2.5.3 High-resolution mass spectrometry (HRMS)

HRMS was performed LC/MSD TOF system (Agilent Technologies) in positive electrospray ionization (ESI) mode. Protonated molecular ions $(M+H)^+$ and ammonium adducts of cholic acid derivatives ions, $[M+NH_4]^+$, were generated by electrospray ionization, which permitted the molecular weight of each molecular species to be determined for empirical formula confirmation.

2.5.4 Gel permeation chromatography (GPC)

GPC was performed on a system consisting of a Waters 600E pump, a Waters 717plus autosampler, a set of two columns (Waters HR6, pore size 1×10^6 Å, and Phenomenex Phenogel, pore size 1×10^4 Å), a Dawn EOS multi-angle laser light scattering detector, and an Optilab rEX interferometric refractometer (both from Wyatt, λ = 690 nm).

The eluent (DMF, 0.01 M LiBr) flow rate was 1.0 $mL \cdot min^{-1}$ and the temperature of the columns was 25 °C. The refractive index *dn/dc* value of the cholic acid polymers was determined to be 0.0885 $mL \cdot g^{-1}$ at 690 nm in DMF (25 °C).

2.5.5 Thermogravimetric analyses (TGA)

TGA were performed on a Hi-Res TGA 2950 thermogravimetric analyzer from TA Instruments under a nitrogen atmosphere. About 2-3 mg of compound was placed in a platinum pan that was heated from 25 to 700 °C at a heating rate of 10 $°C \cdot min^{-1}$ under an atmosphere of nitrogen with a constant purge rate of 60 $mL \cdot min^{-1}$. The thermal decomposition temperature (T_d) was defined as the onset of decomposition. Ferromagnetic transition of the Curie point for a nickel standard was used for temperature calibration.

2.5.6 Differential scanning calorimetry (DSC)

DSC measurements were carried out on a DSC Q1000 differential scanning calorimeter from TA Instruments. The temperature scale was calibrated with an indium standard. A hermetically sealed aluminum pan with a lid was used as the reference and sample pan. The baseline was established by performing a scan with an empty pan. About 2 mg of a compound was weighted into the pan, which was then hermetically sealed with a pin hole-pricked lid then placed on the DSC sample tray. DSC curves were obtained at a heating and cooling rate of 10 $°C \cdot min^{-1}$. The sample chamber was continuously purged with dry nitrogen. The glass-transition temperatures (T_g) were determined from the second scanning curve and they were defined as the inflection point in the change of heat capacity.

2.5.7 Dynamic mechanical analysis (DMA)

Mechanical tests were performed on a DMA 2980 dynamic mechanical analyzer from TA Instruments. For controlled force (stress-strain) experiments, a preload force of 0.01 N and a force ramp 0.2 $N \cdot min^{-1}$ to 18 N were used. Dynamic experiments to measure the T_g were performed at 1 Hz. A preload force of 0.01 N was applied to the sample subjected to

the heating rate of 2 °C·min^{-1} and an oscillation amplitude of 2 μm. The T_g values determined by DMA were defined as the onset in the change of the storage modulus.

3 Results and Discussion

3.1 Monomer syntheses for step-growth polymerizations

In order to synthesize the main-chain bile acid-containing polymers via step-growth polymerization, two different types of heterofunctional monomers were targeted and synthesized (Figure 3.1).

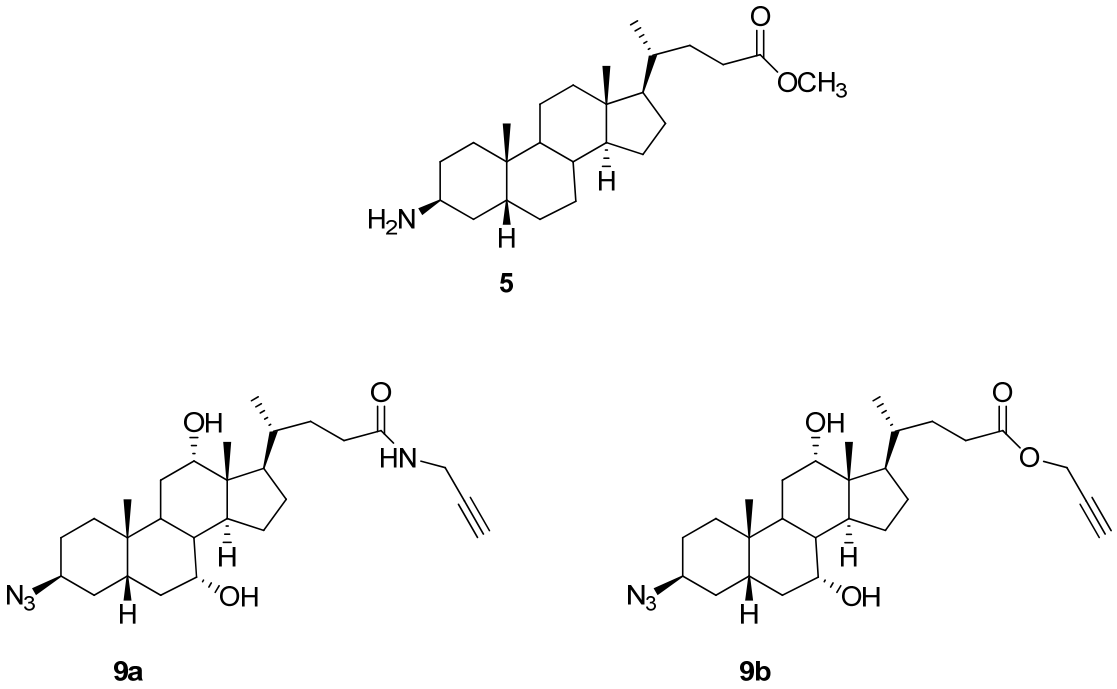

Figure 3.1: The structures of bile acid-based monomers for step-growth polymerizations: **5** for polycondensation reaction and **9a** and **9b** for copper(I)-catalyzed azide-alkyne polyaddition reaction.

Lithocholic acid-based monomer **5** was prepared from lithocholic acid **1** and it was targeted for step-growth polycondensation. Similarly, the synthesis of cholic-based monomers **9a** and **9b** were prepared for step-growth polymerization using the copper(I)-catalyzed azide-alkyne polyaddition reaction.

Cholic acid-based monomers are more hydrophilic than lithocholic acid due to the two extra hydroxyl groups at C7- and C-12-positions. They have an amide linker **9a** as well as an ester linker **9b** attached to the C24-position via amidation or esterification, respectively. In our study, no additional spacer was introduced to the monomer structures in order to evaluate the impact of the bile acid moieties on the materials' properties. However, the rigidity of the monomer unit can influence both the reactivity for step-growth polymerization as well as the thermomechanical properties of the resulting polymers. Therefore, polymers prepared from monomers **5**, **9a** and **9b** are of interest, especially since they are different from those reported previously by our group[15, 79] and others.[14, 31]

3.1.1 Synthesis of the lithocholic acid-based monomer

Heterofunctional lithocholic acid-based monomer **5** was synthesized in four steps as per the experimental section (Figure 2.1). First, **2** was prepared according the procedure previously reported by our group.[80] The methyl ester was used since the esters are more soluble in organic solvents, such as tetrahydrofuran (THF), dichloromethane (DCM), ethyl acetate and chloroform ($CHCl_3$). Moreover, the methyl ester acts as a protecting group and it facilitates the synthesis and purification of **3**-**5** and **10**. The ^{1}H NMR spectrum of the lithocholic acid methyl ester **2** is shown in Figure 3.2. The characteristic resonance signal of the protons at positions C3 and C26 at 3.60 ppm and 3.65 ppm, respectively, confirmed the successful synthesis of **2**.

To synthesize 3β-azido-5β-cholan-24-oic acid methyl ester **4**, the corresponding mesylated **3** was prepared from lithocholic methyl ester **2** and methanesulfonyl chloride (MsCl). The hydroxyl group at the C3-position was activated with methanesulfonyl chloride in the presence of thriethylamine (Et_3N) in DCM.[99] The resulting ^{1}H NMR spectrum of **3** is shown in Figure 3.2. The resonance signal of the methylene proton at the C3-position was identified at 4.65 ppm and the protons of the mesylate group were at 3.00 ppm.

The nucleophilic substitution of the mesylate into the azide using sodium azide was carried out in N,N-dimethylformamide (DMF) at 90 °C under nitrogen.

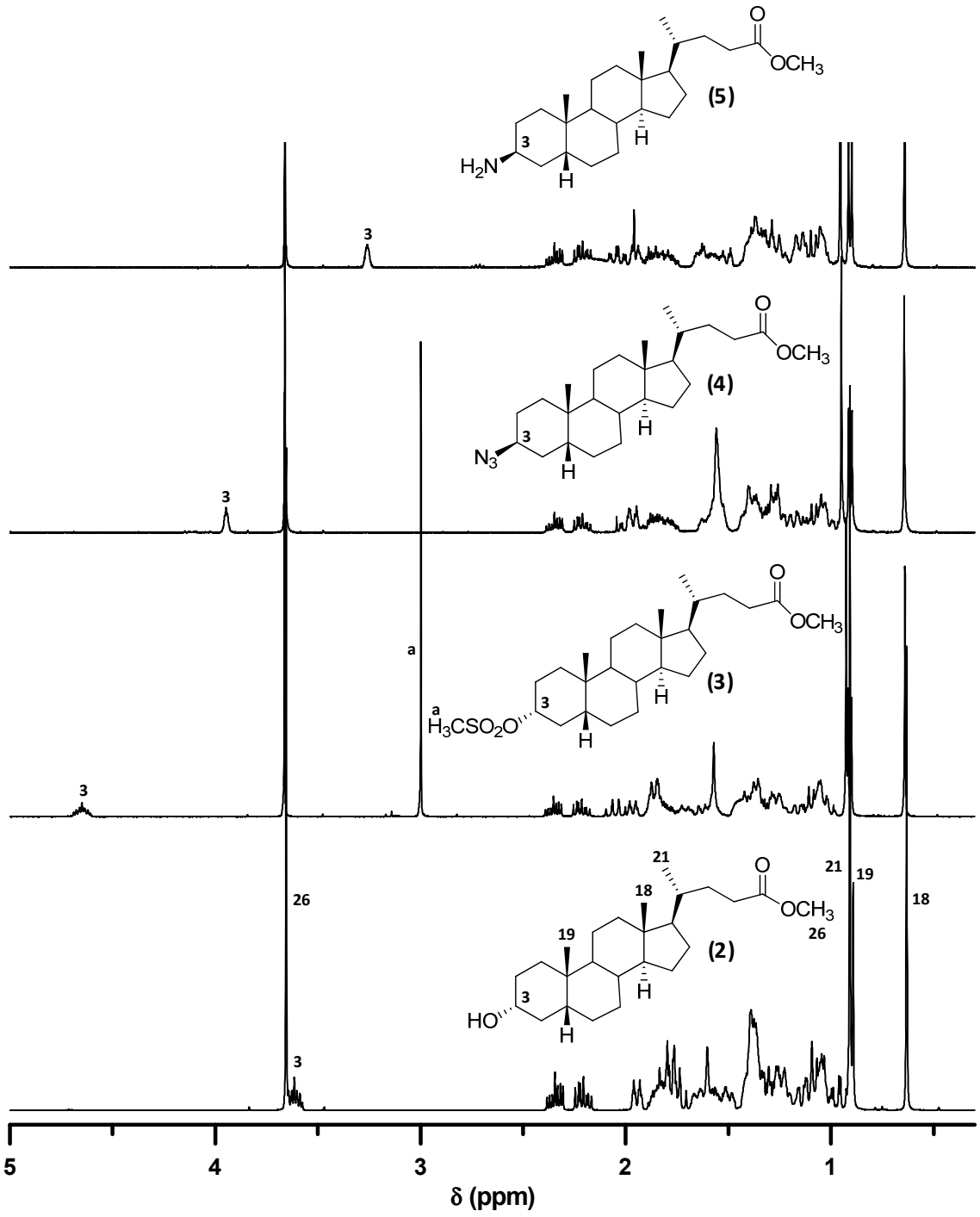

Figure 3.2: ^{1}H NMR spectra of **2**, **3**, **4** and **5** in $CDCl_3$.

The ^{1}H-NMR signal of the CH proton at the C3-position is a clear indicator of the stereochemistry of the molecule as well as for monitoring the reaction progress. The chemical shift change of the methylene protons at the C3-position at 4.65 ppm (broad multiplet, C*H* at equatorial position) of **3** (Figure 3.2) to 3.95 ppm (singlet, CH at the axial position) in the ^{1}H-NMR spectrum of 3β-azido-5β-cholan-24-oic acid methyl ester **4** (Figure 3.2) confirmed the successful conversion of the mesylate into azide. Moreover, the complete substitution to the azide group was also confirmed by the disappearance of the signals ascribed to the CH_3 protons of the mesylate at 3.00 ppm.

Next, 3β-azido-5β-cholan-24-oic acid methyl ester **4** was reduced to 3β-amine-5β-cholan-24-oic acid methyl ester **5**. The bile acid-based azide **4** could be converted into the amine by hydrogenation[103] or by the Staudinger reaction,[100, 104] which is a mild reduction. Triphenylphosphine reacted with the azide **4** to generate a phosphazide. Adding water to the medium led to the bile acid-based amine **5**.

The ^{1}H NMR signal of the CH proton at the C3-position of **5** was seen at 3.26 ppm, and the 3β-configuration remained unchanged during the reduction to obtain **5** (Figure 3.2). The resulting amines,[100] showed limited solubility in common organic solvents, such as THF, DCM, $CHCl_3$, acetone, ethyl acetate, and hexane. However, compound **5** was soluble in methanol.

Table 3.1: ^{1}H NMR chemical shifts (in ppm) of the lithocholic acid-containing **2-5** in $CDCl_3$.

Position	**2**	**3**	**4**	**5**
3	3.60	4.65	3.95	3.26
18	0.63	0.64	0.64	0.64
19	0.89	0.91	0.91	0.91
21	0.91	0.93	0.95	0.96
26	3.65	3.66	3.66	3.66

Additional proof for the successful preparation of **5** was by the FTIR. According to the FTIR spectra in Figure 3.3, the bands at 3516 and 2086 cm^{-1} were attributed to the hydroxyl and azide groups, respectively, confirming that the OH group was transformed into the azide group. The latter was then converted to an amine.

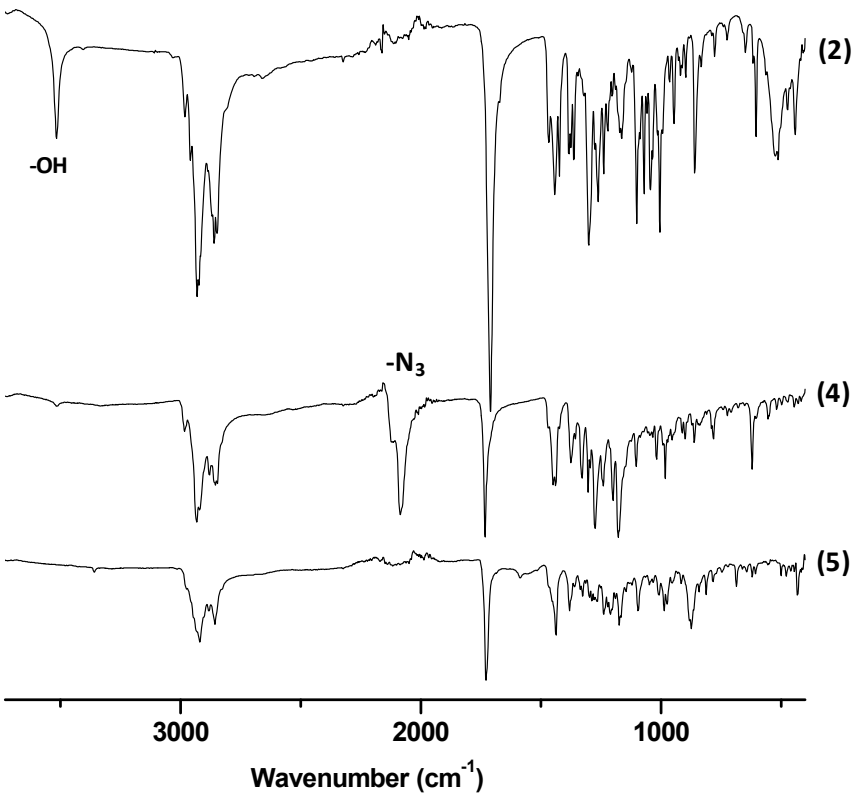

Figure 3.3: The FTIR spectra of **2**, **4** and **5**.

3.1.2 Synthesis of the cholic acid-based monomers

Both the alkyne and azide functionalities were introduced into the same molecule in order to avoid stoichiometric problems for their polymerization. First, the alkyne-functionalized cholanamide **7a** was synthesized by the amidation of carbodiimide-activated

cholic acid **6** with 1-ethyl-3-(3-dimethylaminopropyl) carbodiimide hydrochloride (EDC·HCl) in DMF in 84 % yield. The ^{1}H NMR of **7a** (Figure 3.4) showed the successful coupling according to the signals of the amide group at 8.19 ppm, the C26-methylene at 3.82 ppm and the alkyne of the propargyl group at 3.06 ppm.

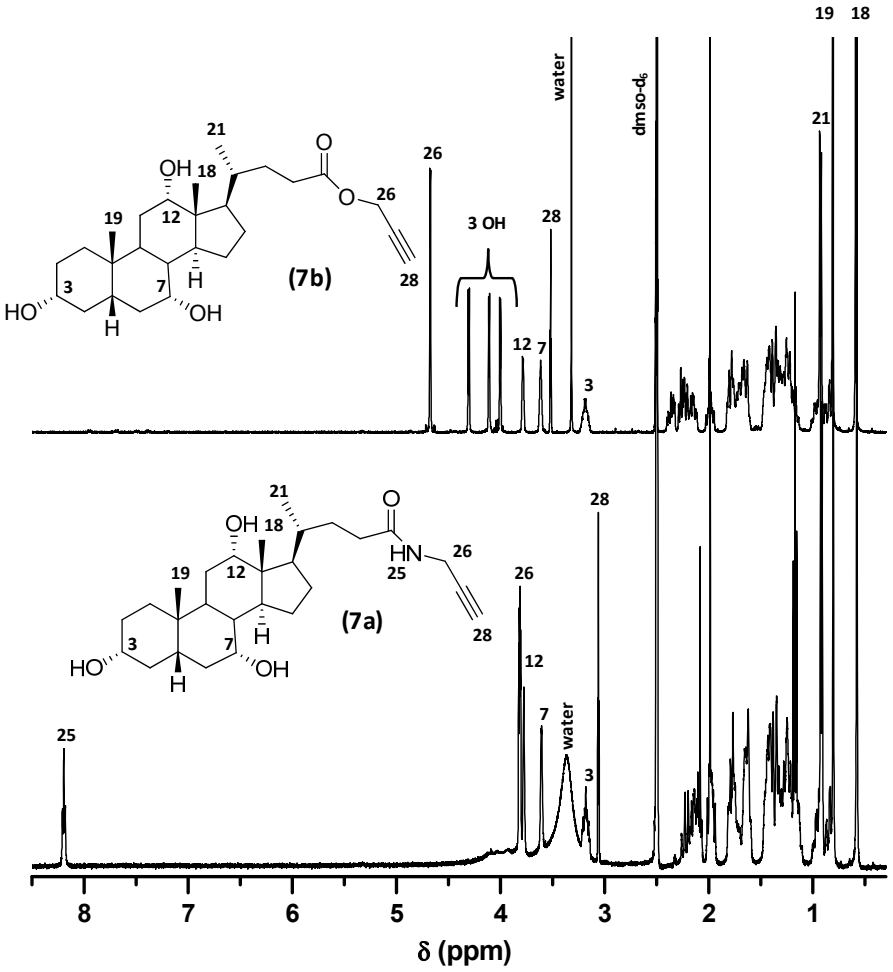

Figure 3.4: ^{1}H NMR spectra of **7a** (bottom) and **7b** (top) in DMSO-d_6.

Using similar reaction conditions, cholanoate **7b** containing a thermal alkyne functionality was obtained in 81 % yield by coupling the carbodiimide-activated cholic acid **6** with propargyl alcohol. The ^{1}H NMR spectrum of compound **7b** is shown in Figure 3.4.

The resonance signal of the protons of the C26-position at 4.67 ppm and the alkyne proton at 3.52 ppm for the propargyl group confirmed the successful esterification.

In order to obtain cholic acid-based azides, **7a** was activated using methanesulfonyl chloride with a 1:1 stoichiometric ratio (**7a**: methanesulfonyl chloride). Due to the poor solubility of **7a** in DCM, the reaction was carried out in pyridine, which served as both the solvent and catalyst.

Figure 3.5 shows the ^{1}H NMR spectrum of **8a**. The CH proton signals of the C3-position with mesylate at 4.50 ppm, and of the C7-position with or without mesylate at 5.12 and 3.88 ppm, respectively, were detected. The two proton resonance signals of mesylate were clearly identified at 2.98 and 3.08 ppm. Although the equatorial hydroxyl group at the C3-position is more reactive than that at the axial C7-position, a mixture of products having activated OH groups at the C3- and C7-positions, with methanesulfonyl chloride, was obtained after the reaction. While only one spot was observed by TLC that was assigned to the main product by activating the C3-position, ^{1}H NMR analysis of different column chromatography fractions confirmed the presence of a mixture of activated compounds. Integrating the ^{1}H NMR peaks revealed that the main fraction from column chromatography (one spot by TLC) contained 15 % of the product having activated OH groups at both the C3- and C7-positions. Therefore, the compound obtained from methanesulfonyl chloride required additional purification by column chromatography. This significantly decreased the yield due to the similar polarity of products activated at the C3-position and both C3- and C7-positions. To overcome this problem, OH groups at C7- and C12-positions had to be protected prior to activation with methanesulfonyl chloride.

Alternatively, activation of the OH group with 4-toluenesulfonyl chloride (TsCl) was used. Activation by tosylating one of the hydroxyl groups of cholic acid derivatives did not require protecting group chemistry. This is because the equatorial hydroxyl group at the C3-position is more reactive than the sterically-hindered hydroxyls at the axial C7- and C12-positions of cholic acid.[103] In addition, the bulky tosylate is less reactive towards the hydroxyls than smaller groups such as triflate or mesylate.[105] This makes it more selective

to reacting at the C3-position. This also avoids the chromatographic purification step of the tosylate prior to the azidation, thus significantly improving the yield.[103]

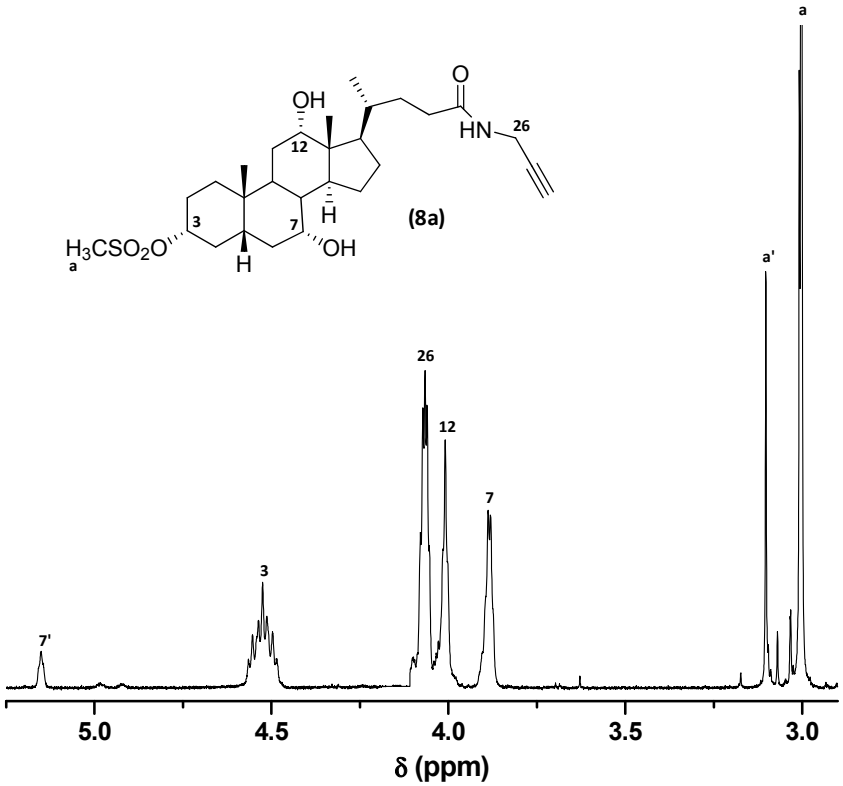

Figure 3.5: ^{1}H NMR spectrum of **8a** in $CDCl_3$ (numbers with prime associated with the product obtained from the reaction of the OH at the C7-position with methanesulfonyl chloride).

With a modified tosylation procedure from Gouin and Zhu,[80] **8b** was obtained in 86 % yield. Selective activation with 4-toluenesulfonyl chloride only at the C3-position was confirmed by the conversion of 3α-CH proton signal at 3.18 ppm of **7a** (Figure 3.4) to 4.25 ppm of **8b** (Figure 3.6), and also only one spot of **8b** was seen by TLC. The ^{1}H NMR spectrum of **8b** is presented in Figure 3.6. No change in the chemical shift was observed for the axial CH protons signals at the C7- and C12- positions at 3.58 and 3.75 ppm, respectively, confirming that only the hydroxyl group at C3 was substituted.

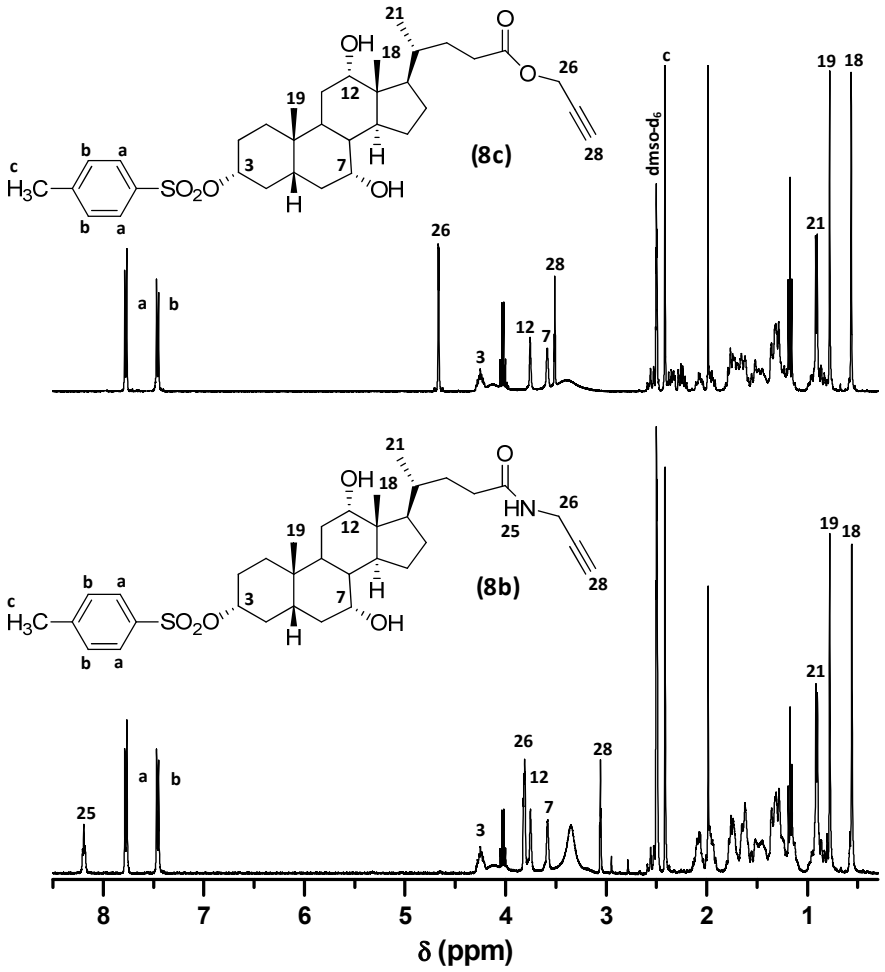

Figure 3.6: ^{1}H NMR spectra of **8b** (bottom) and **8c** (top) in DMSO-d_6.

Similarly, **7b** was reacted with 4-toluenesulfonyl chloride yielding a C3-activated product. The ^{1}H NMR spectrum of **8c** is shown in Figure 3.6. Thus, no column chromatography was required for this step prior to azidation.

Different conditions for the azidation of 3α-mesyloxy-5β-cholan-24-oic acid methyl ester **3** were used for preparing **8a**, **8b** and **8c** due to the presence of unprotected alkyne groups. While high reaction temperatures (80-90 °C) were used in the case of 3α-mesyloxy-5β-cholan-24-oic acid methyl ester **3**, the nucleophilic substitution of mesylate or tosylate by an azide for **8a**, **8b** and **8c** was conducted at 45 °C. This was to improve the solubility of

sodium azide (NaN_3) in DMF. Mild conditions were required to avoid side reactions, such as the undesired polymerization. But these lead to longer reaction times.

As reported earlier, an inversion in the configuration of the equatorial 3α to axial 3β occurs during the azidation with sodium azide. This is typical of an S_N2 substitution.[103] Complete substitution of the tosylate to an azide was important to increase the yield and significantly simplify purification of the final product **9a** or **9b**. Therefore, an excess of sodium azide was used to improve the yield.

The ^{1}H NMR signal of the CH proton of cholic acid derivatives at the C3-position is a clear indicator of both the stereochemistry and reaction progress. The NMR signals of the equatorial 3α-proton of **7a** or **7b** at 3.18 ppm and **8b** or **8c** at 4.25 ppm were broad multiplets (Table 3.2; Figure 3.4 and Figure 3.6, respectively). Meanwhile, the axial 3β proton signal of **9a** and **9b** at 3.99 ppm (Table 3.2; Figure 3.7) was sharp, similar to the axial CH protons at the C7- and C12-positions at 3.62 ppm and 3.78 ppm, respectively.

The structures of **7a**, **7b**, **9a** and **9b** also were confirmed by ^{13}C NMR (Table 3.3), FTIR spectroscopy and mass spectrometry (experimental section).

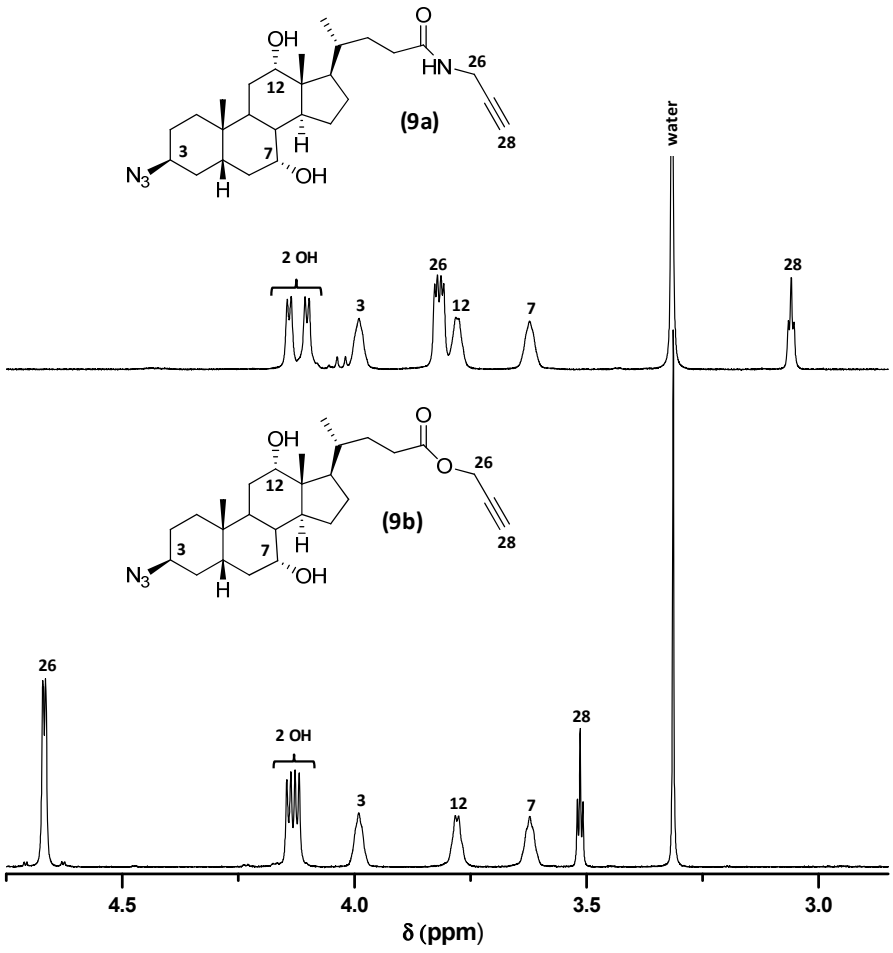

Figure 3.7: ^{1}H NMR spectra of **9a** (top) and **9b** (bottom) in DMSO-d_6.

Table 3.2: ^{1}H NMR chemical shifts (in ppm) of the cholic acid-containing compounds in DMSO-d_6.

Position	**7a**	**8b**	**9a**	**7b**	**8c**	**9b**
3	3.18	4.25	3.99	3.18	4.25	3.99
7	3.61	3.58	3.62	3.62	3.58	3.62
12	3.78	3.75	3.78	3.78	3.76	3.78
18	0.58	0.56	0.58	0.59	0.57	0.59
19	0.81	0.78	0.85	0.81	0.78	0.85
21	0.92	0.92	0.92	0.93	0.91	0.92
25	8.19	8.19	8.19	-	-	-
26	3.82	3.81	3.81	4.67	4.67	4.67
28	3.06	3.06	3.06	3.52	3.51	3.51

Table 3.3: ^{13}C NMR chemical shifts (in ppm) of the cholic acid-containing compounds in DMSO-d_6.

Carbon	**7a**	**9a**	**7b**	**9b**
3	70.31	58.26	70.32	58.36
7	66.13	66.05	66.13	66.15
12	70.89	70.88	70.87	70.96
18	12.25	12.23	12.22	12.30
19	22.53	22.63	22.51	22.73
21	17.00	17.00	16.77	16.88
24	172.26	172.24	172.49	172.58
26	31.46	31.45	51.33	51.44
27	81.31	81.30	78.47	78.57
28	72.60	72.59	77.33	77.43

Alternatively, **9a** and **9b** could be prepared by activating the OH group at the C3-position with 4-toluenesulfonyl chloride followed by sodium azide substitution. These were then coupled with propargyl amine or propargyl alcohol via the carboxylic group of cholic acid (Figure 3.8, right). While the reactivities of the compounds in both strategies are similar, the solubility of cholic acid-based amides **7a**, **8a** or **8b** and esters **7b** or **8c** in common organic solvents is much higher than 3α-(4-methylphenyl)sulfonyloxy-7α,12α-dihydroxy-5β-cholan-24-oic acid **7c** or 3β-azido-7α,12α-dihydroxy-5β-cholan-24-oic acid **8d**.

Similar procedures for the tosylation of **7a** or **7b** afforded 3α-(4-methylphenyl)sulfonyloxy-7α,12α-dihydroxy-5β-cholan-24-oic acid **7c** in 68 % yield. However, a higher temperature (90 °C) was used for the azidation reaction due to the absence of the unprotected alkyne group.

Another synthetic route may be used for the synthesis of monomer **9a** or **9b**. Due to the poor solubility of cholic acid-based **7c** and **8d**, the yield of monomer **9a** (Figure 3.8, right) was much lower than in the case of **9a**, which was prepared by first coupling at the C24-position (Figure 3.8, left). Thus, this alternate synthetic route was not used further for the synthesis of cholic acid-based amide and ester monomers (**9a** and **9b**).

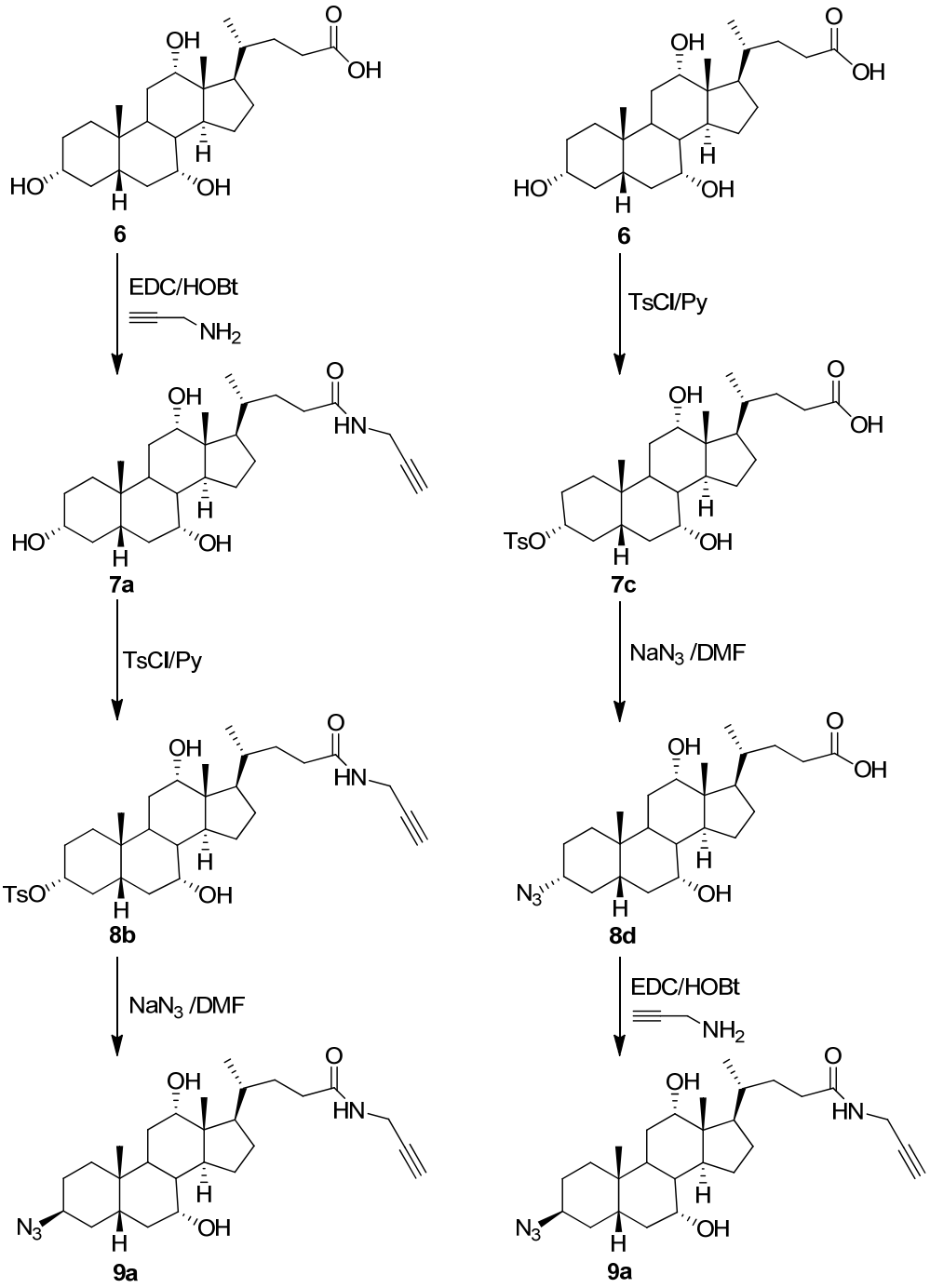

Figure 3.8: Two routes for the synthesis of ω-alkyne-α-azide cholic acid derivative **9a** from cholic acid **6**.

3.2 Polymer syntheses

3.2.1 Synthesis of bile acid-based polymers via polycondensation

The polycondensation of monomers based on cholic acid and deoxycholic acid cannot be done at high temperature due to the presence of additional reactive sites at the C7- and C12-positions. These may cause branching and crosslinking of the resulting polymers.[76] Alternatively, polyesters can be prepared at room temperature via carbodiimide coupling due to the higher reactivity of C3-OH position than the C7- and C12-OH.[14] The stereochemistry of the C3-position changed from the more reactive equatorial to the less reactive axial orientation, when C3-OH activated with methanesulfonyl chloride or 4-toluenesulfonyl chloride was substituted with sodium azide. Therefore, only lithocholic acid with one OH group was used in order to synthesize the polymers via polycondensation. Due to the low solubility of the lithocholic acid-based monomer **5**, melt polymerization was conducted. High temperatures and long reactions are essential to obtain high molecular weight polymers via polycondensation.[106] The melting point (T_m) of **5** was 127 °C, as determined by DSC using a heating 10 °C·min^{-1}. Thermogravimetric analysis (TGA) showed a high-temperature stability of **5** with an onset of decomposition at 210 °C (Figure 3.9). Therefore, lithocholic acid-based monomer **5** was polymerized in bulk at 180 °C under vacuum to obtain the polyamides (Figure 2.4). When melt polycondensation was conducted with monomer **5** for 8 h or higher, insoluble polymers were obtained. The solubility of obtained polymers were tested in common organic solvents such as $CHCl_3$, DCM, THF, ethyl acetate, toluene, methanol and even DMF and DMSO.

The FTIR spectra of the polyamide **10** (Figure 3.10) exhibited a characteristic absorption band for N–H stretching at 3223 cm^{-1}, corresponding to a secondary amide. The bands at 2927 and 2862 cm^{-1} were attributed to the aliphatic C–H stretching. The presence of the amide carbonyl group (amide-I band) was indicated by a strong band at 1643 cm^{-1}.

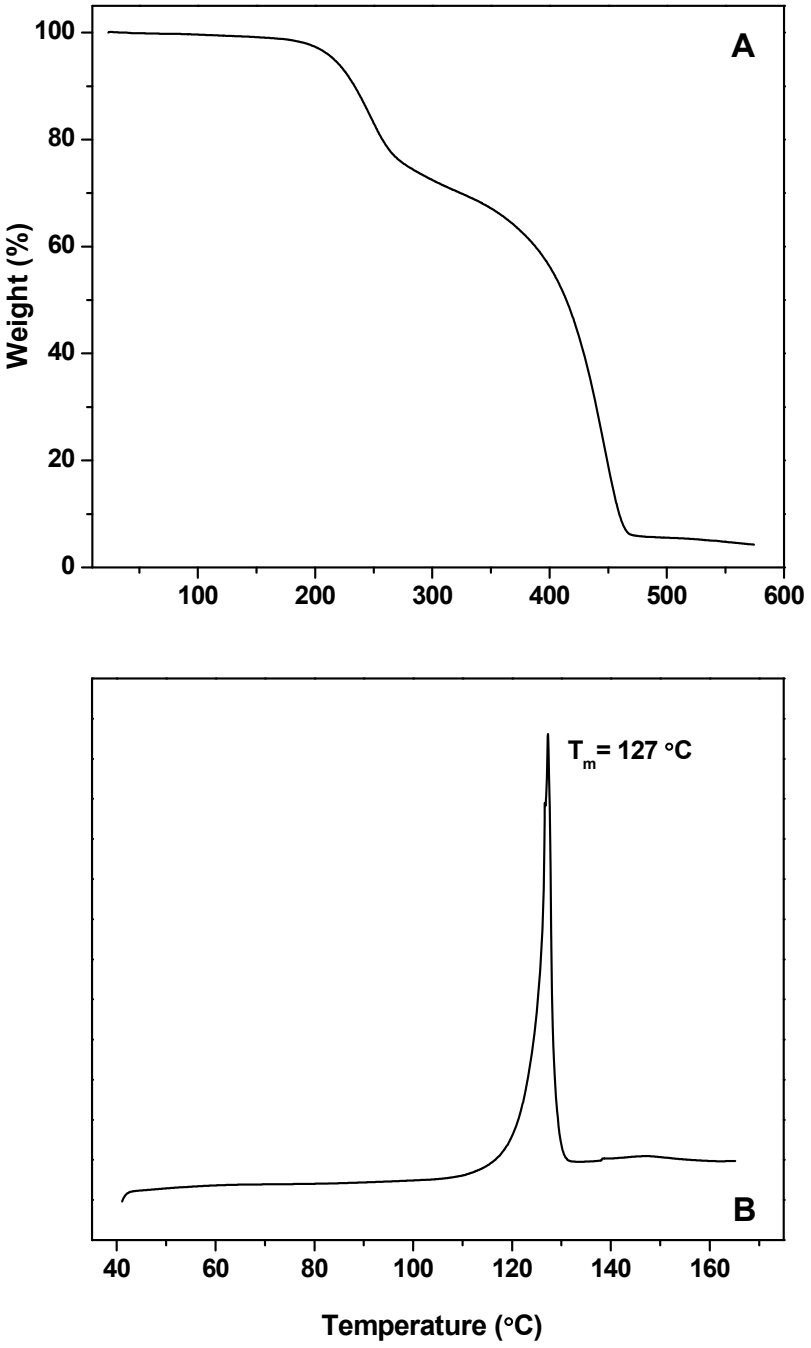

Figure 3.9: (A) TGA trace of lithocholic acid-based monomer **5**; (B) DSC heating curve of the first thermal cycle for compound **5**. Heating and cooling rate: 10 °C·min^{-1}.

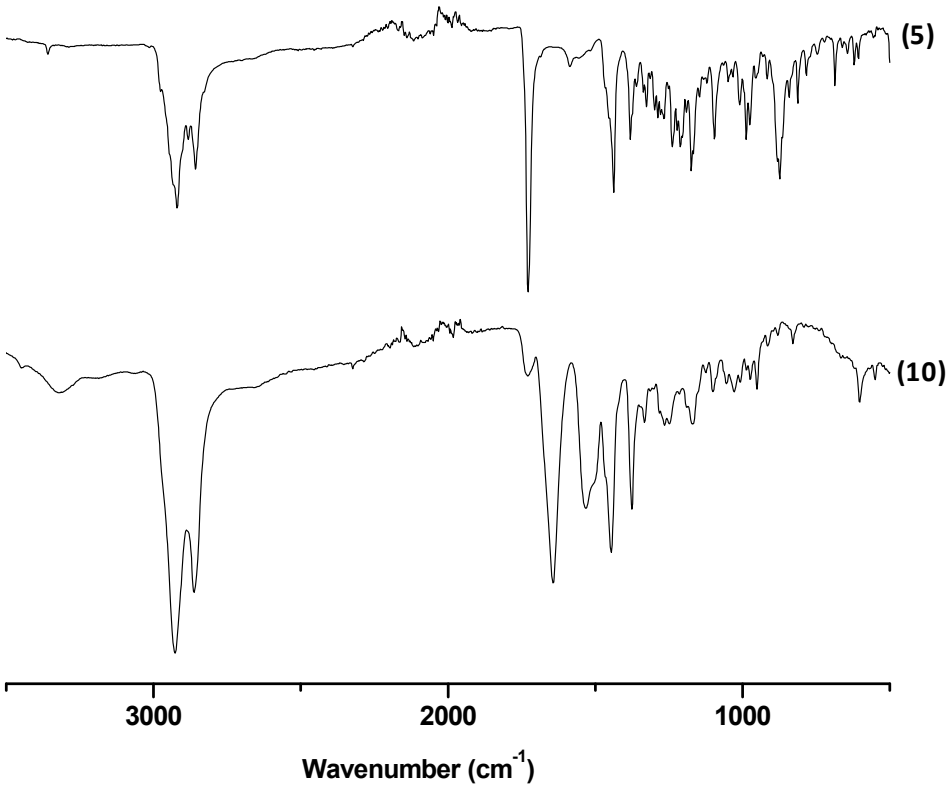

Figure 3.10: The FTIR spectra of **5** (top) and **10** (bottom).

The band at 1531 cm^{-1} was attributed to the N–H bending vibration (amide-II band).[107] The reaction success was confirmed by the disappearance of a strong band of the ester carbonyl group at 1729 cm^{-1}.

The low solubility of polyamide **10** after 8 h or higher may be due to the rigid steroid structure and the hydrogen bonds of the amide group as well as the high molecular weight of polymers. Polymerization under the same conditions for 5 h yielded a soluble product in chloroform. Gel permeation chromatography (GPC) revealed that the product was a low molecular weight oligomer with $M_n \sim 2\ 500\ g \cdot mol^{-1}$ (PDI ~ 1.56). The GPC analysis was performed with the sample after precipitating in diethyl ether (Figure 3.11).

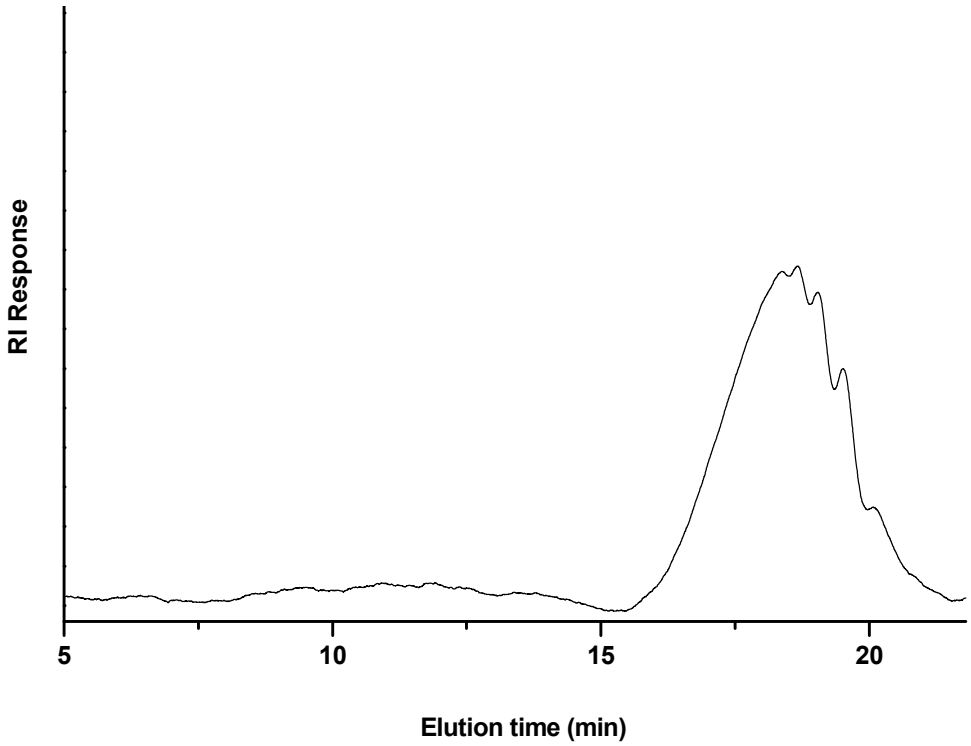

Figure 3.11: GPC chromatogram of oligomer **10**: $CHCl_3$; flow rate: 1 $mL \cdot min^{-1}$; temperature: 25 °C.

The ^1H NMR spectra of monomer **5** and oligomer **10** in $CDCl_3$ are shown in Figure 3.12. The resonance signal of the CH protons at the C3-position at 3.26 ppm was shifted to 4.17 ppm after polycondensation. The concomitant vanishing of the proton resonance signals of the methyl ester group protons at C26 as well as the appearance of the amide signals at 5.66 ppm clearly confirmed the formation of the amide bonds between the lithocholic acid moieties.

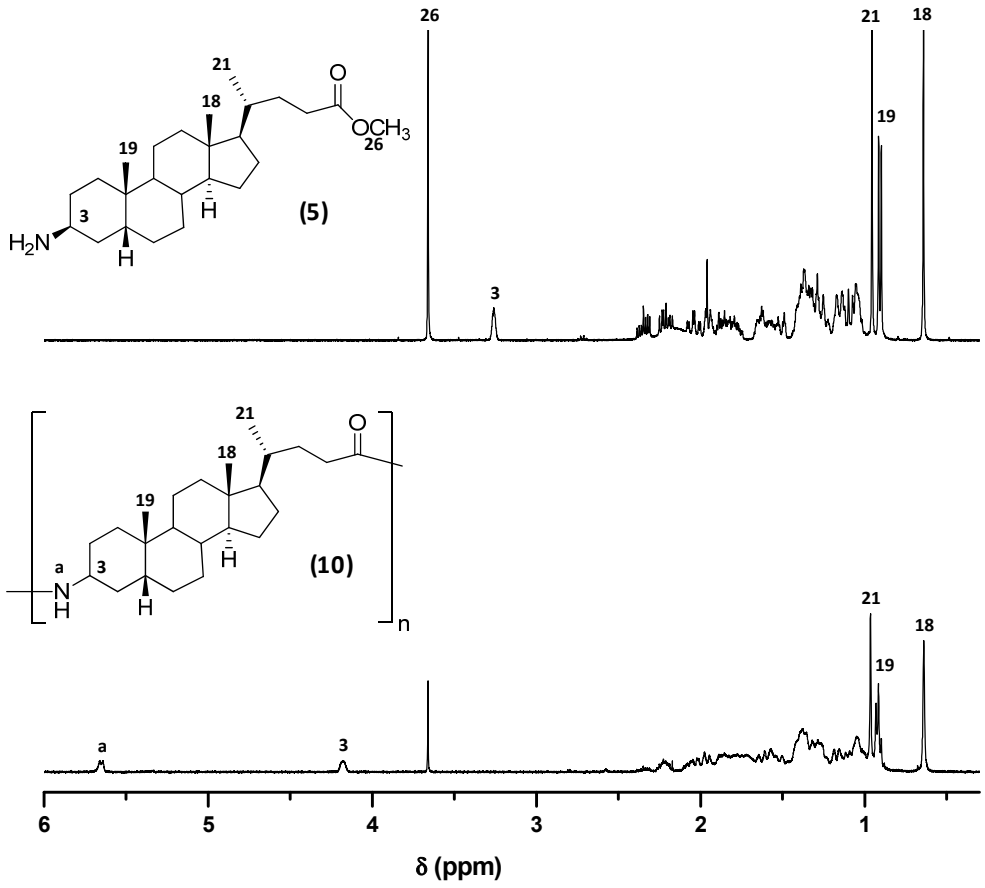

Figure 3.12: ^{1}H NMR spectra of **5** (top) and **10** (bottom) in $CDCl_3$.

3.2.2 Synthesis of bile acid-based polymers via copper(I)-catalyzed azide-alkyne cycloaddition

The step-growth polymerization reaction conditions of the heterofunctional cholic acid derivatives **9a** and **9b** by alkyne-azide coupling (Figure 2.5) are summarized in Table 3.4. The ^{1}H NMR analysis of **11** in DMSO-d_6 confirmed the formation of 1,4-disubstituted triazole rings through the emergence of characteristic signals from the triazole at 7.90 ppm and the C3-proton adjacent to the triazole at 4.59 ppm. Further evidence was from the disappearance of the alkyne signals at 3.06 ppm and the C3-proton adjacent to the azide group at 3.99 ppm (Figure 3.13).

Table 3.4: Polymerization conditions and the polymer properties.

polymer	catalyst[a]	M_n [b]	M_w/M_n [b]	DP[c]
11	CuBr/PMDETA	23 900	1.69	51
12	CuBr/PMDETA	25 500	1.63	54
13	$CuSO_4 \cdot 5H_2O$/SA	5 200	1.48	11, 10[d]

[a] Polymerization catalyzed by CuBr/PMDETA (N,N,N',N",N"-pentamethyldiethylene triamine) in DMF at 80 °C for 120 h or by $CuSO_4 \cdot 5H_2O$/sodium ascorbate (SA) in a *t*-BuOH/H_2O mixture at 60 °C for 120 h. [b] M_n and M_w ($g \cdot mol^{-1}$): number- and weight-average molecular weights obtained by GPC analysis. [c] Degree of polymerization. [d] Calculated from ^{1}H NMR data.

The polymerization of **9b** was accompanied by the disappearance of the ^{1}H NMR resonance signals of the alkyne group proton at 3.51 ppm and the C3-proton adjacent to the azide group at 3.99 ppm. There also was the emergence of the triazole proton at 8.17 ppm, and a C3-proton adjacent to the triazole at 5.10 ppm (Figure 3.14).

For all the polymers, the GPC analyses showed a monomodal molecular weight distribution (Figure 3.15) and a relatively low polydispersity index of 1.6-1.7. The polyamide **11** and polyester **12** had a number-average molecular weight of 23 900 and 25 500 $g \cdot mol^{-1}$, respectively, corresponding to a degree of polymerization of over 50 in both cases (Table 3.4). This indicated that there was no significant difference in the reactivities of **9a** and **9b**.

The polymerization of **9a** was also carried out in a *tert*-butanol/water (*t*-BuOH/H_2O) mixture and it was catalyzed by $CuSO_4 \cdot 5H_2O$/sodium ascorbate (SA) under nitrogen. A few minutes after starting the reaction (~ 15 min), the resulting polymer started to precipitate. The stirring was continued for 120 h. After purification, the polymer **13** was poorly soluble in common organic solvents, such as chloroform, dichloromethane or tetrahydrofuran, but it dissolved in DMF and DMSO.

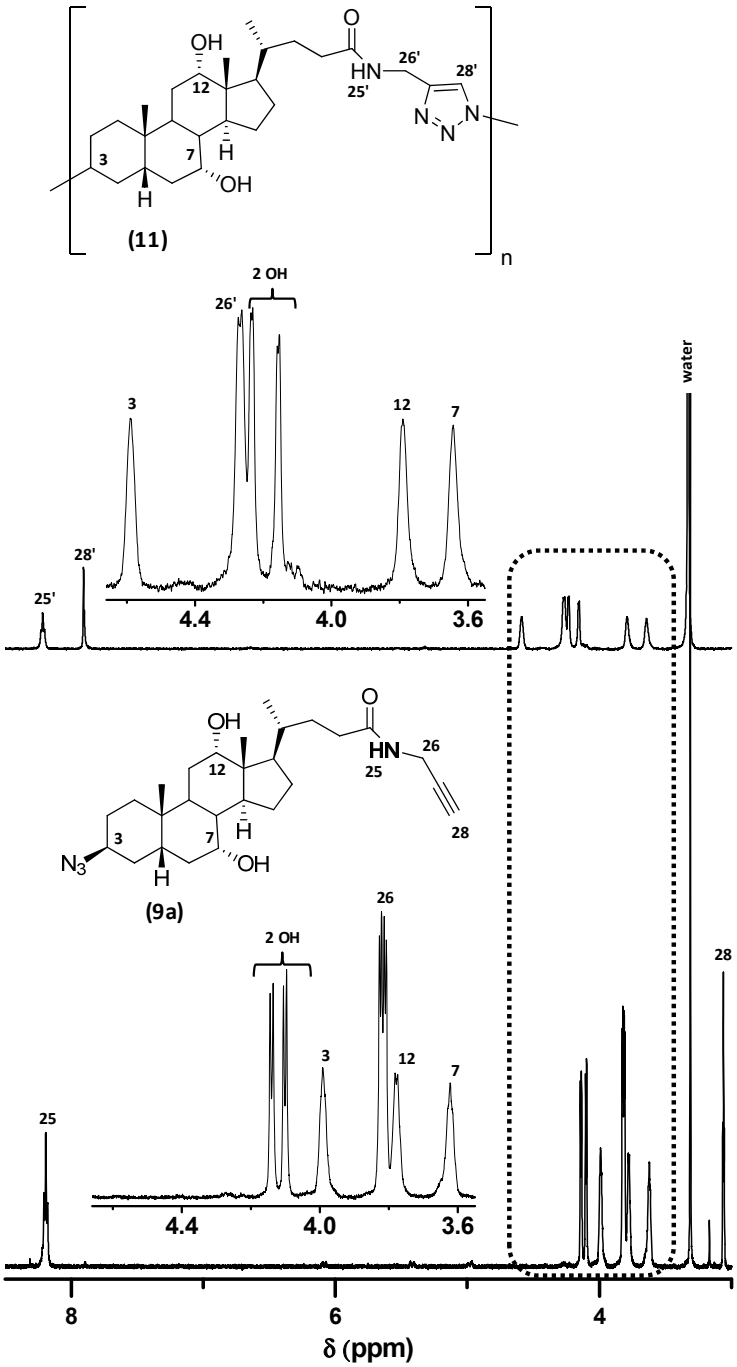

Figure 3.13: ^{1}H NMR spectra of the heterofunctional monomer (bottom) **9a** and of the corresponding polyamide **11** (top) recorded at room temperature in DMSO-d_6. The insets correspond to the expanded regions of the spectra marked with dashed lines.

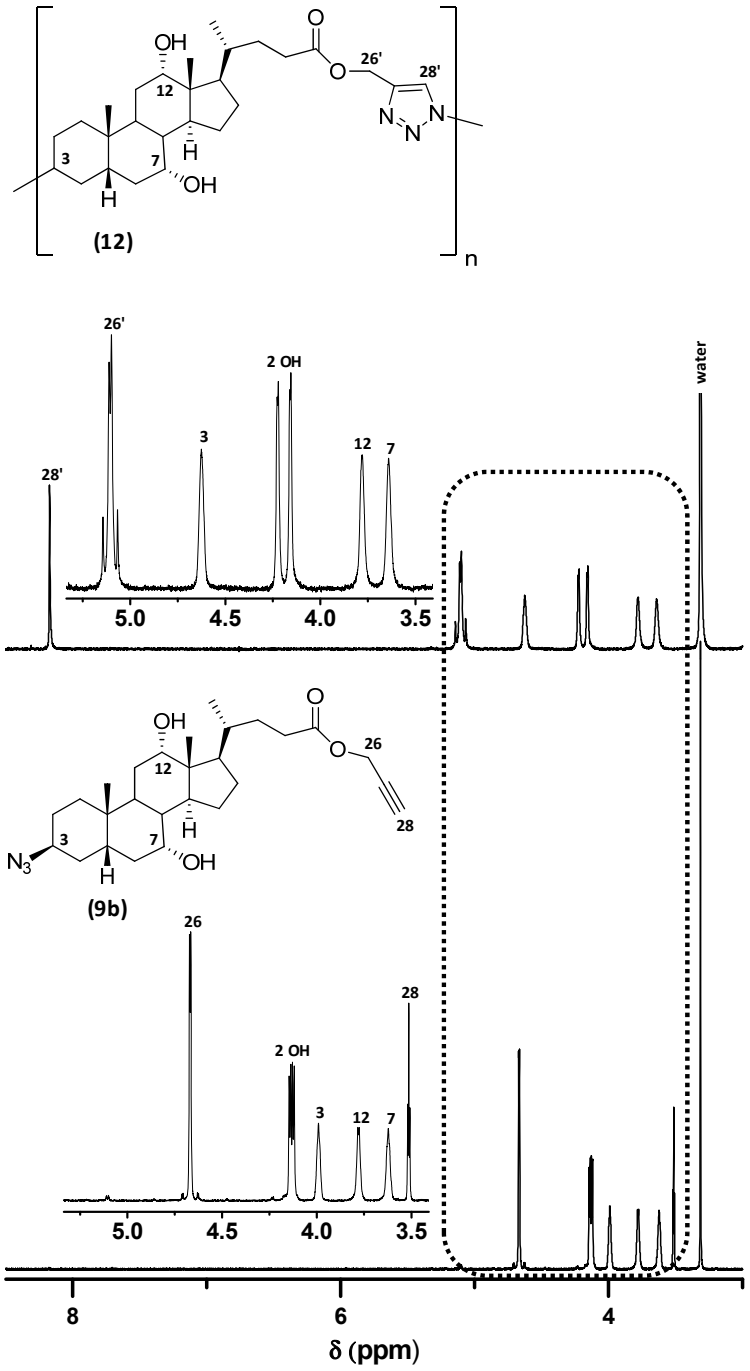

Figure 3.14: ^{1}H NMR spectra of the heterofunctional monomer (bottom) **9b** and of the corresponding polyester **12** (top) recorded at room temperature in DMSO-d_6. The insets correspond to the expanded regions of the spectra marked with dashed lines.

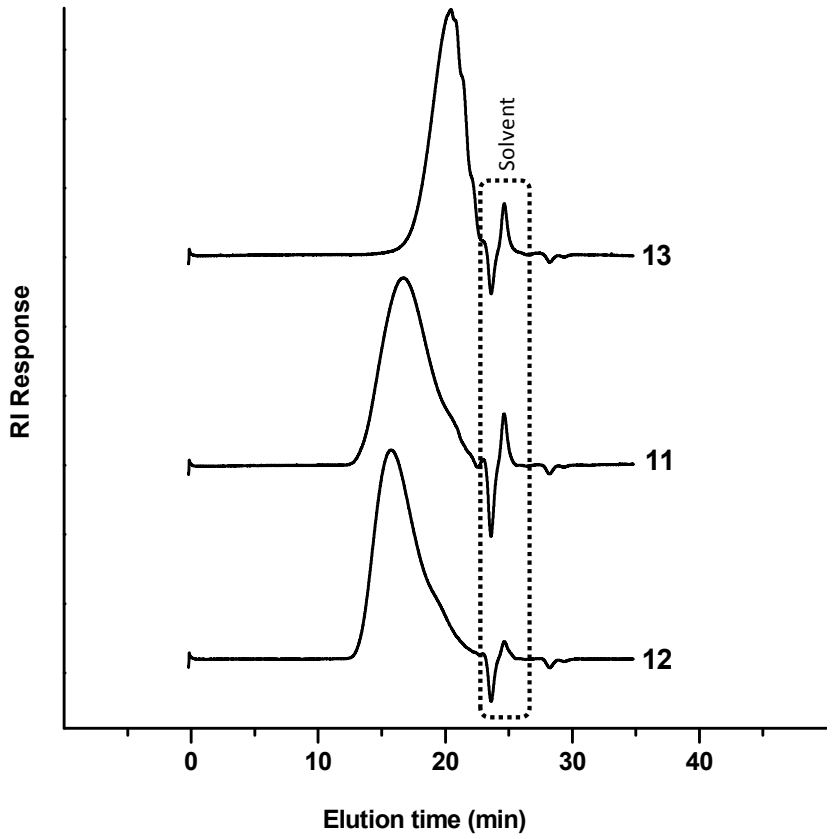

Figure 3.15: GPC chromatograms of polyamides **11** and **13**, and polyester **12**: DMF; flow rate: 1 mL·min^{-1}; temperature: 25 °C.

The molecular weight (M_n) was low (5 200 g·mol^{-1}, Table 3.4), most likely due to the poor solubility of the polyamide formed in *t*-BuOH/H_2O. Since the molecular weight in this case was relatively low, it was also estimated from ^{1}H NMR (Table 3.4). This was done by comparing the integrated area of the alkyne end group signal at 3.06 ppm to the triazole signal in the main chain at 7.90 ppm (Figure 3.16).

In comparison, the polymerization of **9a** in dry DMF at 80 °C with CuBr/PMDETA as the catalyst, where no precipitation occurred, led to a 5-fold increase in the molecular weight of the polyamide. Owing to their high molecular weights, neither polyamide **11** nor polyester **12** showed the azide and alkyne end group signals in ^{1}H and ^{13}C NMR spectra (Figure 3.13 - 3.14, Table 3.5 - 3.6).

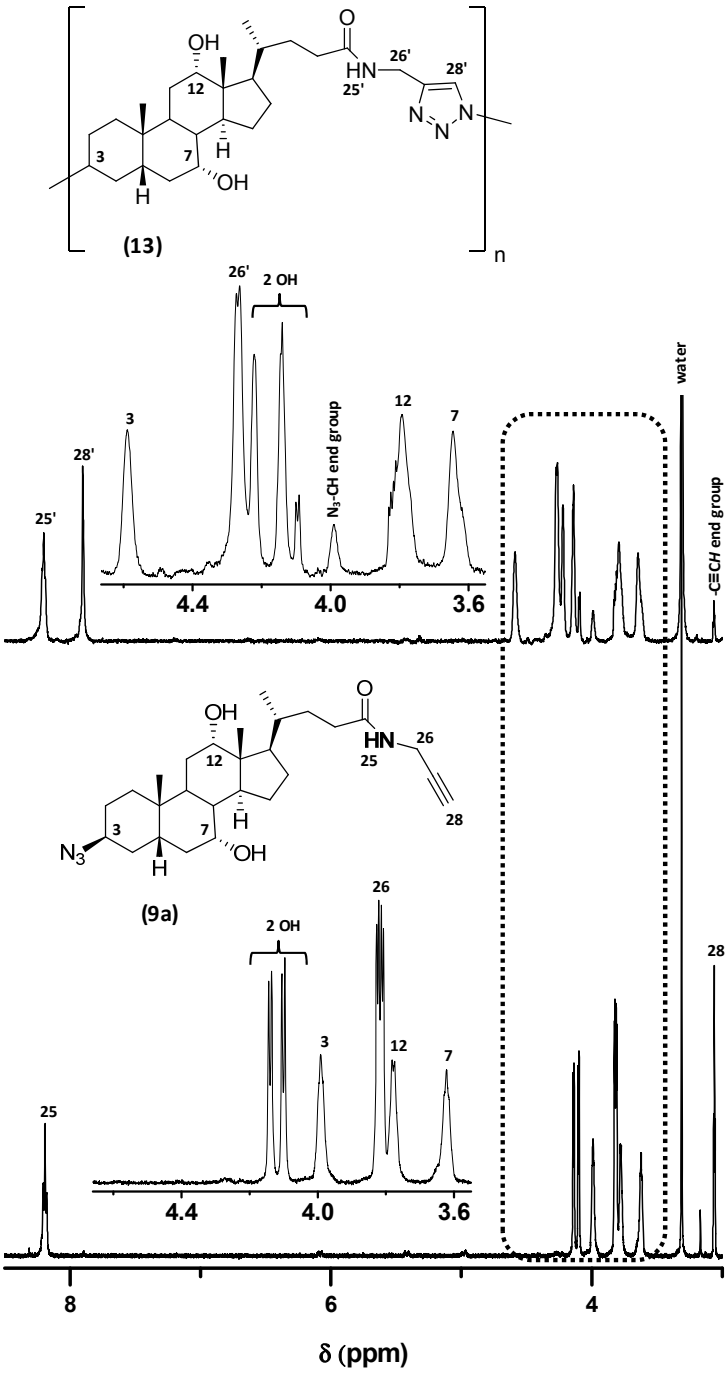

Figure 3.16: ^{1}H NMR spectra of the heterofunctional monomer (bottom) **9a** and of the corresponding polyamide **13** (top) recorded at room temperature in DMSO-d_6. The insets correspond to the expanded regions of the spectra marked with dashed lines.

Table 3.5: ^{1}H NMR chemical shifts (in ppm) of the cholic acid-containing polymers in DMSO-d_6.

Position	**11**	**12**	**13**
3	4.59	4.63	4.59; 3.99*
7	3.64	3.64	3.64
12	3.79	3.78	3.80
18	0.58	0.56	0.58
19	0.79	0.78	0.85
21	0.92	0.90	0.92
25	8.22	-	8.20
26	4.27	5.10	4.27
28	-	-	3.06*
28'	7.91	8.17	7.90

Table 3.6: ^{13}C NMR chemical shifts (in ppm) of the cholic acid-containing polymers in DMSO-d_6.

Carbon	**11**	**12**	**13**
3	55.69	55.90	55.69; 58.26*
7	66.08	66.07	66.08
12	70.91	70.87	70.91
18	12.24	12.19	12.24
19	22.66	22.64	22.65
21	17.04	16.80	17.04
24	172.41	172.95	172.40
26	31.54	56.94	31.54
27	-	-	81.31*
27'	121.72	123.77	121.73
28	-	-	72.60*
28'	144.35	144.36	144.38

* value for the end group

Additional proof for the formation of main-chain cholic acid-based polymers is shown in the FTIR spectra of the obtained polytriazoles **11**-**13** (Figure 3.17).

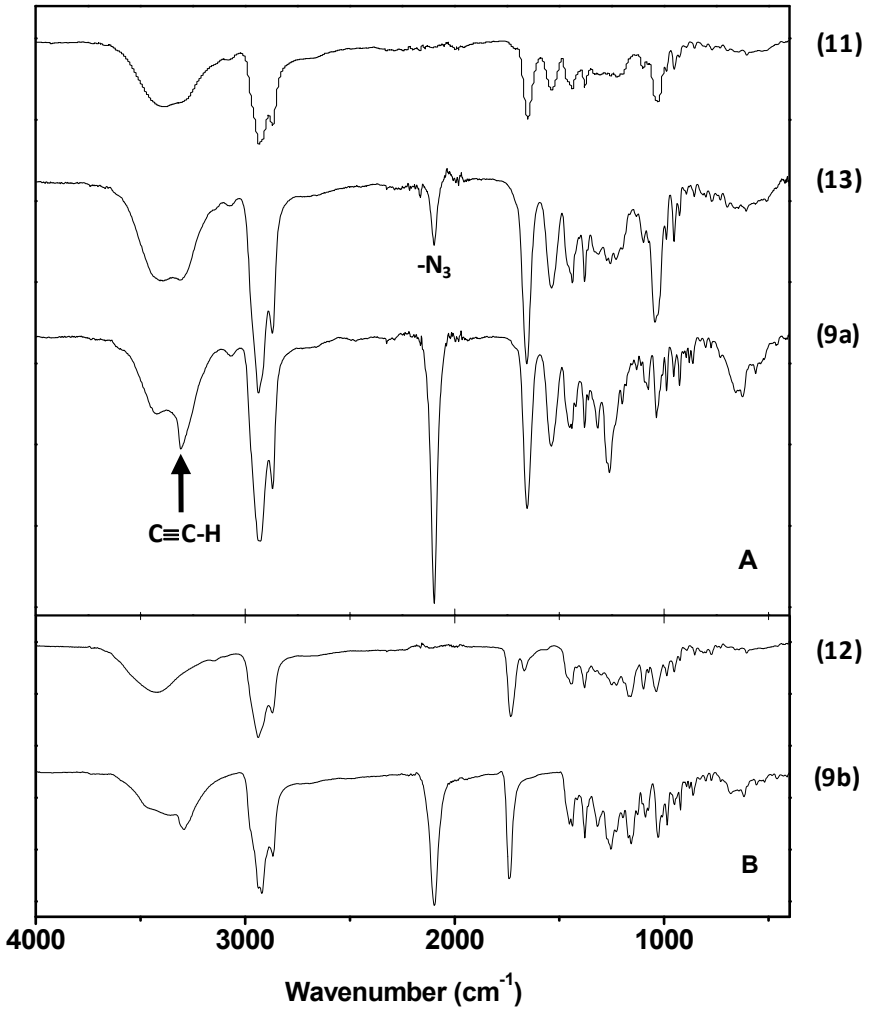

Figure 3.17: (A) (top) FTIR spectra of **9a**, polyamides **13** and **11**, (B) (bottom) FTIR spectra of **9b** and polyester **12**.

The bands at 3306 and 2095 cm^{-1} of **9a** disappeared in the spectrum of polyamide **11** and polyester **12** after the polymerization, indicating that most of the -C≡CH and $–N_3$ groups were transformed to triazole rings.

3.3 Thermal and mechanical properties of bile acid-based polyamides and polyesters

Thermogravimetric analysis (TGA), differential scanning calorimetry (DSC), and dynamic mechanical analysis (DMA) were conducted on polymer films cast from DMF solutions (100 mg/mL). These were done to study the effect of the chemical structure on the thermal behavior of polymers. Thermograms and calorimetric curves of the samples are presented in the Figure 3.18 and the results are summarized in Table 3.7.

Table 3.7: Thermomechanical properties of polymer films

polymer	T_g (°C)[a]		T_d (°C)[b]	E (MPa)[c]
	DSC	DMA		
11	161 ± 0.6	155 ± 2.0	372 ± 3.0	659 ± 29
12	137 ± 0.8	139 ± 1.5	307 ± 6.0	282 ± 26
13	167 ± 1.6	N/A	365 ± 4.0	N/A

[a]Glass transition temperature determined by differential scanning calorimetry (DSC) and dynamic mechanical analysis (DMA). [b]Temperature corresponding to the onset of decomposition in thermogravimetric analysis. [c] Young's modulus measured from stress-strain curves at 30 °C.

All the polymers showed high resistance to thermal degradation with degradation onset temperatures, 307 °C ≤ T_d ≤ 372 °C. The polyamides were more thermally stable than the polyesters. The glass transition temperatures (T_g), determined by DSC, were in the range of 137 - 167 °C. None of the polymers exhibited melting transitions below the degradation temperature, which points to the amorphous nature of the materials. This behavior corresponds well with that of a rigid polyester prepared by the direct polycondensation of cholic acid, which showed a low crystallinity.[14] Our earlier observations on main chain-functional bile acid-based polymers also showed an amorphous character.[86]

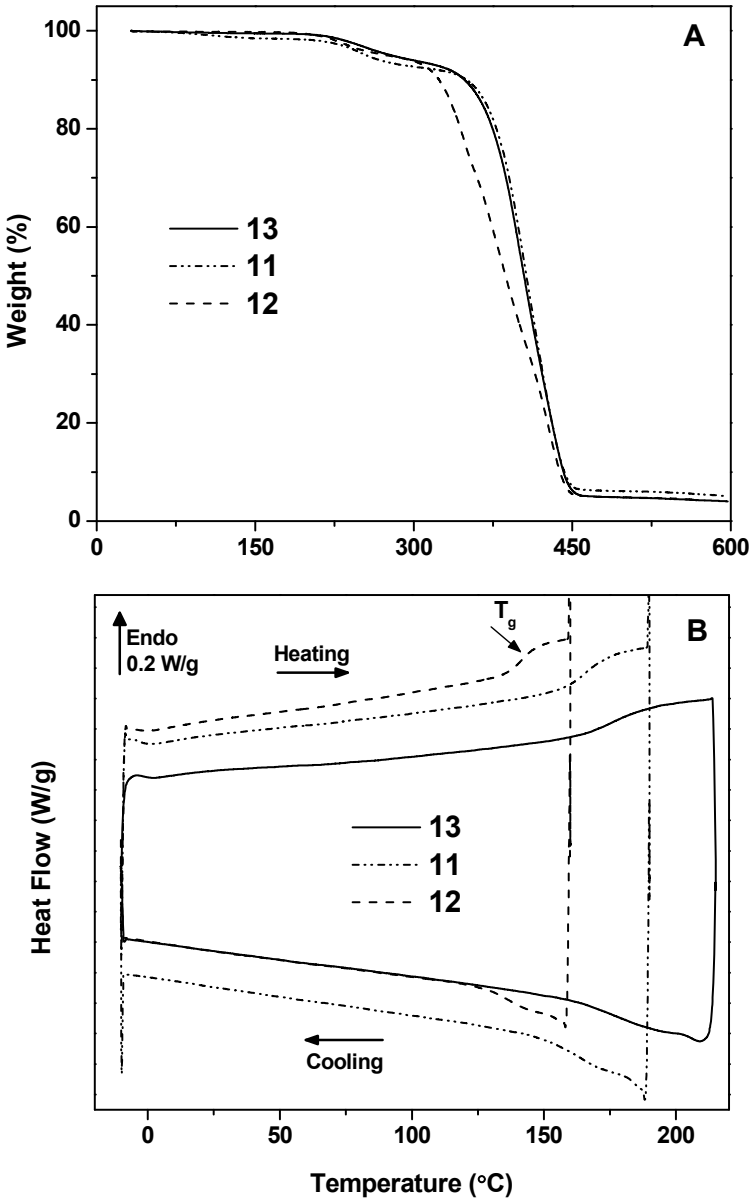

Figure 3.18: (A) TGA traces of polyamides **11** (dash-dot), **13** (solid), and polyester **12** (dash); (B) Heating and cooling curves of the second thermal cycles for polyamides **11** (dash-dot), **13** (solid) and polyester **12** (dash) by DSC. Heating and cooling rate: 10 °C·min^{-1}. Arrow points to the glass transition temperature (T_g) of **12**.

The triazole linker may contribute to the high T_g because of its proximity to the steroid ring. This imposes strong steric constraints along the polymer backbone and thus increases the chain rigidity, as well as through hydrogen bonding.[90] The replacement of the amide by an ester in the polymers of similar molecular weight (**11** and **12**) decreased the T_g by ca. 24 °C and the T_d by ca. 65 °C (Table 3.7). This is a result of the higher rigidity and thermal stability of amide-containing polymers. A similar effect of the chemical structure on the T_g was observed with cholic acid and lithocholic acid-based main chain-functional polyester-amides and polyesters bearing long alkyl spacers between the bile acid moieties. Both the amide and multiple hydroxyls of the cholic acid significantly increase the T_g.[86] Usually, the T_g decreases with increasing spacer length. As expected, the absence of a spacer between the steroid ring and the azide leads to a higher T_g for the triazole-linked polyester than the one obtained by Pandey and coworkers.[31]

Figure 3.19 shows the evolution of the storage modulus E' of the polyamide **11** and polyester **12** films with temperature, allowing the determination of T_g from the onset of the slope. The results were in accordance with those determined by DSC (Table 3.7).

Linear stress-strain response was observed for both polymers (Figure 3.20) with high values of Young's modulus (Table 3.7), characteristic of brittle polymers with amorphous character or low crystallinity. The polyamide had a higher Young's modulus than the polyester, confirming the enhanced hardness of the material caused by the amide bonds. The modulus of **11** at 30 °C was comparable to the one of a main chain-functional lithocholic acid-based polyester-amide bearing two amide bonds per repeating unit.[15] This further emphasizes the importance of the chemical structure of linkers on the polymer mechanical properties, but also warrants studies of the triazole-linked polymers based on other bile acids.

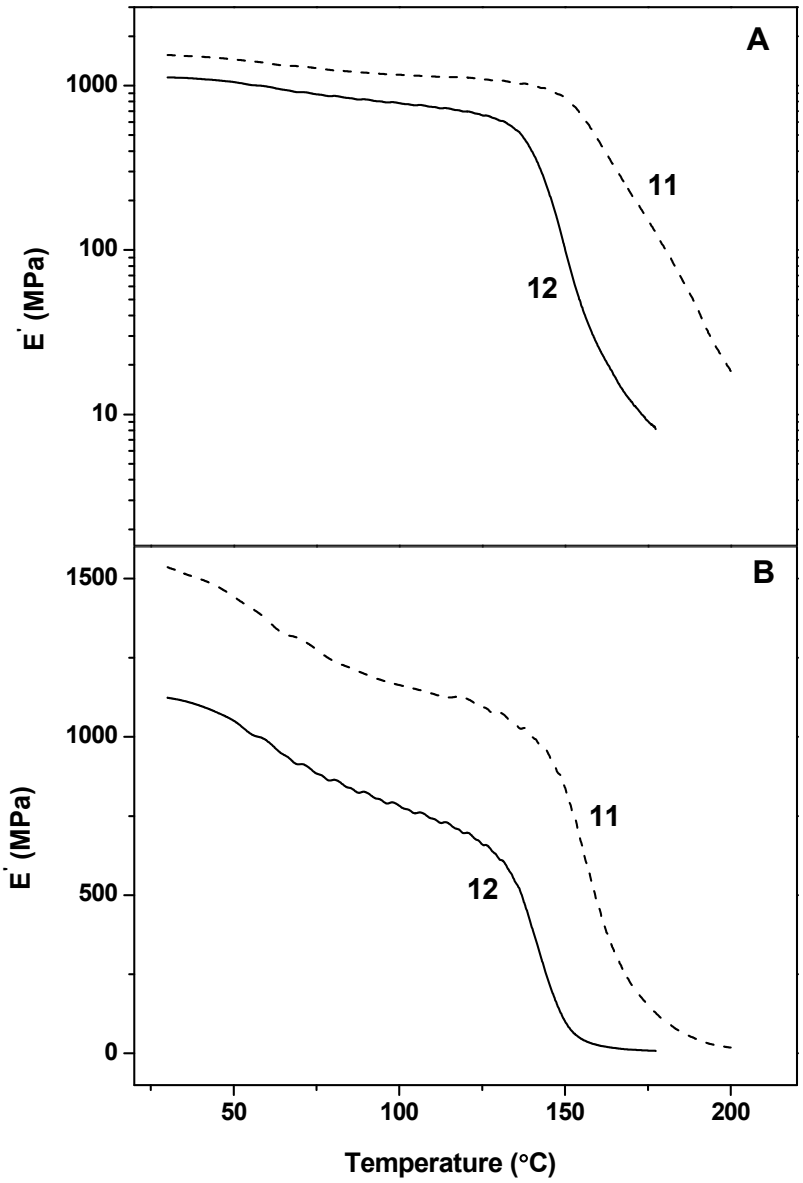

Figure 3.19: Evolution of the storage modulus of **11** and **12** with temperature determined by DMA at a frequency of 1 Hz, plotted with the logarithmic (A) and normal (B) scales. Measurements were made on rectangular samples (4 x 10 mm), with a preload force of 0.01 N, an amplitude of 2 μm, and a temperature sweep rate of 2 °C·min^{-1}.

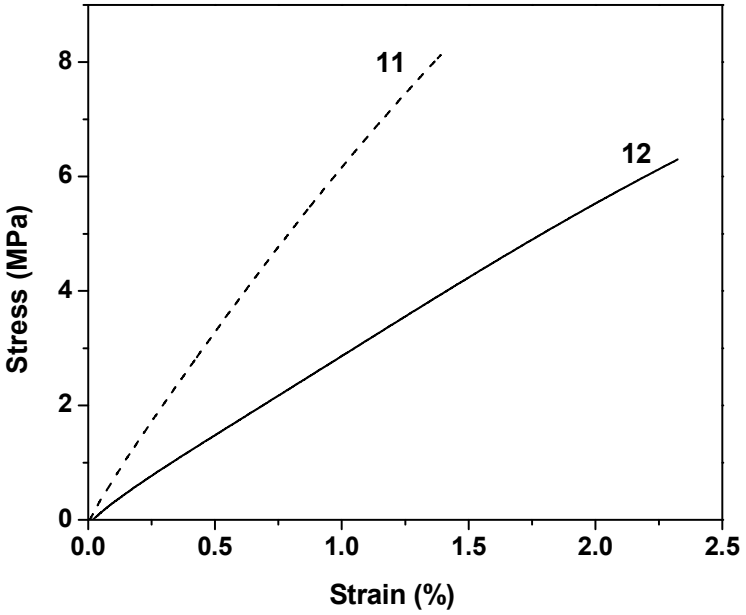

Figure 3.20: Stress-strain curves of polyamide **11** (dash) and polyester **12** (solid) obtained at 30 °C.

4 Conclusions

4.1 Polyamides obtained via polycondensation

The lithocholic acid-based monomer was successfully synthesized from lithocholic acid in four steps in good yield under mild conditions. The same synthetic strategy can be applied to other bile acids and related compounds. However, polycondensation conditions (high temperatures, vacuum) as well as the poor solubility of the bile acid-based derivatives limit the choice of monomer to lithocholic acid derivative since there are only two reactive groups on the steroid skeleton.

A lithocholic acid derivative was polymerized in bulk, yielding poorly soluble polymers in common organic solvents. A different reaction time was used to prepare polyamides having different molecular weights. Under 5 h, a soluble oligomer was obtained. In contrast, when the polymerization time was increased to 8 h or more, insoluble polyamides were obtained. The poor solubility of these polymers hindered further characterization and assessed their physical and mechanical properties.

4.2 Polyamides and polyesters obtained via CuAAC

The copper(I)-catalyzed azide-alkyne cycloaddition (CuAAC) is an attractive method for synthesizing triazole-linked polymers having a variety of functional groups.

Cholic acid was directly converted in high yields to monomers bearing azide and alkyne groups without any spacer groups. The azidation of the monomers occurred directly at the C3-position on the bile acid skeleton. A novel class of triazole-linked polyamides and polyesters derived from cholic acid was successful prepared by copper(I)-catalyzed step-growth polymerization of heterofuctional monomers in high yields. The polyamides were made for the first time and their properties have been compared to the polyester analogs.[108]

Polymers were synthesized under homogeneous and heterogeneous conditions yielding polymers with different molecular weights. The polymers synthesized under homogeneous conditions with a copper(I) bromide catalyst had moderate molecular weights

while heterogeneous conditions yielded polymers with low molecular weights and unimodal molecular weight distributions (PDI < 1.7). These polymers had very good solubility in polar organic solvents.

Triazole-linked polyamides and polyesters bearing cholic acid moiety in the main chain were thermally stable up to 307 °C. They had high glass transition temperatures and Young's moduli that were dependent on the chemical structure of the linker (amide *versus* ester). The polyamides tended to have higher T_g and higher moduli than their polyester counterparts.

4.3 Perspectives

This family of triazole-linked polymers may be further expanded by the inclusion of other bile acids or fatty acids. The microwave-assisted copper-mediated azide-alkyne coupling (CuAAC) may help to reduce the reaction times and to obtain bile acid-based polymers with relatively high molecular weights. It may also be interesting to use solvent- and catalyst-free strategies for preparing these polymers. This is because of thermal azide-alkyne cycloaddition has already proven to be effective in the synthesis of main chain-functionalized polymers and polymer networks. It may be useful to study the degradation of these polymers in a biological environment with the presence of enzymes.

It would be interesting to study the structural effects on the thermomechanical properties by introducing and changing the length and the nature of the spacer linkers between the bile acid moieties (ester, amide, triazole, urethane or imine) in the polymer main chain.

5 References

1. Michel, V. *Prog. Polym. Sci.* **2007,** *32*, (8–9), 755-761.
2. Sokolsky-Papkov, M.; Agashi, K.; Olaye, A.; Shakesheff, K.; Domb, A. J. *Adv. Drug Delivery Rev.* **2007,** *59*, (4–5), 187-206.
3. Nair, L. S.; Laurencin, C. T. *Prog. Polym. Sci.* **2007,** *32*, (8–9), 762-798.
4. Mano, J. F.; Silva, G. A.; Azevedo, H. S.; Malafaya, P. B.; Sousa, R. A.; Silva, S. S.; Boesel, L. F.; Oliveira, J. M.; Santos, T. C.; Marques, A. P.; Neves, N. M.; Reis, R. L. *J. R. Soc., Interface* **2007,** *4*, (17), 999-1030.
5. Constantinidis, I.; Rask, I.; Long Jr, R. C.; Sambanis, A. *Biomaterials* **1999,** *20*, (21), 2019-2027.
6. Yu, L.; Dean, K.; Li, L. *Prog. Polym. Sci.* **2006,** *31*, (6), 576-602.
7. Puppi, D.; Chiellini, F.; Piras, A. M.; Chiellini, E. *Prog. Polym. Sci.* **2010,** *35*, (4), 403-440.
8. Parenteau-Bareil, R.; Gauvin, R.; Berthod, F. *Materials* **2010,** *3*, (3), 1863-1887.
9. Zhang, J.; Xia, W.; Liu, P.; Cheng, Q.; Tahi, T.; Gu, W.; Li, B. *Mar. Drugs* **2010,** *8*, (7), 1962-1987.
10. Vroman, I.; Tighzert, L. *Materials* **2009,** *2*, (2), 307-344.
11. Kim, C.; Lee, S. C.; Kang, S. W.; Kwon, I. C.; Kim, Y.-H.; Jeong, S. Y. *Langmuir* **2000,** *16*, (11), 4792-4797.
12. Zhang, X.; Li, Z. Y.; Zhu, X. X. *Biomacromolecules* **2008,** *9*, (9), 2309-2314.
13. Shao, Y.; Lavigueur, C.; Zhu, X. X. *Macromolecules* **2012,** *45*, (4), 1924-1930.
14. Zuluaga, F.; Valderruten, N. E.; Wagener, K. B. *Polym. Bull.* **1999,** *42*, (1), 41-46.
15. Gautrot, J. E.; Zhu, X. X. *Macromolecules* **2009,** *42*, (19), 7324-7331.
16. Zou, T.; Cheng, S.-X.; Zhang, X.-Z.; Zhuo, R.-X. *J. Biomed. Mater. Res., Part B* **2007,** *82B*, (2), 400-407.
17. Giguère, G.; Zhu, X. X. *Biomacromolecules* **2010,** *11*, (1), 201-206.
18. Virtanen, E.; Kolehmainen, E. *Eur. J. Org. Chem.* **2004,** *16*, 3385-3399.
19. Gautrot, J. E.; Zhu, X. X. *J. Biomater. Sci., Polym. Ed.* **2006,** *17*, (10), 1123-1139.

20. Mukhopadhyay, S.; Maitra, U. *Curr. Sci.* **2004,** *87*, (12), 1666-1683.
21. Portincasa, P.; Moschetta, A.; Palasciano, G. *Lancet* **2006,** *368*, 230-239.
22. Danielsson, H.; Sjoevall, J., *New Comprehensive Biochemistry, Vol. 12: Sterols and Bile Acids*. Elsevier: 1985; p 447.
23. Sabine, J., *Cholesterol*. Dekker: 1977; p 489.
24. Jenkins, G.; Hardie, L. J., *Bile Acids Toxicology and Bioactivity*. Royal Society of Chemistry: 2008; p 163
25. Zhang, J.; Zhu, X. *Science in China Series B-Chemistry* **2009,** *52*, (7), 849-861.
26. Zakrzewska, J.; Markovic, V.; Vucelic, D.; Feigin, L.; Dembo, A.; Mogilevsky, L. *J. Phys. Chem.* **1990,** *94*, (12), 5078-5081.
27. Carey, M. C.; Small, D. M. *Arch. Intern. Med.* **1972,** *130*, (4), 506-27.
28. Zhu, X. X.; Nichifor, M. *Acc. Chem. Res.* **2002,** *35*, (7), 539-546.
29. Nair, P. P.; Kritchevsky, D., *The Bile Acids: Chemistry, Physiology, and Metabolism*. Plenum: New York, 1971; Vol. 1, p 3-9.
30. Gautrot, J. E.; Zhu, X. X. *Angew. Chem. Int. Ed.* **2006,** *118*, (41), 7026-7028.
31. Kumar, A.; Chhatra, R. K.; Pandey, P. S. *Org. Lett.* **2009,** *12*, (1), 24-27.
32. Kim, I. S.; Kim, S. H. *Int. J. Pharm.* **2001,** *226*, (1-2), 23-29.
33. Huh, K. M.; Lee, K. Y.; Kwon, I. C.; Kim, Y.-H.; Kim, C.; Jeong, S. Y. *Langmuir* **2000,** *16*, (26), 10566-10568.
34. Kim, I.-S.; Kim, S.-H.; Cho, C.-S. *Macromol. Rapid Commun.* **2000,** *21*, (17), 1272-1275.
35. Zhang, J.; Wang, X. D.; Zhao, B. H.; Li, C. X. *Chem. Lett.* **2006,** *35*, (1), 40-41.
36. Kim, I.-S.; Jeong, Y.-I.; Kim, S.-H. *Arch. Pharmacal Res.* **2000,** *23*, (1), 87-89.
37. Zou, T.; Li, S.-L.; Cheng, S.-X.; Zhang, X.-Z.; Zhuo, R.-X. *J. Biomed. Mater. Res., Part A* **2007,** *83A*, (3), 696-702.
38. Fu, H.-L.; Cheng, S.-X.; Zhang, X.-Z.; Zhuo, R.-X. *J. Controlled Release* **2007,** *124*, (3), 181-188.
39. Fu, H.-L.; Zou, T.; Cheng, S.-X.; Zhang, X.-Z.; Zhuo, R.-X. *J. Tissue Eng. Regener. Med.* **2007,** *1*, (5), 368-376.

40. Zhang, H.; Tong, S.-Y.; Zhang, X.-Z.; Cheng, S.-X.; Zhuo, R.-X.; Li, H. *J. Phys. Chem. C* **2007,** *111*, (34), 12681-12685.
41. Fu, H.-L.; Yu, L.; Zhang, H.; Zhang, X.-Z.; Cheng, S.-X.; Zhuo, R.-X. *J. Biomed. Mater. Res., Part A* **2007,** *81A*, (1), 186-194.
42. Chen, W.-Q.; Wei, H.; Li, S.-L.; Feng, J.; Nie, J.; Zhang, X.-Z.; Zhuo, R.-X. *Polymer* **2008,** *49*, (18), 3965-3972.
43. Giguère, G.; Zhu, X. X. *J. Polym. Sci., Part A: Polym. Chem.* **2007,** *45*, (17), 4173-4178.
44. Luo, J.; Giguère, G.; Zhu, X. X. *Biomacromolecules* **2009,** *10*, (4), 900-906.
45. Strandman, S.; Le Dévédec, F.; Zhu, X. X. *Macromol. Rapid Commun.* **2011,** *32*, (15), 1185-1189.
46. Li, C.; Lavigueur, C.; Zhu, X. X. *Langmuir* **2011,** *27*, (17), 11174-11179.
47. Lavigueur, C.; Zhu, X. X. *RSC Adv.* **2012,** *2*, (1), 59-63.
48. Hu, X.; Zhang, Z.; Zhang, X.; Li, Z.; Zhu, X. X. *Steroids* **2005,** *70*, (8), 531-537.
49. Gauthier, M. A.; Zhang, Z.; Zhu, X. X. *ACS Appl. Mater. Interfaces* **2009,** *1*, (4), 824-832.
50. Gauthier, M. A.; Simard, P.; Zhang, Z.; Zhu, X. X. *J. R. Soc., Interface* **2007,** *4*, (17), 1145-1150.
51. Zhang, Y. H.; Zhu, X. X. *Macromol. Chem. Phys.* **1996,** *197*, (10), 3473-3482.
52. Wang, Y. J.; Zhang, J.; Zhu, X. X.; Yu, A. *Polymer* **2007,** *48*, (19), 5565-5571.
53. Ahlheim, M.; Hallensleben, M. L.; Wurm, H. *Polym. Bull.* **1986,** *15*, 497-501.
54. Zhu, X. X.; Moskova, M.; Denike, J. K. *Polymer* **1996,** *37*, (3), 493-498.
55. Zhang, Y. H.; Akram, M.; Liu, H. Y.; Zhu, X. X. *Macromol. Chem. Phys.* **1998,** *199*, (7), 1399-1404.
56. Benrebouh, A.; Zhang, Y. H.; Zhu, X. X. *Macromol. Rapid Commun.* **2000,** *21*, (10), 685-690.
57. Benrebouh, A.; Avoce, D.; Zhu, X. X. *Polymer* **2001,** *42*, (9), 4031-4038.
58. Kim, J. B.; Lee, B. W.; Kang, J. S.; Seo, D. C.; Roh, C. H. *Polymer* **1999,** *40*, (26), 7423-7426.

59. Idziak, I.; Gravel, D.; Zhu, X. X. *Tetrahedron Lett.* **1999,** *40*, (52), 9167-9170.
60. Liu, H. Y.; Avoce, D.; Song, Z. J.; Zhu, X. X. *Macromol. Rapid Commun.* **2001,** *22*, (9), 675-680.
61. Hao, J. Q.; Li, H.; Zhu, X. X. *Biomacromolecules* **2006,** *7*, (3), 995-998.
62. Nichifor, M.; Carpov, A. *Eur. Polym. J.* **1999,** *35*, (12), 2125-2129.
63. Nichifor, M.; Stanciu, M. C.; Zhu, X. X. *React. Funct. Polym.* **2004,** *59*, (2), 141-148.
64. Xu, Q.; Yuan, X.; Chang, J. *J. Appl. Polym. Sci.* **2005,** *95*, (3), 487-493.
65. Yuan, X.-B.; Li, H.; Zhu, X.-X.; Woo, H.-G. *J. Chem. Technol. Biotechnol.* **2006,** *81*, (5), 746-754.
66. Lee, K. Y.; Jo, W. H.; Kwon, I. C.; Kim, Y.-H.; Jeong, S. Y. *Langmuir* **1998,** *14*, (9), 2329-2332.
67. Lee, K. Y.; Jo, W. H.; Kwon, I. C.; Kim, Y.-H.; Jeong, S. Y. *Macromolecules* **1998,** *31*, (2), 378-383.
68. Lee, K. Y.; Kim, J. H.; Kwon, I. C.; Jeong, S. Y. *Colloid Polym. Sci.* **2000,** *278*, (12), 1216-1219.
69. Kwon, S.; Park, J. H.; Chung, H.; Kwon, I. C.; Jeong, S. Y.; Kim, I.-S. *Langmuir* **2003,** *19*, (24), 10188-10193.
70. Park, J. H.; Kwon, S.; Nam, J.-O.; Park, R.-W.; Chung, H.; Seo, S. B.; Kim, I.-S.; Kwon, I. C.; Jeong, S. Y. *J. Controlled Release* **2004,** *95*, (3), 579-588.
71. Kim, K.; Kwon, S.; Park, J. H.; Chung, H.; Jeong, S. Y.; Kwon, I. C.; Kim, I.-S. *Biomacromolecules* **2005,** *6*, (2), 1154-1158.
72. Yoo, H. S.; Lee, J. E.; Chung, H.; Kwon, I. C.; Jeong, S. Y. *J. Controlled Release* **2005,** *103*, (1), 235-243.
73. Park, K.; Kim, K.; Kwon, I. C.; Kim, S. K.; Lee, S.; Lee, D. Y.; Byun, Y. *Langmuir* **2004,** *20*, (26), 11726-11731.
74. Shaikh, V. A. E.; Maldar, N. N.; Lonikar, S. V.; Rajan, C. R.; Ponrathnam, S. *J. Appl. Polym. Sci.* **2006,** *100*, (3), 1995-2001.
75. Orienti, I.; Gianasi, E.; Aiedeh, K.; Zecchi, V. *J. Pharm. Belg.* **1996,** *51*, (3), 125-130.

76. Ahlheim, M.; Hallensleben, M. L. *Makromol. Chem., Rapid Commun.* **1988,** *9*, (5), 299-302.
77. Noll, O.; Ritter, H. *Macromol. Rapid Commun.* **1996,** *17*, (8), 553-557.
78. Stanciu, M. C.; Nichifor, M.; Simionescu, B. C. *Rev. Roum. Chim.* **2009,** *54*, (11-12), 951-955.
79. Gouin, S.; Zhu, X. X.; Lehnert, S. *Macromolecules* **2000,** *33*, (15), 5379-5383.
80. Gouin, S.; Zhu, X. X. *Steroids* **1996,** *61*, (11), 664-669.
81. Gouin, S.; Zhu, X. X. *Langmuir* **1998,** *14*, (15), 4025-4029.
82. Krasko, M. Y.; Ezra, A.; Domb, A. J. *Polym. Adv. Technol.* **2003,** *14*, (11-12), 832-838.
83. Matsusaki, M.; Hang Thi, T.; Kaneko, T.; Akashi, M. *Biomaterials* **2005,** *26*, (32), 6263-6270.
84. Gautrot, J. E.; Zhu, X. X. *Chem. Commun.* **2008**, 1674-1676.
85. Strandman, S.; Gautrot, J. E.; Zhu, X. X. *Polym. Chem.* **2011,** *2*, (4), 791-799.
86. Thérien-Aubin, H.; Gautrot, J. E.; Shao, Y.; Zhang, J.; Zhu, X. X. *Polymer* **2010,** *51*, (1), 22-25.
87. Manzini, B.; Hodge, P.; Ben-Haida, A. *Polym. Chem.* **2010,** *1*, (3), 339-346.
88. Gangwal, J. J.; Kulkarni, M. G. *J. Appl. Polym. Sci.* **2011,** *122*, (1), 220-232.
89. Kolb, H. C.; Finn, M. G.; Sharpless, K. B. *Angew. Chem., Int. Ed.* **2001,** *40*, (11), 2004-2021.
90. Chow, H.-F.; Lau, K.-N.; Ke, Z.; Liang, Y.; Lo, C.-M. *Chem. Commun.* **2010,** *46*, (20), 3437-3453.
91. Qin, A.; Lam, J. W. Y.; Tang, B. Z. *Chem. Soc. Rev.* **2010,** *39*, (7), 2522-2544.
92. Meldal, M. *Macromol. Rapid Commun.* **2008,** *29*, (12-13), 1016-1051.
93. Guo, J.; Wei, Y.; Zhou, D.; Cai, P.; Jing, X.; Chen, X.-S.; Huang, Y. *Biomacromolecules* **2011,** *12*, (3), 737-746.
94. Tsarevsky, N. V.; Sumerlin, B. S.; Matyjaszewski, K. *Macromolecules* **2005,** *38*, (9), 3558-3561.

95. Binauld, S.; Damiron, D.; Hamaide, T.; Pascault, J.-P.; Fleury, E.; Drockenmuller, E. *Chem. Commun.* **2008**, 4138-4140.
96. Besset, C. l.; Pascault, J.-P.; Fleury, E.; Drockenmuller, E.; Bernard, J. *Biomacromolecules* **2010,** *11*, (10), 2797-2803.
97. Pospieszny, T.; Małecka, I.; Paryzek, Z. *Tetrahedron Lett.* **2012,** *53*, (3), 301-305.
98. Li, W.; Li, X.; Zhu, W.; Li, C.; Xu, D.; Ju, Y.; Li, G. *Chem. Commun.* **2011,** *47*, (27), 7728-7730.
99. Pore, V. S.; Aher, N. G.; Kumar, M.; Shukla, P. K. *Tetrahedron* **2006,** *62*, (48), 11178-11186.
100. Ryu, E.-H.; Ellern, A.; Zhao, Y. *Tetrahedron* **2006,** *62*, (29), 6808-6813.
101. del Amo, V.; Siracusa, L.; Markidis, T.; Baragana, B.; Bhattarai, K. M.; Galobardes, M.; Naredo, G.; Perez-Payan, M. N.; Davis, A. P. *Org. Biomol. Chem.* **2004,** *2*, (22), 3320-3328.
102. Vatmurge, N. S.; Hazra, B. G.; Pore, V. S.; Shirazi, F.; Deshpande, M. V.; Kadreppa, S.; Chattopadhyay, S.; Gonnade, R. G. *Org. Biomol. Chem.* **2008,** *6*, (20), 3823-3830.
103. Denike, J. K.; Moskova, M.; Zhu, X. X. *Chem. Phys. Lipids* **1995,** *77*, (2), 261-267.
104. Tian, W. Q.; Wang, Y. A. *J. Org. Chem.* **2004,** *69*, (13), 4299-4308.
105. Stang, P. J.; Anderson, A. G. *J. Org. Chem.* **1976,** *41*, (5), 781-785.
106. Odian, G., *Principles of Polymerization, 4th Edition*. Wiley: New Jersey, 2004; p 768
107. Sojitra, P.; Patel, K. *High Perform. Polym.* **2011,** *23*, (8), 565-574.
108. Ivanysenko, O.; Strandman, S.; Zhu, X. X. *Polym. Chem.* **2012,** *3*, 1962-1965.

Appendix

Requirements for high molecular weight in step-growth polymerization[1]

There are few critical requirements for SGP to obtain linear high molecular weight polymers. First, the perfect stoichiometric balance of the two difunctional monomers must be introduced, or self-balancing reaction is necessary. For example, a single difunctional monomer can generate polymer, such as in the case of ε-aminocaproic acid, an internal balance within the monomer is provided. Second, high degree monomer purity is required. The products of degradation or impurities lead to a stoichiometric imbalance while the monofunctional monomers act as a chain stopper and no further reaction is possible at that end of the chain. If the monomer functionality is greater than two, then the resulting polymer is either highly branched, or a crosslinked, three-dimensional network. Third, the reaction responsible for the polymerization must be a very high yield reaction with the absence of side reactions.

Polymerization reaction of heterofunctional monomer (A-B monomer) and two monofunctional monomers (A-A and B-B monomers) can be written in the general form:

$$N_0A-B \rightarrow A-B-\left[A-B\right]-_{N_0-2}\ A-B$$
$$N_0A-A+N_0B-B \rightarrow A-A-\left[B-B-A-B\right]-_{N_0-1}\ B-B$$

where N_0 is the number of monomer molecules at the beginning of the reaction. At any given stage of the reaction, if N or 2N functional groups, respectively, have remained unreacted, then there will be N or 2N molecules in the mixture, regardless of size. The total number of functional groups of either type A or B that have reacted is N_0-N. The extent of a reaction at a given stage of the polymerization is defined by *P*, which is the ratio of the number of reacted molecules to the initial number of molecules.

The degree of polymerization, DP is the original number of the molecules divided by the remaining number of molecules and approaches a number equal to the original number of the molecules as N approaches one. DP can be expressed by

$$DP = \frac{N_0}{N_0(1-P)} = \frac{1}{1-P}$$

Consider a reaction to be pushed to 90 % completion, DP is 10. Moreover, 98 % yield reaction is necessary in order to obtain DP=50 at which many polymers begin to exhibit useful mechanical properties. In case of a reaction having the same conversion but with 2 % impurity, the molecular weight is cutting in a half.

1. Stille, J. K. *J. Chem. Educ.* **1981,** *58*, (11), 862-866.